MODELING OF CIRCADIAN-IMMUNE INTERACTIONS

by

PANTELEIMON D. MAVROUDIS

A Dissertation submitted to the

Graduate School-New Brunswick

Rutgers, The State University of New Jersey

in partial fulfillment of the requirements

for the degree of

Doctor of Philosophy

Graduate Program in Chemical and Biochemical Engineering

written under the direction of

Ioannis (Yannis) P. Androulakis, PhD

and approved by

_____

_____

_____

_____

New Brunswick, New Jersey

October, 2014

Abstract of the Dissertation

Modeling of Circadian-Immune interactions

by

PANTELEIMON D. MAVROUDIS

Dissertation Director:

Ioannis P. Androulakis

Dysregulation of the inflammatory response is a critical component of many clinically challenging disorders such as sepsis. Inflammation is a biological process designed to lead to healing and recovery, ultimately restoring homeostasis; however, the failure to fully achieve those beneficial results can leave a patient in a dangerous persistent inflammatory state. One of the primary challenges in developing novel therapies in this area is that inflammation is comprised of a complex network of interacting pathways. Here, we discuss our approaches towards addressing this problem through computational systems biology, with a particular focus on how the presence of biological rhythms and importantly circadian (~24hr) and the disruption of these rhythms may be applied in a translational context. By leveraging the information content embedded in physiologic variability, and its loss under acute inflammatory response we aim to gain insight into the underlying physiology.

Heart rate variability (HRV) has been studied as a potential prognostic marker in inflammation-linked diseases. We modeled the interactions between human endotoxemia mediators and the autonomic nervous system in order to understand the loss of HRV in presence of stress, allowing for the rationalization of experimental observations in the framework of a quantitative model. Furthermore, by modeling the flow of circadian information from the environmental light/dark cycles to the systemic cortisol level and ultimately to the single immune cell level, we identified critical dynamics that confer robust synchronization and rhythmicity both of which are characteristics associated with well-being. Lastly, by considering the disparate role of cortisol as an immunopermissive and immunosuppressive agent, we elucidated the dynamics leading to a time of day dependence of body's inflammatory response. These results denote the critical importance of physiological rhythms in homeostasis and stress, and elucidate the potential to derive critical information by the analysis of variability and its source both at the systemic and at the single cell level.

Ackowledgment

First and most important, I thank my advisor Ioannis P. Androulakis for his inspiration and guidance. My family for supporting me and Fani for being the closest person I had all these years. I would like to dedicate this work to all of them.

Table of contents

List of Tables

List of illustrations

Figure B 3: Administration of LPS stimulus at cortisol's zenith (z) and nadir (n) levels. A: Cortisol profile when LPS is introduced at zenith (z) and nadir (n) levels. B: Maximum P_{ens} levels calculated for 24hr following LPS introduction at zenith or nadir levels. C: Suppressive (Supp, red line) and permissive (perm, blue line) effects in homeostasis (solid lines) and when LPS is introduced at cortisol's zenith level. Dotted point indicates the time of the stimulus. D: Suppressive (Supp, red line) and permissive (perm, blue line) effects in homeostasis (solid lines) and when LPS is introduced at cortisol's nadir levels. Permissive profile represents the cortisol mediated induction of cytokine receptors through mineralocorticoid receptor ($\frac{k_{fr,2} \cdot FMR(N)}{K_{fr,2} + FMR(N)}$) whereas suppressive the cortisol mediated inhibition of cytokines through glucocorticoid receptor ($\frac{k_{fr} \cdot FGR(N)}{K_{fr} + FGR(N)}$). Dotted point indicates the time of the stimulus. 175

Chapter 1: Introduction

1.1: Systemic inflammation

In response to a stressor, such as an injury or an infection, the body mounts an inflammatory response aimed at resolving the deleterious effects of the stressor and restoring homeostasis, such as through the healing of a wound or the elimination of a bacterial infection. Normally, inflammation successfully results in a return to homeostasis. However, when anti-inflammatory mechanisms fail to adequately counterbalance proinflammatory activity, the body can reach a state of prolonged, unresolving systemic inflammation. This dysregulated inflammatory state can cause significant harm to the body, even in the absence of any exogenous stressor.

Further complicating this issue is our general inability to effectively modulate persistent inflammatory states. Clinically, this represents a major challenge. For instance, therapies for the management and control of inflammation in septic patients are limited (Martin, Mannino et al. 2003) and the only recently approved novel therapy (activated protein C) failed to show improved outcome in a repeat phase III clinical trial (Angus 2011). Furthermore, novel therapies aimed at treating rheumatoid arthritis and inflammatory bowel disease with anti-cytokine therapies have shown promise in recent years, but similar strategies have not produced such promising results in treating sepsis (Marshall 2003).

In order to develop novel strategies to approach the clinical management of inflammation-linked diseases, we need to obtain a more fundamental

understanding of the mechanisms driving inflammation. A useful experimental tool that has helped with progression toward these goals is the human endotoxemia model (Lowry 2005), which consists of the injection of low doses of endotoxin (lipopolysaccharide, LPS) in healthy human volunteers. This evokes many signs and symptoms characteristic of systemic inflammation, making it a practical experimental model of systemic inflammation in humans. Furthermore, it is becoming increasingly apparent that issues of physiologic variability are tightly intertwined with inflammation. The existence of a homeostatic state does not imply that physiology is at a constant level during health; to the contrary, there is rich variability both at circadian and other time scales in many physiological processes, including those related to inflammation. This is particularly interesting in light of the hypothesis originally put forth by Godin and Buchman that the connectivity of a physiological system is related to the variability in its output, and that dysregulated inter-organ communication in disease may be reflected in decreased variability in output signals (Godin and Buchman 1996). These issues can also be studied in the context of human endotoxemia, since endotoxemia results in a significant loss of physiologic variability (often called “decomplexification”) at multiple scales (Rassias, Holzberger et al. 2005).

1.2: Human endotoxemia and physiologic variability

Human endotoxemia is the response to the elective administration of endotoxin (lipopolysaccharide, LPS), a component of the outer membrane of

Gram-negative bacteria that is recognized by the innate immune system and provokes an inflammatory response. Although acute, systemic inflammation is of course not reflective of all of the physiological changes occurring in complex disease such as sepsis, human endotoxemia does precipitate signs and symptoms characteristic of clinical sepsis (Lowry 2005) acute respiratory distress syndrome (ARDS) (Buttenschoen, Kornmann et al. 2008)and trauma (Shanker, Coyle et al.). These physiological changes include transcriptional responses in immune cells, secretion of cytokines and hormones, and changes in autonomic activity (Lowry 2009). All of these effects stem from responses generated by the binding of LPS to toll-like receptor 4 (TLR4), thus activating innate immune cells and stimulating pathways linked to the production of inflammatory genes such as the NF-κB, JAK-STAT, and MAPK signaling pathways (Foteinou, Calvano et al. 2009; Scheff, Mavroudis et al. 2013). This transcriptional activity leads to the production and release of both proinflammatory and anti-inflammatory cytokines, mediators of the inflammatory response and the return to homeostasis, respectively. This initial inflammatory response to LPS also propagates through afferent nervous signaling to the central nervous system (CNS), which then forms a feedback loop to regulate the progression immune response through modulating sympathetic and parasympathetic activity, which may be reflected in increased heart rate (HR) and decreased heart rate variability (HRV) (Godin, Fleisher et al. 1996). In particular, central regulation plays a role in governing the inflammatory response both through autonomic activity itself (Tracey 2002) and though the activation of the hypothalamic-pituitary-adrenal (HPA) axis

and the subsequent release of anti-inflammatory hormones such as cortisol (Beishuizen and Thijs 2003).

Many of the components involved in the inflammatory response contain homeostatic rhythmic variability, and advances in clinical and experimental tools make assaying the state of these rhythms increasingly plausible. Figure 1.1 shows several of these homeostatic rhythms, including mediators directly involved in inflammation such as cytokines and immunomodulatory hormones, as well as oscillatory components that give rise to patterns in heart rate (HR) that are disrupted in inflammation such as breathing pattern, blood pressure rhythms, and autonomic activity. Underlying every biochemical oscillator is some type of negative feedback mechanism (Novak and Tyson 2008). Possibly the simplest system to consider is a protein that acts as a transcription factor by inhibiting the transcription of its own mRNA. Given appropriate time delays in transcription, translation, and translocation, as well as appropriate rate constants, this simple single-gene system oscillates. Real physiological systems typically consist of much more complex networks comprised of multiple feedback loops. Even still, physiological rhythms are of clinical interest because characteristics of those patterns convey information about the underlying system that is producing them, beyond simply measuring the mean value of a signal. For instance, in some cases, the network structure giving rise to rhythms can be reverse engineered from the pattern of rhythmicity (Pigolotti, Krishna et al. 2007). Given that negative feedback loops are critical in maintaining homeostasis and acute responsiveness, perturbations in negative feedback loops culminating in altered rhythmic

patterns can reveal information about the integrity of the negative feedback system (Veldhuis, Keenan et al. 2008).

Clinically, patterns in physiological signals represent a broad source of potential diagnostic and prognostic markers. For instance, perturbations in the rhythmicity of heart beats precede the onset of neonatal sepsis (Griffin, O'Shea et al. 2003). At a much longer time scale, circadian variations in plasma cortisol concentration, a factor that has been linked to immune dysfunction, has been associated with chronic stress resulting from depression (Yehuda, Teicher et al. 1996), obesity (Rosmond, Dallman et al. 1998), psychological stress (Polk, Cohen et al. 2005), and cancer (Mormont and Levi 1997; Sephton, Sapolsky et al. 2000; Sephton, Lush et al. 2013). The loss of rhythmicity in these cases may reflect an underlying loss in the regulation of negative feedback control systems.

To take full advantage of the information conveyed by altered rhythmicity in a biological signal, the mechanism behind the change in rhythmicity must be known. Lacking this, variability-based metrics can still yield significant clinical uses purely based on observed correlations, which is often the case for applications of HRV analysis. More mechanistic detail would allow for understanding of what physiological processes drive changes in HRV, potentially opening the door to novel and more refined therapeutic approaches. In this context, controlled experimental and mathematical models represent critical avenues by which mechanisms giving rise to both the homeostatic generation of rhythms and the alteration of rhythms in disease can be explored.

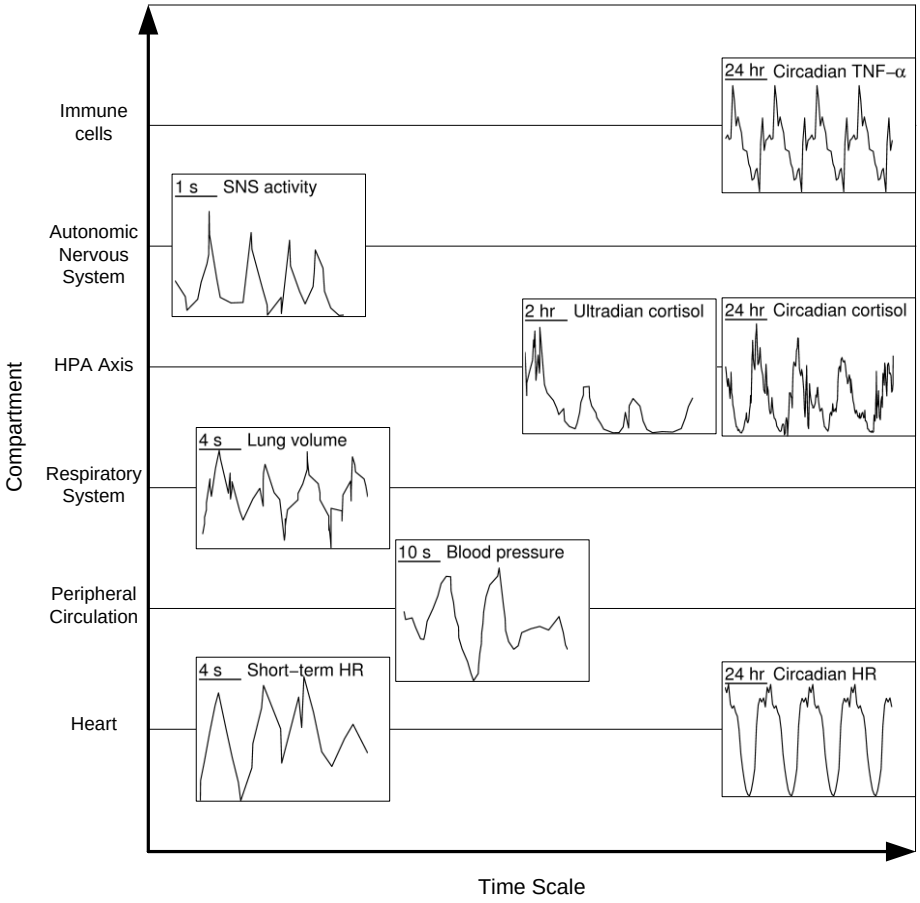

Figure 1. 1: Homeostatic rhythms, at a variety of time scales, which contribute to altered physiologic variability in endotoxemia. TNF-α data: (Petrovsky and Harrison 1998). SNS activity data: (Donadio, Cortelli et al. 2008). Circadian cortisol data: (Brown, Meehan et al. 2001). Ultradian cortisol data: (Charloux, Gronfier et al. 1999). Lung volume, blood pressure, and short-term HR data: (Seydnejad and Kitney 2001). Circadian HR data: (Octavio, Rodriguez et al. 2004). TNF-α is an inflammatory cytokine that has a clear circadian pattern in response to LPS stimulation. Autonomic signaling in inflammation contributes both to changes in cardiac function and modulation of the inflammatory response. Cortisol is an anti-inflammatory hormone. Blood pressure and respiratory rhythms contribute to short-term patterns in HR, which are diminished in endotoxemia.

1.3: Outline of dissertation

Especially due to its potential use as a prognostic marker in inflammatory diseases and sepsis, the quantification of beat-to-beat heart rate variability (HRV) represents a critically important physiological dimension. In Chapter 2 we investigate the use of a physiologically based model that aims to explore the interactions between human endotoxemia and the autonomic nervous system in order to understand the loss of HRV in response to stress.

HRV is a systemic signal that represents the systemic variability of the body mediated from multiple rhythms. In Chapter 3 we aim to understand the source of variability in the body beginning from the single cell level and extending on the systemic level. Furthermore, we try to explore the flow of circadian information in the body, beginning from the environmental light/dark cycles and ending on the circadian secretion of inflammatory parameters. Based on this, in Chapter 4 we present two semi-mechanistic models that describe the entrainment of peripheral immune cell clocks to cortisol circadian rhythm, and the entrainment of cortisol rhythmicity to environmental light/dark cycles. As a whole, this chapter investigates the flow of circadian information from the environment to peripheral clocks of the body through the use of physiologically based models.

In Chapter 5 we link cortisol's circadian rhythmicity with its disparate effects in inflammatory response. In particular, we explore the convolution of cortisol's immuno-permissive/suppressive effects throughout the day, and using as a test-bed the acute inflammatory response we investigate the dynamics resulting in an optimal time of day dependent response.

The results of our efforts point towards the importance of physiologic variability in homeostasis as well as in the inflammatory response. Furthermore, through our modeling we underline the necessity of an optimal orchestration between inter- and intra-organ variability that ultimately results in an effective dynamic function of the body.

Chapter 2: Heart Rate Variability and Human Endotoxemia

2.1: Introduction

Heart rate variability (HRV) is generally defined as the quantification of the distribution of time intervals between successive heartbeats. Reduction in HRV, a manifestation of altered autonomic function under stress, is potentially a useful predictor of outcome in myocardial infarction (Kleiger, Miller et al. 1987), congestive heart failure (Ponikowski, Anker et al. 1997), diabetic neuropathy (Pagani 2000), and neonatal sepsis (Lake, Richman et al. 2002). Diminished HRV has also been observed in critically ill patients in intensive care units (Morris, Norris et al. 2007), which motivates interest in HRV as a critical variable in the recovery from critical illness (Lowry and Calvano 2008). Due to this clinical relevance, dynamic characteristics of HRV have been assessed by time domain, frequency domain (Task 1996), and nonlinear metrics (Peng, Havlin et al. 1995; Lake, Richman et al. 2002). The majority of HRV research has thus far focused on the interpretation of the patterns of HRV (Lahiri, Kannankeril et al. 2008) rather than linking cellular-level mechanisms to patterns (Buchman 2009). The realization that health may be

characterized by a certain degree of variability of human heart signals motivates the hypothesis that appropriate physiologic variability is the manifestation of robust dynamics of control signals whose fluctuations equip the host with the ability to anticipate external and internal disturbances. We hypothesize that these variable dynamics are driven by the convergence of rhythmic physiological signals on the heart via autonomic modulation.

Studying the effects of critical illness on HRV requires a clinical model that can be experimentally evaluated in great detail. Responses observed in human endotoxemia experiments mimic observed responses in systemic inflammation in intensive care unit (ICU) patients, albeit over different timescales (Haimovich, Reddell et al. 2010), thus making the human endotoxemia model an excellent platform for exploring mechanistic underpinnings of the systemic inflammatory response. A key component in the response to endotoxemia is a decrease in HRV, concomitant with imbalances in autonomic activity reflected by perturbed autonomic oscillatory responses in HR (Godin, Fleisher et al. 1996; Rassias, Holzberger et al. 2005; Jan, Coyle et al. 2009; Jan, Coyle et al. 2010).

The dynamic signals evoked in an inflammatory response are propagated to the sinoatrial (SA) node of the heart to assess how HRV is perturbed in endotoxemia. Previously, endotoxemia-induced changes in HR and HRV have been described by physicochemical relations which begin to elucidate the signals that give rise to altered phenotypes (Foteinou, Calvano et al. 2010; Foteinou, Calvano et al. 2011). However, this neglects that HR and HRV are both derived from the same physiological process, the beats of the heart, and that the contraction of the heart as initiated by firing neurons at the SA node is

a noisy, discrete process. This motivates the development of a more mechanistic model to produce discrete heartbeat signals that can then be used to calculate HR and HRV, providing a basis for the development of autonomic dysfunction in endotoxemia. In this Chapter we propose a semi-mechanistic mathematical model linking endotoxemia to cardiac function through an integral pulse frequency modulation (IPFM) model (Bayly 1968) that produces discrete heartbeats as output based on autonomic modulation of the heart. Variability is considered both at high frequencies (autonomic oscillations) and much lower frequencies (circadian rhythms). Outputs of the model, namely HR and HRV, are shown to accurately capture experimentally-observed phenomena in human endotoxemia studies. Furthermore, the links between autonomic activity and cardiac function are explored, as well as how these communication links are affected by acute stress. Understanding the loss of variability of cardiac function in endotoxemia serves as a step towards gaining insight into similar changes in HRV observed clinically in response to stress (Haimovich, Reddell et al. 2010). It is important to consider how the communication between the autonomic nervous system and the heart in endotoxemia (Sayk, Vietheer et al. 2008) will affect both measureable parameters of HRV and the mechanistic underpinnings that give rise to altered cardiac function. Thus, connections between processes at the cellular, molecular, and neural levels are quantitatively linked to HRV. This work builds towards translational applications of systems biology (Vodovotz, Csete et al. 2008; Foteinou, Calvano et al. 2009) by moving towards an understanding of the relationship between fundamental biological processes and clinical outcomes.

2.2: Material and Methods

2.2.1: Human endotoxemia model and HRV

Bacterial endotoxin, a component of the outer cell membrane of gram-negative bacteria, is an important mediator in the pathophysiology of gram-negative bacterial sepsis (Opal, Scannon et al. 1999). This complex macromolecule induces its injurious effects by a non-cytotoxic interaction with CD14-bearing inflammatory cells, such as macrophage-monocytes, circulating neutrophils and lung epithelial cells. These effector cells are activated through a family of Toll-like receptors and subsequently release a network of inflammatory products as also described in Chapter 1. These host-derived mediators function in concert to induce the systemic inflammatory response syndrome (SIRS) (Parrillo 1993) leading to a variety of clinical disorders, including adult respiratory distress syndrome (ARDS) (Miyata and Torisu 1986; Bayston and Cohen 1990). Elective administration of endotoxin to otherwise healthy human volunteers has been used to study systemic inflammation and gain insight into behavior of inflammatory mediators encountered in acute, as well as chronic, inflammatory disease. Human endotoxemia precipitates signs and symptoms characteristic of clinical sepsis (Lowry 2005; Andreasen, Krabbe et al. 2008) and ARDS (Buttenschoen, Kornmann et al. 2008), inducing a reduction in HRV (Godin, Fleisher et al. 1996; Rassias, Holzberger et al. 2005). While we do not argue that the human endotoxin (lipopolysaccharide=LPS) challenge model precisely replicates an acute infectious or sepsis condition, human endotoxin challenge does serve as a useful model of toll-like receptor 4 (TLR4) agonist-induced systemic

inflammation by providing a reproducible experimental platform tying systemic inflammation to physiological signal generation and alterations in HRV. As an example, it has recently been demonstrated that LPS challenge induces transient dynamic changes in leukocyte gene expression similar to day 1 trauma patients (Shanker, Coyle et al.; Scheff, Mavroudis et al. 2012; Scheff, Mavroudis et al. 2013).

In an effort to establish quantitative relationships among the components involved in endotoxemia, we developed a mathematical model of human endotoxemia (Foteinou, Calvano et al. 2009; Foteinou, Calvano et al. 2009). A detailed description of the components of the mathematical model is given in Appendix A and the network structure is displayed in Figure 2.1. At the cellular level, recognition of LPS by TLR4 on immune cells leads to the activation of the NF-κB pathway and ultimately the production of both pro-inflammatory (*P*) and anti-inflammatory (*A*) cytokines, which are proximal mediators of the systemic inflammatory response (Opal and DePalo 2000) and antagonistically work towards the self-regulation and resolution of inflammation. At the neuroendocrine level, the hypothalamic-pituitary-adrenal (HPA) axis and the sympathetic nervous system (SNS) are the primary stress response pathways by which the central nervous system (CNS) regulates the immune response (Sternberg 2006). This was modeled by assuming that the production and release of counter-regulatory anti-inflammatory endogenous hormones cortisol (*F*) and epinephrine (*EPI*) respond to pro-inflammatory cytokines, and then these hormones feed-back to modulate the transcriptional response in leukocytes. In addition, circadian rhythms in model components, both at the level of immune cells and CNS activity, were considered by

accounting for diurnal patterns in the release of the hormones cortisol and melatonin (*M*), which then propagate their circadian rhythmicity to other variables (Scheff, Calvano et al. 2010).

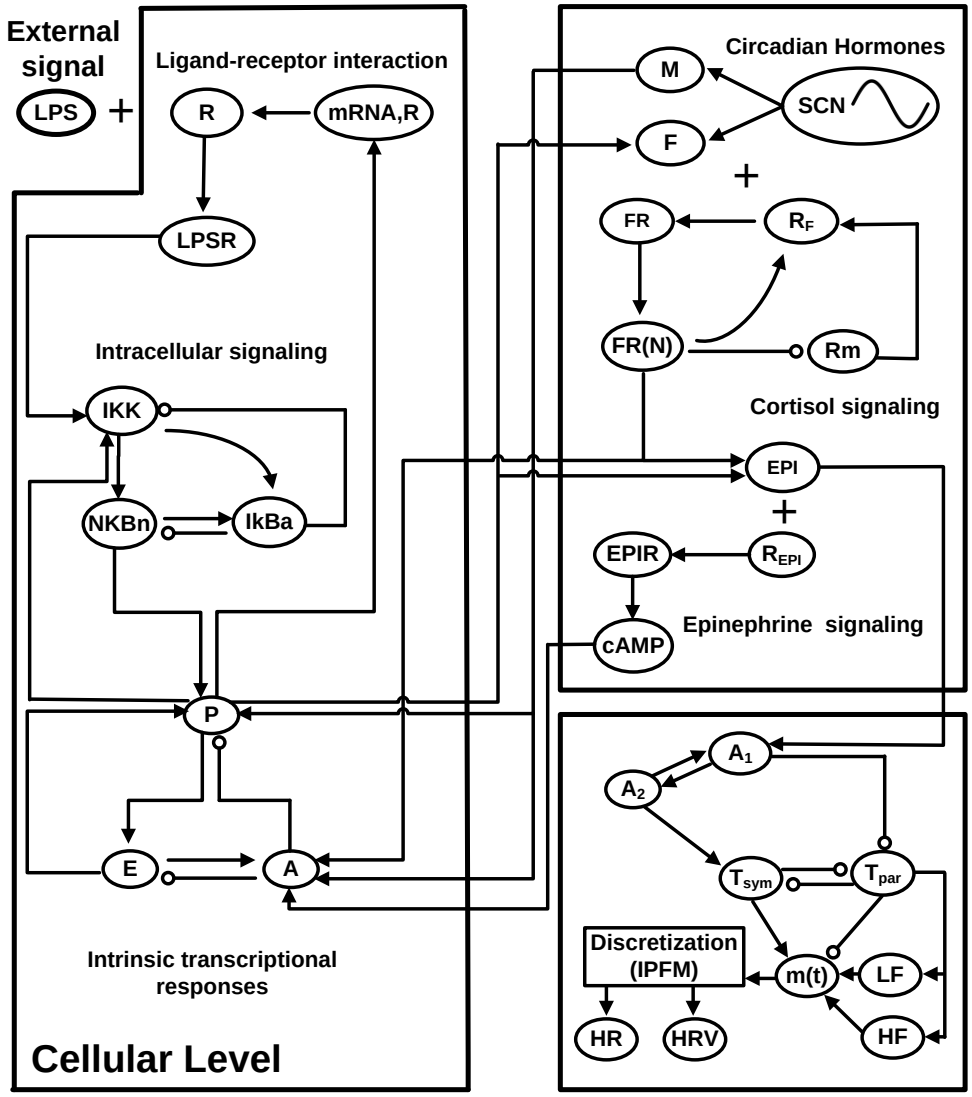

Figure 2.1: Network structure. At the cellular level, LPS is recognized by its receptor, activating the NF-κB signaling cascade that provokes a significant transcriptional response consisting primarily of pro-inflammatory (P) and anti-inflammatory (A) signaling as well as a decrease in cellular bioenergetic processes (E). Neuroendocrine-immune crosstalk results in

the secretion of stress hormones cortisol (F) and epinephrine (EPI), which serve as immunoregulatory branches of the central nervous system. They are also centrally regulated to obey circadian dynamics. Finally, these signals propagate to the heart, where HR and HRV are modulated in a systemic inflammatory response.

Previous efforts of our group explored the principles of the Warner model (Warner and Cox 1962) to describe the influences of the antagonistic relationship between the sympathetic and parasympathetic branches of the autonomic nervous system on the firing at the SA node of the heart (Foteinou, Calvano et al. 2011). Autonomic activity at the SA node of the heart can be inferred based on blood epinephrine concentration (Foteinou, Calvano et al. 2011), which has a circadian pattern with a peak during the middle of the day, slightly lagging the diurnal behavior of cortisol (Kronfol, Nair et al. 1997; Dimitrov, Benedict et al. 2009; Scheff, Calvano et al. 2010). A_1 (Eq. 2.1a) represents the neurotransmitter concentration at the SNS nerve ending, which is associated with blood norepinephrine concentration and is assumed to be similarly responsive to endotoxemia as epinephrine (Schaller, Waeber et al. 1985). Plasma norepinephrine ultimately influences the local concentration at the SA node as described by A_2 (Eq. 2.1b). This produces antagonistic changes in effective local sympathetic (Eq. 2.1c) and parasympathetic (Eq. 2.1d) activity. These relationships were used to develop a physicochemical model of the effect of endotoxemia on HR (Foteinou, Calvano et al. 2011).

$$\frac{dA_1}{dt} = K_{a1} \cdot (EPI - A_1) - K_{a2} \cdot (A_2 - A_1) \qquad (2.1a)$$

$$\frac{dA_2}{dt} = K_{a2} \cdot \left(A_1 - A_2 \right) \qquad (2.1b)$$

$$\frac{dT_{sym}}{dt} = \frac{K_{a3} \cdot A_2 \cdot (K_C - T_{sym})}{\left(1 + k_{T_{sym}, T_{T_{par}}} \cdot T_{par} \right)} - K_{a4} \cdot T_{sym} \qquad (2.1c)$$

$$\frac{dT_{par}}{dt} = \frac{K_{in, T_{par}}}{\left(1 + k_{T_{par}, T_{sym}} \cdot T_{sym} \right) \cdot A_1} - K_{out, T_{par}} \cdot T_{par} \qquad (2.1d)$$

When combining Eq. 2.1 with our circadian model (Scheff, Calvano et al. 2010), described in the Appendix A, we observe that the effective sympathetic (T_{sym}) and parasympathetic (T_{par}) modulation of HR and HRV exhibit diurnal patterns as imposed by central circadian regulation. Experiments measuring muscle sympathetic nerve activity show that it is responsive to light (Saito, Shimizu et al. 1996) and that during sleep, sympathetic activity decreases (Gherghel, Hosking et al. 2004). Based on experimental evidence that parasympathetic activity can be estimated by respiratory sinus arrhythmia measured by the spectral analysis of heart rate, it has been shown that parasympathetic activity also follows circadian dynamics (Burgess, Trinder et al. 1997), as measured by both time domain (pNN50) and frequency domain metrics (Burger, Charlamb et al. 1999). These oscillatory dynamics, leading to short-term HRV and long-term circadian rhythms in HR and HRV, have not yet been studied in a model that links autonomic activity to the beating of the heart within the context of an integrated model of inflammation. Below, variability in HR is studied in terms of these rhythmic signals through the development of a model linking the inflammatory response with alterations in the pattern of discrete heart beats.

2.2.2: Modeling autonomic influence on cardiac dynamics

To describe how internal signals representing cellular and molecular processes responsive to endotoxemia are propagated to the heart, the oscillatory signals giving rise to variability in HR must first be accounted for. We hypothesize that the convergence of these variable autonomic signals, representing both circadian rhythms and higher frequency oscillations, gives rise to the characteristic patterns of variability in HR. Thus, the first step towards developing a more mechanistic model of cardiac function in endotoxemia is describing the nature of autonomic regulation at the SA node of the heart. Three sources of oscillations are considered: sympathetic and parasympathetic oscillations and circadian rhythms.

HRV is typically calculated based on a series of RR intervals, which are generated from ECG signals by measuring the time interval between successive R waves. In the frequency domain of RR intervals, the power spectrum is typically divided into two frequency bands: low frequency (LF, 0.04-0.15 Hz) and high frequency (HF, 0.15-0.4 Hz). While the precise autonomic underpinnings of HF and LF power are unclear and likely indirect (Karemaker 1999), HF is related to vagal activity and LF responds to changes in both vagal and sympathetic tone; thus, the ratio LF/HF may give some insight into the relative autonomic control of HR. Incorporating higher-frequency oscillations in autonomic modulation of HR allows for the production of a more biologically realistic heartbeat signal.

Long-term circadian oscillations in autonomic activity at the SA node influence the diurnal pattern of heartbeats. Sympathetic activity increases HR, while parasympathetic activity decreases HR; therefore, combining models that represent autonomic activity in inflammation (Foteinou, Calvano et al. 2011) and circadian rhythms in inflammation (Scheff, Calvano et al. 2010) generates variables reflecting circadian rhythms in sympathetic and parasympathetic activity at the SA node. These circadian autonomic activities lead to diurnal patterns in both HR and HRV (Huikuri, Niemela et al. 1994; Korpelainen, Sotaniemi et al. 1997; Nakagawa, Iwao et al. 1998). Circadian rhythms are hypothesized to express sympathetic activity as proportional to autonomic modulation and parasympathetic activity as inversely proportional. Circadian rhythms are included to represent autonomic influences on the SA node, specifically slowly evolving circadian rhythms.

The inclusion of autonomic activity through a modified Warner-type model (Eq. 2.1), stimulated by central hormonal circadian rhythms allow for the assessment of changes in autonomic control of heart rate variability (Chiu and Kao 2001). When sympathetic activity increases, the SA autonomic modulation is expected to increase, corresponding to more frequent firing and thus higher HR. When parasympathetic activity increases, the opposite occurs and HR decreases. Our model aims to introduce circadian variability in the autonomic modulation of the SA node, through the connections to our endotoxemia model via T_{sym} (Eq. 2.1c) and T_{par} (Eq. 2.1d), which are ultimately linked to circadian rhythms in HR that match well with experimental data showing that HR peaks during the day and is lower at night (Nakagawa, Iwao et al. 1998).

HF and LF power have been observed to exhibit circadian rhythms under normal conditions (Huikuri, Niemela et al. 1994; Korpelainen, Sotaniemi et al. 1997; Nakagawa, Iwao et al. 1998). In human endotoxemia, HF and LF power both decrease acutely before recovering (Godin, Fleisher et al. 1996; Jan, Coyle et al. 2009; Jan, Coyle et al. 2010). Both circadian and acute responses may be explained by the link between vagal activity and HF and LF oscillations. Suppressing vagal activity leads to decreases in both HF and LF power, contrary to the outdated view that HF reflects only vagal activity and LF reflects only sympathetic activity (Task 1996). Experimental data of circadian rhythms in HF and LF are in phase with the predicted circadian oscillations in T_{par} in 1.2. Further, in human endotoxemia, T_{par} decreases to reflect diminished parasympathetic activity during the acute systemic inflammatory response (Foteinou, Calvano et al. 2011). Thus, we hypothesize that the variable amplitudes of HF and LF oscillations are governed by parasympathetic activity.

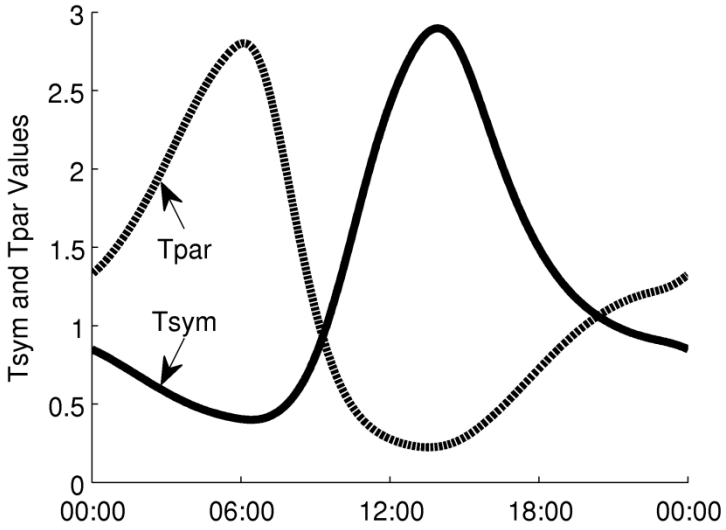

Figure 2.2: Circadian rhythms in the effective sympathetic and parasympathetic activity (Tsym and Tpar) at the sinus node of the heart. Diurnal rhythms from the circadian release of

cortisol propagate through epinephrine, ultimately influencing Tsym and Tpar, which oscillate out of phase in homeostasis.

HF and LF oscillations are assumed to contribute in an additive manner to SA node autonomic modulation as two sinusoids. In (Brennan, Palaniswami et al. 2002), HF and LF oscillations are similarly modeled as sinusoids with frequencies 0.334 Hz and 0.025 Hz, respectively. The LF frequency is set so low (below the LF range) because it is meant to also allow for realistic changes in very low frequency (VLF, <0.05 Hz) activity. However, this impedes the direct calculation of LF and HF powers because the peak in the power spectrum is so narrow that it hardly influences the power in the LF frequency band. Therefore, in Eq. 2.2, the mean values of the frequencies in the HF and LF bands were used. Then, the peaks in the power spectrum fall directly within the HF and LF bands, facilitating the use of standard methods of calculating HF and LF power to study model output. The amplitudes of the HF and LF sinusoids depend on T_{par}, which produces homeostatic circadian rhythms in HRV (Huikuri, Niemela et al. 1994; Korpelainen, Sotaniemi et al. 1997; Nakagawa, Iwao et al. 1998) as well as acute suppression of HRV in endotoxemia (Godin, Fleisher et al. 1996; Jan, Coyle et al. 2009; Jan, Coyle et al. 2010).

The aforementioned assumptions are succinctly summarized in the model of Eq. 2.2. The effective autonomic modulation at the SA node depends on contributions including circadian and higher frequency modulation of the heart as well as a constant activity level which gives rise to the mean resting HR.

$$m(t) = \underbrace{HR}_{\substack{\text{constant}\\ \text{activity}\\ \text{level}}} + \underbrace{k_{circ}\left(T_{sym} + \frac{1}{T_{par}}\right)}_{\substack{\text{circadian}\\ \text{variability}}} + \underbrace{k_{osc}\left(1 + k_{par,LF}T_{par}\right)\sin\left(f_{LF}t\right)}_{\text{LF/sympathetic oscillations}} + \underbrace{k_{osc}\left(1 + k_{par,HF}T_{par}\right)\sin\left(f_{HF}t\right)}_{\text{HF/sympathetic oscillations}} \tag{2.2}$$

Table 2.1: Frequencies for the HF and LF bands are set to the mean value of the standard limits of those bands. The other parameters are set manually. In practice, the parameters in the IPFM model would need to be tuned to an individual subject due to significant person-to-person variability in cardiac dynamics, such as the mean heart rate and the amplitude of circadian rhythms.

Parameter	**Value**	**Parameter**	**Value**
HR	1	$k_{par,HF}$	1
$\mathbf{k_{osc}}$	0.05	f_{HF}	0.275
$\mathbf{k_{par,LF}}$	0.5	k_{circ}	0.04
$\mathbf{f_{LF}}$	0.105		

2.2.3: Generation of discrete heartbeats

Autonomic activity influences the heart by modulating the pattern of discrete heartbeats by altering the concentration of neurotransmitters at the SA node. An idealized neuron functions by sensing local neurotransmitter concentration and, when that concentration crosses a threshold, the postsynaptic neuron fires. This type of neural-based discretization process occurs at the sinoatrial (SA) node of the heart, which normally initiates the electrical impulses that trigger contraction of cardiac tissue. As the SA node is innervated by both sympathetic and parasympathetic branches of the autonomic nervous system and the imbalance between these branches is critical to the loss of HRV, an ideal model would be one that dynamically controls the time interval of integration between successive firings based on autonomic activity as defined in Eq. 2.2.

A continuous signal can be converted to discrete events via an integrate-and-fire model in which the signal is repeatedly integrated until it reaches a threshold, thus signifying an event. One realization of an integrate-and-fire model which can discretize a continuous signal is an integral pulse frequency modulation (IPFM) model. IPFM models allow for the translation of a continuous signal into a discrete series of events, conceptually similar to the behavior of a neuron (Bayly 1968). A continuous input signal $m(t)$ represents modulation of neural firing, such as is defined in Eq. 2.2 to represent modulation at the SA node. Then, the times of firings are found by repeatedly

integrating *m(t)* until a threshold Δ has been reached: $\int_{t_k}^{t_{k+1}} m(t)dt = \Delta$. Δ is set to 1 in all simulations performed here.

This produces a vector *t* with elements t_k to represent the *k*th discrete event. In our model of heartbeat generation, *m(t)* represents autonomic modulation of the heart and the discrete events produced through the IPFM model represent heartbeats initiated by the SA node (Chiu and Kao 2001; Brennan, Palaniswami et al. 2002). HR is modulated by shifting the mean value of *m(t)* up (increased HR) or down (decreased HR). And because of variations in autonomic activity, the output of the IPFM model (heartbeats) will contain some variability. There are two primary mechanisms by which HRV is modulated through this model. Most directly, changes in HRV are driven by variable amplitudes of the HF and LF oscillators in Eq. 2.2. When the amplitude of these oscillators decreases, *m(t)* becomes more and more flat until there is very little beat-to-beat variability. However, even with constant amplitudes for HF and LF, HRV can still change because RR intervals become shorter as the mean value of *m(t)* shifts up due to circadian influences from T_{sym} and T_{par},. Thus, the observed decrease in variability as assessed by HRV metrics is partially reflecting the changing mean value of heart rate (Niklasson, Wiklund et al. 1993). This initially may seem analogous to what is observed when sympathetic activity increases, such as in exercise where there seems to be an inverse relationship between HR and HRV (Javorka, Zila et al. 2002). However, looking at the raw HR data in these cases makes it clear that the amplitude of oscillations in HR is lost in concert with increased mean HR. Therefore, if the amplitude of these oscillations, and thus HRV, is to be

dynamic, it must be represented with a model that has the ability to alter the amplitude of oscillatory components, as in Eq. 2.2.

2.2.4: Calculation of HRV

A variety of HRV parameters are assessed, spanning the time domain (SDNN, the standard deviation of normal-to-normal heartbeat intervals), frequency domain (HF, LF, and associated measures), and nonlinear analysis (sample entropy). All parameters are calculated over epochs that are 5 minutes in length, as is typical in the analysis of HR data (Task 1996). Each of the i epochs of RR intervals is denoted by RR_i. The time domain measure, SDNN, is simply the standard deviation of interbeat intervals generated by the IPFM model, defined in Eq. 2.3.

$$SDNN_i = \text{stdev}(RR_i) \tag{2.3}$$

The frequency domain statistics are calculated from mean-subtracted RR interval sequences based on the output of MATLAB's pyulear function with an order of 12, which implements an autoregressive model using the Yule-Walker algorithm to estimate the power spectral density. Then, HF and LF values represent the area under the curve in linear units over the appropriate frequency ranges of 0.15-0.4 Hz and 0.04-0.15 Hz respectively. HF_n and LF_n are normalized values, defined as $HF_n=HF/(HF+LF)$ and $LF_n=LF/(HF+LF)$. The LF/HF ratio is also computed.

Sample entropy (*SampEn*) (Richman and Moorman 2000) is calculated using the implementation available on PhysioNet (http://www.physionet.org/physiotools/sampen/). *SampEn* is defined as the

negative natural logarithm of the estimated conditional probability that two subseries of *m* points that have all matched within a tolerance *r* continue to match within that tolerance at the next point. Therefore, a low value of *SampEn* means that the input series has a very regular structure, and high values correspond with high entropy, irregular signals.

2.2.5:Generation of Poincaré maps and their geometric properties

Poincaré maps of RR intervals are generated for the scenarios described above. These plots are derived from a time series of RR intervals by plotting each value RR(i) on the x-axis versus its successive value RR(i+1) on the y-axis. Thus, if the system generated two consecutive RR intervals that were identical, that point would lie directly on the 45° diagonal. Variability in the Poincaré map can be quantified by calculating the standard deviation along this diagonal line and perpendicular to the diagonal line. These values, called *SD1* and *SD2*, are visualized by plotting an ellipse whose axes are equal to *SD1* and *SD2*. *SD1* and *SD2* have been used to roughly represent short-term and long-term variability in HR due to their intuitive, geometric interpretations (Brennan, Palaniswami et al. 2001).

2.3: Results

Circadian and higher-frequency variability in autonomic modulation at the SA node is taken into account in Eq. 2.2, allowing for simulation of homeostasis and the biologically rhythms present in homeostasis. Based on this, Figure 2.3 shows the homeostatic model output. *m(t)* has a clear circadian

pattern in Figure 2.3A and also exhibits higher-frequency variability in Figure 2.3B. Both the mean value and the amplitude of variability of *m(t)* are under diurnal regulation. Circadian rhythms in HR (Figure 2.3C) and HRV as assessed by SampEn and SDNN (Figure 2.3D) are present in model output. HF and LF power, visualized on the power spectra in Figure 2.3E-F representing 00:00 and 12:00 respectively, also contain significant diurnal variability.

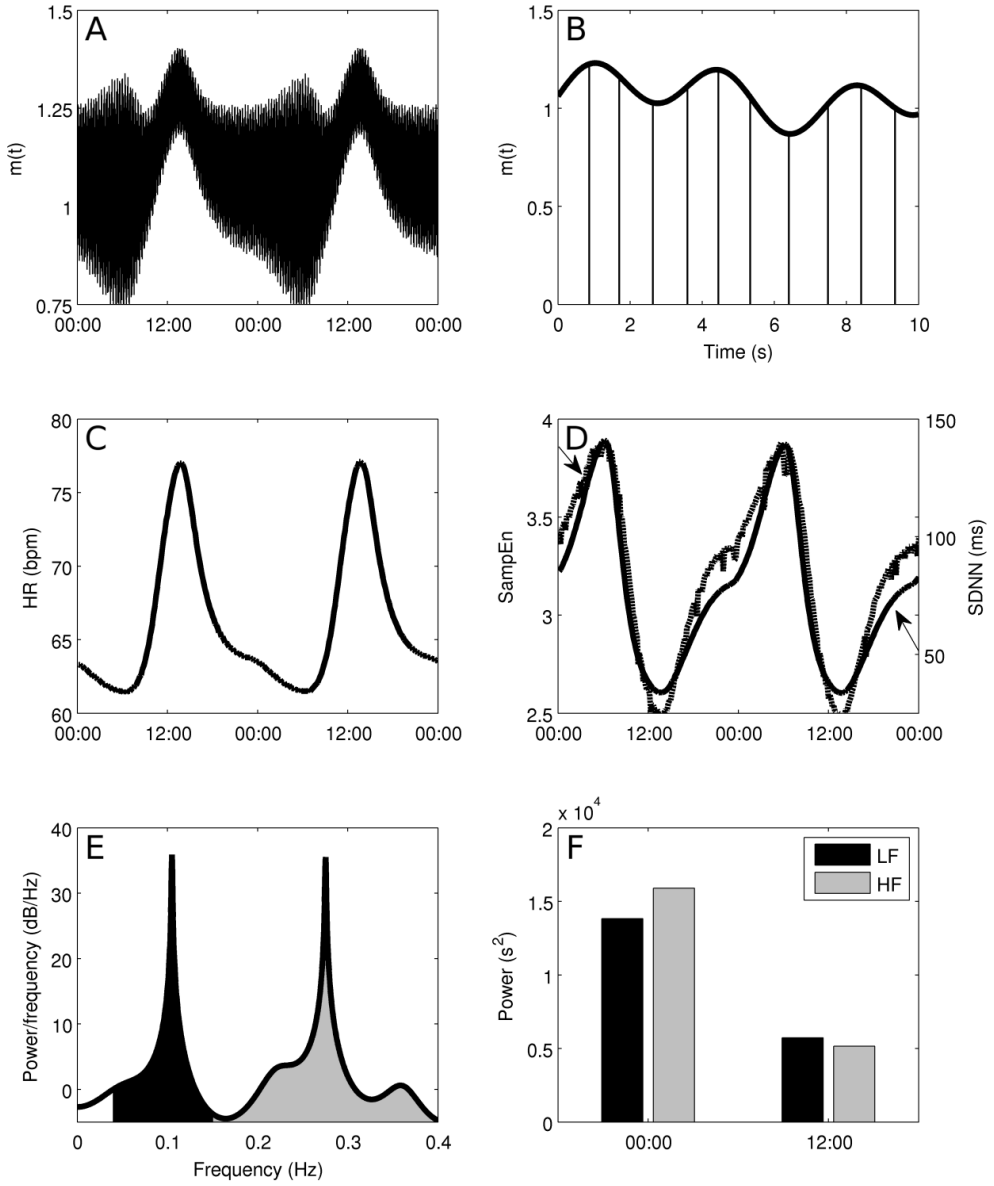

Figure 2.3: Autonomic modulation at the SA node of the heart, shown at two scales (A and B), leading to circadian rhythms in smoothed HR (C) and HRV (D), as assessed by time domain (SDNN, solid line) and nonlinear (SampEn, dashed line) metrics. E shows a power spectrum calculated from a 5 minute window of RR intervals at 12am. Two peaks, representing LF and HF oscillations, are present. LF and HF values are calculated as the area under this curve, 0.04-0.15 Hz for LF and 0.15-0.4 Hz for HF. F shows how that these HF and LF values undergo significant changes throughout the daily circadian cycle.

The addition of beat-to-beat variability in RR intervals permits the visualization of the RR interval time series via the Poincaré maps in Figure 2.4. Four maps are shown, evenly spaced throughout the day: 00:00, 06:00, 12:00, and 18:00. Inset in each figure is the state of T_{par} at the time when the map is generated. The ellipses have axes equal to the standard deviations of the points along the diagonal and perpendicular to the diagonal (Brennan, Palaniswami et al. 2001). The mean value of the RR interval (roughly the center of the mass of points) moves, illustrating long term variability due to circadian changes in the mean value of *m(t)*.

Local variability (roughly the spread of points) also undergoes significant changes throughout the day as shown in Figure 2.5 where the HF and LF values are plotted over time, exhibiting clear circadian patterns.

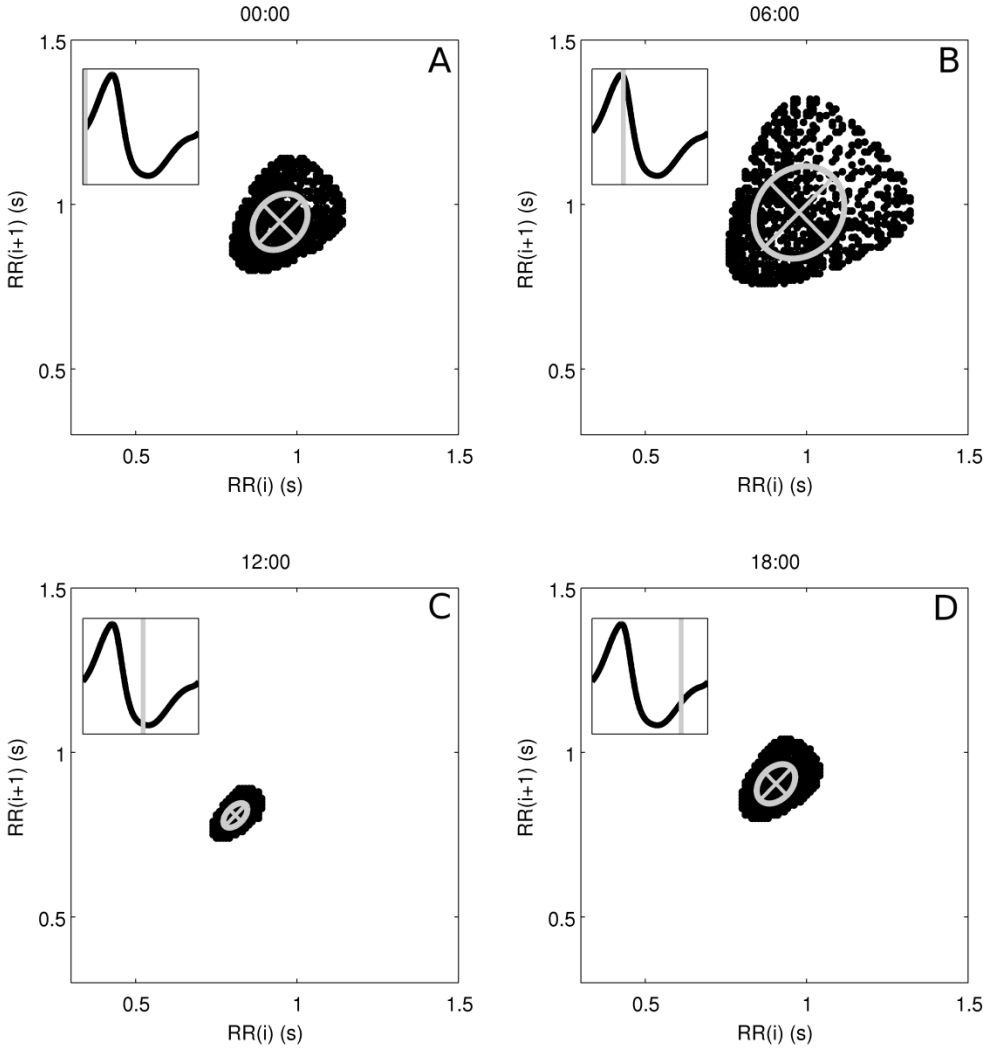

Figure 2. 4 : Poincaré maps of RR intervals in homeostasis, at 00:00 (A), 06:00 (B), 12:00 (C), and 18:00 (D). Inset in each figure is the circadian pattern of T_{par} and the region that was used to generate the Poincaré map. The ellipses represent the dispersion of points as the axes are equal to the standard deviation of points on each axis. The major and minor axes of the ellipses are drawn on the figure, representing the standard deviations along the y=x diagonal (SD1) and the y=-x diagonal (SD2). A large circadian pattern in the geometry of the Poincaré maps is observed, ranging from a maximum of (SD1, SD2) = (0.13, 0.15) in B to a minimum of (0.027, 0.046) in C.

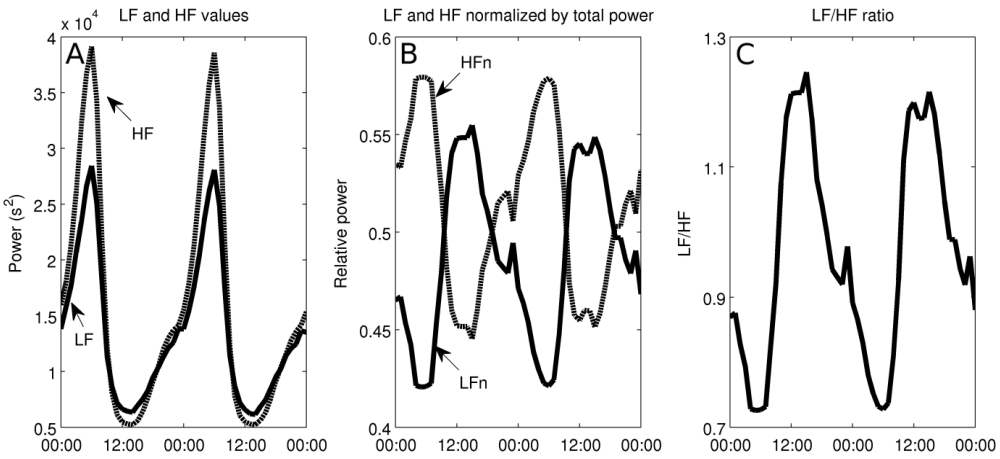

Figure 2.5: LF and HF values are calculated, as shown in Figure 2.3E, at many points throughout the simulation, and these values are plotted as functions of time. A: Circadian rhythms in LF and HF; B: normalized LF and HF (LFn=LF/(LF+HF), HFn=HF/(LF+HF)); and C: the LF/HF ratio. LF and HF are in phase, but their normalized values are out of phase.

An acute dose of LPS is given at 20:00, thus provoking a simulated systemic inflammatory response. As described in detail in Appendix A, LPS is recognized by TLR4 on immune cells and instigates a wide range of transcriptional responses, including those that lead to the release of pro-inflammatory cytokines. These cytokines serve as mediators in neuroendocrine-immune communication, leading to the central release of stress hormones such as cortisol and catecholamines. Figure 2.6 shows how this acute disturbance propagates through the system, from pro-inflammatory mediators to anti-inflammatory hormones, finally leading to an increase in T_{sym} and a decrease in T_{par}, which then provoke changes in cardiac dynamics in response to acute stress. In response to changes in T_{sym} and T_{par}, the autonomic modulation of the SA node, $m(t)$ as given in Eq. 2.2, is shifted up

and the amplitudes of its higher-frequency oscillatory components are diminished in Figure 2.6E.

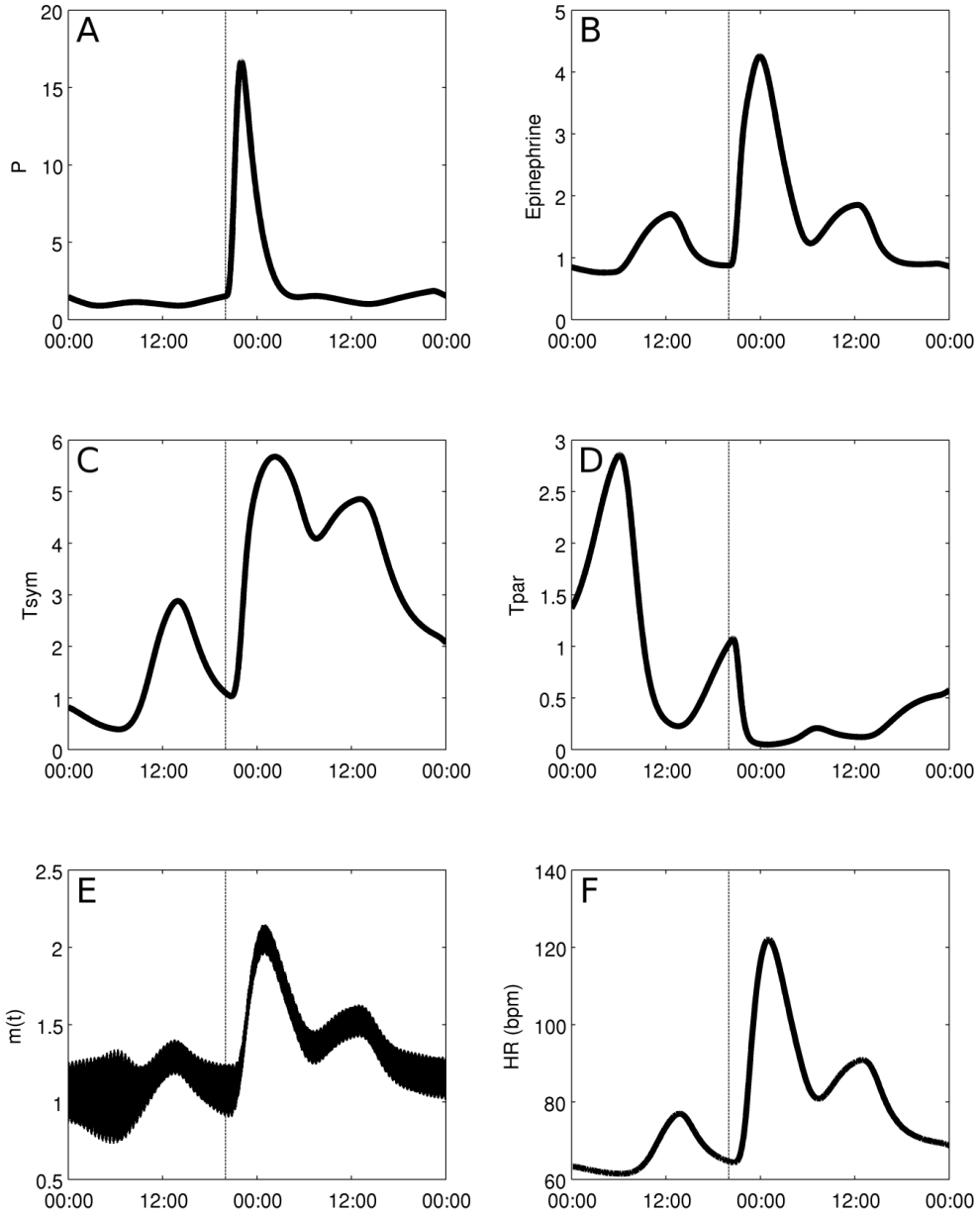

Figure 2 6: Response to a dose of LPS given at 20:00. Changes propagate through proinflammatory cytokines secreted by immune cells (A) to neuroendocrine-mediated effects (epinephrine release in B; autonomic activation in C and D) to the activity of the heart, reflected by changes in effective autonomic modulation (E) and HR (F).

Figure 2.7 shows how LF and HF both decrease while the LF/HF ratio increases, in agreement with experimental data (Godin, Fleisher et al. 1996; Jan, Coyle et al. 2009; Jan, Coyle et al. 2010). The Poincaré maps displayed in Figure 2.8 show a significant tightening that begins directly after LPS injection and reaches maximal tightening several hours later. Figure 2.7D shows the output of two HRV parameters, SDNN and SampEn. Both parameters capture the circadian pattern prior to LPS and both show an acute decrease after LPS treatment, but the decrease in SampEn is much larger than the decrease in SDNN relative to the normal circadian rhythms observed in each parameter. The above results concerning LPS all study the system response to a dose of LPS at the same time point. The computational model presented here allows for a more broad exploration of the circadian influence on the endotoxemia response, shown in Figure 2.9 where LPS is given at 5:00 and 12:00, illustrating the maximum differences in responses as quantified by HRV.

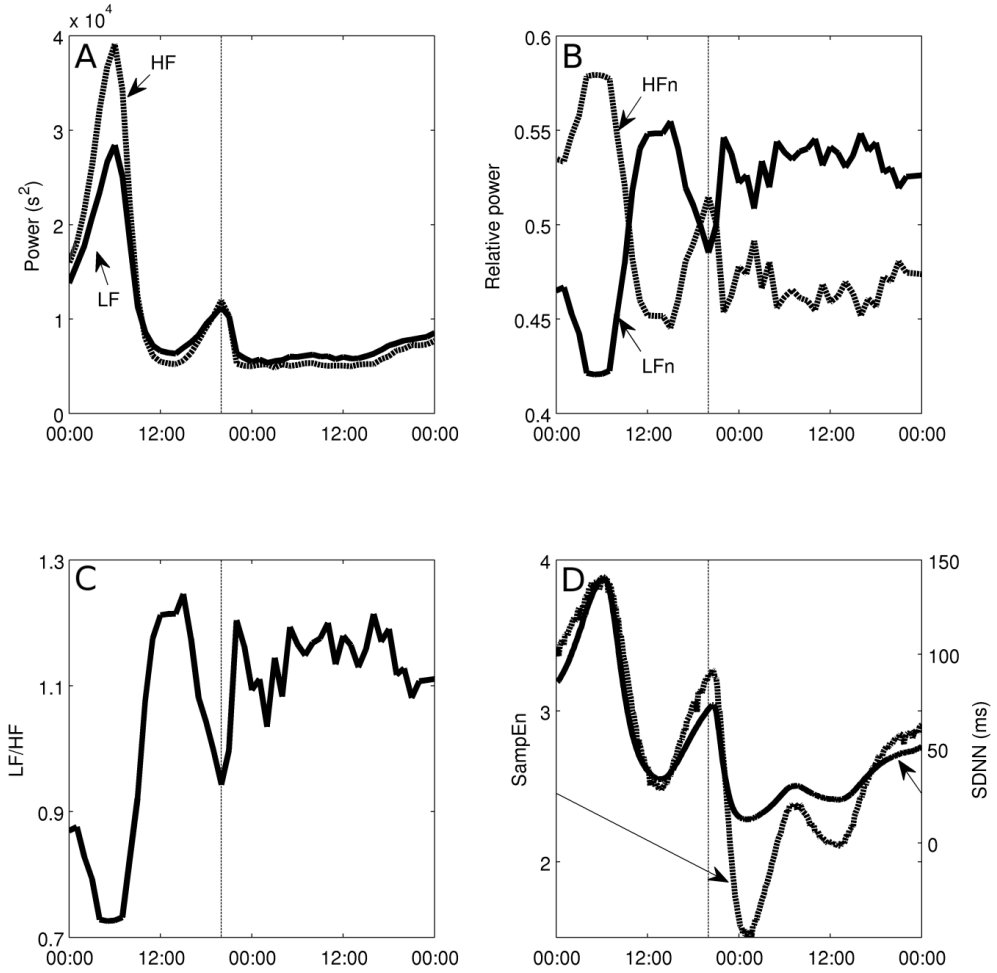

Figure 2.7: Changes in HRV in response to a dose of LPS given at 20:00. Both LF and HF are suppressed (A), but relative values (B) and the LF/HF ratio (C) show that HF is more strongly suppressed than LF. SampEn (dashed line) and SDNN (solid line) both decrease in response to LPS, but SampEn decreases more relative to the amplitude of its normal circadian rhythm.

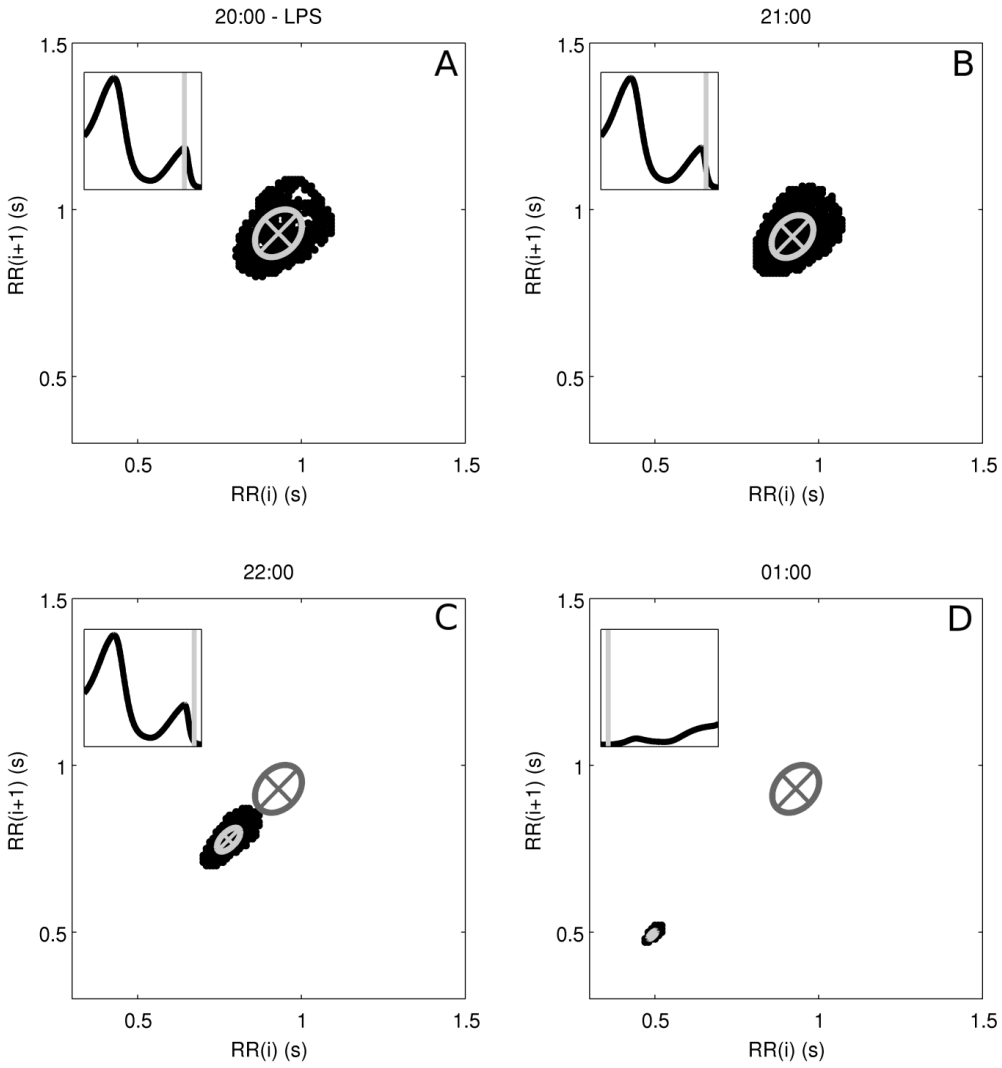

Figure 2.8: Poincaré maps showing the response to a dose of LPS at 20:00, showing maps at 20:00 (A), 21:00 (B), 22:00 (C), and 01:00 (D). Inset in each figure is the circadian pattern of T_{par} and the region that was used to generate the Poincaré map; in D, the next 24 hours are shown. After injection, the points on the map shift down and to the left, reflecting decreased RR intervals and decreased HR. The points also become more tightly distributed, illustrating the loss of HRV in endotoxemia. D shows the Poincaré map at 01:00, which is when HRV is most suppressed. The ellipses represent the dispersion of points as the axes are equal to the standard deviation of points on each axis. A change in the geometry of the Poincaré maps is observed, ranging from a maximum of (SD1, SD2) = (0.060, 0.082) at the time of injection in B to a minimum of (0.0060, 0.017) in C. The pre-LPS fitted ellipse from A is shown in C and D to illustrate the difference in both the mean and the distribution of points during the acute response.

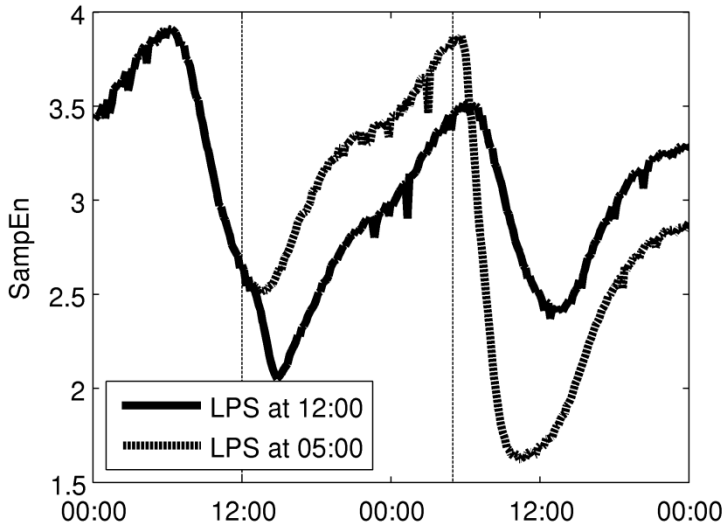

Figure 2. 9: There is a circadian dependence on the response of the model to a dose of LPS. The maximum difference is observed between LPS given at 5:00 and 12:00, HRV, as quantified by HRV.

To determine the model response to decoupling between the heart and the autonomic nervous system, the amplitude of HF and LF oscillations, k_{osc} in Eq. 2.2, is halved. Figure 2.10 shows how SDNN changes under these conditions by showing a 24-hour period of diminished k_{osc} in between one day on each side of normal conditions. The amplitude of circadian rhythms in SDNN and the magnitude of SDNN are both diminished in the decreased coupling region.

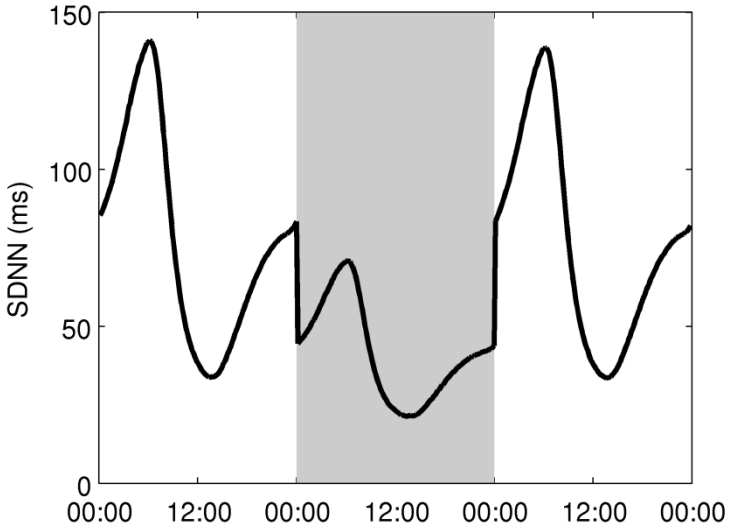

Figure 2.10: Decoupling between the autonomic nervous system and the heart is simulated by decreasing coupling by 50% during the shaded area in the figure. Both the amplitude of circadian rhythms and the magnitude of HRV (assessed by SDNN) are diminished.

2.4: Discussion

The components required to link neuroendocrine-immune interactions with circadian and higher-frequency autonomic variability in HR are combined through our proposed model (Eq. 2.2), which incorporates circadian control of cardiac function via autonomic activity along with HF and LF oscillations. While hormonal circadian rhythms alone produce circadian rhythms in model output, some higher frequency oscillations are required to produce the local variability that is observed in real heartbeat signals. HF and LF power is dependent on vagal signaling, and more specifically it is known that HF and LF are diminished under human endotoxemia (Godin, Fleisher et al. 1996; Jan, Coyle et al. 2009). Thus, Eq. 2.2 represents the dependence of HF and LF oscillatory amplitudes on T_{par}. Figure 2.3A displays a clear change in the shape of *m(t)* as the local oscillations have very different amplitudes

depending on the position in the circadian cycle. Power spectra, taken at 00:00 and 12:00 respectively which are close to times at which T_{par} is at its maximum and minimum values, processed to calculate the HF and LF values shown in Figure 2.3F LF and HF show a significant drop in the area under the curve of the power spectrum over those frequency ranges throughout the normal diurnal cycle. These HF and LF powers, calculated more frequently, are shown in Figure 2.5. Though raw LF and HF are in phase, HF is suppressed more strongly so that the normalized values LFn and HFn are actually out of phase (Godin, Fleisher et al. 1996; Jan, Coyle et al. 2009). A similar pattern is seen in Figure 2.7A-C after an acute dose of LPS. Both LF and HF decrease, but the decrease in HF is more profound, so that the LFn increases relative to HFn. Thus, the LF/HF ratio remains elevated throughout the recovery phase, illustrating continued imbalance between sympathetic and parasympathetic modulation at the SA node (Godin, Fleisher et al. 1996; Jan, Coyle et al. 2009).

In Figure 2.6 and Figure 2.7, changes in T_{sym}, T_{par}, and the HRV parameters are persistent for over 24 hours after an LPS injection while all other variables in the model recover to their baseline conditions within 24 hours. Run for a longer period of time, these model variables recover within a couple days. Despite this, HRV parameters do recover to within the normal range of circadian variability within 24 hours. In studies where LPS is given to humans and ECGs are recorded for 24 hours as the inflammatory response is initiated and then resolves in a self-limited response, HRV has generally been observed to recover within 24 hours post-injection (Alvarez, Katsamanis Karavidas et al. 2007).

The HF and LF sinusoids in Eq. 2.2 are assumed to mechanistically arise somewhere outside of the model. Biologically, LF and HF oscillations arise largely from vasomotor activity and respiration under control conditions, respectively (Lombardi, Malliani et al. 1996). As *m(t)* represents only the autonomic modulation specifically at the SA node of the heart, the transduction of the signals producing HF and LF oscillations to the heart must be considered. So, the terms that modulate the amplitude of these sinusoids based on the level of T_{par} represent the ability of the oscillatory signals to be reflected in neurotransmitter concentrations at the SA node, based on the observed relationship between vagal signaling and HF and LF components of HR. Vagal activity modulates LF and HF oscillations in HR and without this vagal activity, LF and HF responses are blunted (Karemaker 1999). In other words, the HF and LF peaks that appear in the power spectrum of HR depend on the autonomic nervous system to communicate these signals to the SA node. Thus, LF and HF give some indication as to the coupling between the heart and the autonomic nervous system, which is of particular interest as HR is relatively easy to assess noninvasively. Indeed, in endotoxemia, an increase in regularity is observed in HR, neutrophil function, and plasma cortisol levels (Rassias, Holzberger et al. 2005), in line with theoretical expectations of the response of decoupled biological systems (Pincus 1994) and the results shown in Figure 2.10 where variability is lost under decoupling. Although these results show an instant decoupling rather than a gradual process as likely occurs *in vivo*, decoupling may be important in adverse conditions such as endotoxemia when interorgan communication is diminished (Godin and Buchman 1996; Godin, Fleisher et al. 1996). Clinically, assessing the

interorgan communication by means such as evaluating HF and LF is critical to understanding and assessing the extent of injury in multiple organ dysfunction syndrome (MODS) and sepsis (Schmidt, Müller-Werdan et al. 2007). HF and LF most directly measure cardiac-autonomic coupling, but they can also be used as accessible proxies for measuring general interorgan communication (Schmidt, Müller-Werdan et al. 2007). In addition, drugs that normally alter heart rate by autonomic modulation fail to have an effect in endotoxemia (Sayk, Vietheer et al. 2008). Thus, the effect of endotoxemia on the heart can be viewed as a decoupling between the autonomic nervous system and the SA node. This decoupling represents a potential mechanism for the observed decreased complexity and increased regularity in physiological signals (Pincus 1994; Buchman 1996). The recovery of HRV following injury can then be viewed as a recoupling of autonomic and cardiac systems, and more generally a recoupling of organ systems in the recovery phase. The model presented here begins to decipher the nature of this relationship through the variable *m(t)* which represents the communication link between the autonomic nervous system and the heart.

One of the fundamental contributions of the described modeling work is the incorporation of circadian rhythms in both HR and HRV parameters. This is of particular interest due to the loss of circadian rhythms observed in inflammation (Lowry 2009) and the interplay between inflammatory mediators and molecular circadian machinery both centrally in the suprachiasmatic nucleus (SCN) and in peripheral tissues (Haimovich, Calvano et al. 2010; Scheff, Calvano et al. 2010). The circadian dependence of this model is shown in Figure 2.9 where identical doses of LPS are given at two

different times, 0:500 and 12:00. These two times produce a maximal difference in responses, as the diurnal peak in cortisol occurs between these time points, and this primes the system for a robust anti-inflammatory response. Thus, before this hormonal priming occurs, a significantly larger decrease in HRV (quantified by SampEn) is observed. However, in both cases, the overall dynamics of the system (an acute response and recovery to baseline) are similar. These computational results match with clinical observations that sepsis patients are at elevated risk of mortality from 02:00 to 06:00, before the circadian peak in cortisol secretion (Hrushesky, Langevin et al. 1994). Considering this type of circadian dependence on responses to pathogens, and also to therapies, is important in optimizing treatment of inflammatory disease (Hrushesky and Wood 1997). In Figure 2.6, circadian rhythms in cardiac function are blunted in response to a dose of LPS as the LPS-induced acute increase in T_{sym} and acute decrease in T_{par} overwhelm the normal diurnal pattern of those variables. In Figure 2.7A, the decrease in both LF and HF in response to endotoxemia is only slightly larger than the physiologic changes in LF and HF due to circadian rhythms. This is because, in the model, T_{par} is predicted to pass relatively close to zero in its diurnal cycle, so in endotoxemia, there is not much further for it to fall. While this result may seem unintuitive, it matches with experimental results showing that the drop from maximum to minimum values during circadian rhythms in HF and LF (Huikuri, Niemela et al. 1994; Korpelainen, Sotaniemi et al. 1997; Nakagawa, Iwao et al. 1998) and the depression in HF and LF due to endotoxemia (Godin, Fleisher et al. 1996; Jan, Coyle et al. 2009; Jan, Coyle et al. 2010) can both be anywhere from 50% to 90% depending on experimental

protocol. However, by looking at Poincaré maps (compare Figure 2.4 and Figure 2.8) or by assessing HRV by other metrics such as SDNN and SampEn as in Figure 2.7D, it is clear that there is a significant increase in regularity in response to LPS that is fundamentally different than what is observed in normal circadian patterns. This illustrates the importance of assessing multiple variability/regularity metrics to tease out subtle patterns in HR data.

An advantage of the model presented here, relative to a continuous physicochemical model of either HR or HRV, is that it produces discrete beats as output. This allows both HR and HRV to be derived from a single variable signal, as they are experimentally, and it allows for comparison of the performance of HRV metrics. Figure 2.7D is provocative in this regard as it shows SDNN and SampEn, two common HRV parameters, both are able to capture normal circadian dynamics as well as the acute response to LPS; however, when their axes are aligned such as in Figure 2.7D so that the amplitude of circadian rhythms is equal for both parameters, it is clear that SampEn is much more significantly suppressed in endotoxemia. Thus, by taking a more mechanistic approach that models heartbeats rather than attempting to directly estimate changes in HRV, these types of quantitative differences can be discovered.

The representation of neurotransmitter concentration at the SA node (Foteinou, Calvano et al. 2011) is conceptually based on the Warner model (Warner and Cox 1962) of sympathetic and vagal influences of HR. A similar idea is explored in the work of Chiu and Kao (Chiu and Kao 2001) in which an IPFM model is modulated by the vagal and sympathetic outputs of the Warner model. The work presented in this paper goes a step further by

ultimately linking the model of autonomic modulation at the SA node with a larger, well-established model of human endotoxemia to explore changes in cardiac output specifically within this context. This introduces some additional complexity into *m(t)* since the amplitude of HF and LF oscillations depend on a nonlinear model, and also circadian influences are directly incorporated through T_{sym} and T_{par}. In general, one cannot assume that this type of multimodal input signal will be effectively transduced through an IPFM model without the addition of significant distortion (Nakao, Norimatsu et al. 1997). However, the power spectra in Figure 2.3 clearly show that the HF and LF frequency components are strongly present in the short-term variability of IPFM-generated HR.

By linking cardiac dynamics with a detailed model of the inflammatory response, we have begun to explore the mechanistic underpinnings that may underlie the relationship between autonomic dysfunction and modulated HR and HRV in endotoxemia, and by extension, possible decoupling among other organ systems. The mechanism-based approach (Vodovotz, Constantine et al. 2009) of the endotoxemia model allows for the future investigation of the relationship between neuroendocrine-immune state and cardiac function. This linking of processes at the molecular and cellular level with outcomes at the systemic level (namely clinically accessible variables such as HR and HRV) is an important step towards developing translational applications of systems biology.

Chapter 3: System biology of circadian-immune interaction

Variations at the beating of the heart and the subsequent HRV, represent critical manifestations of physiologic variability. In order to gain insight into the dynamics driving systemic variability and particularly circadian variability at the inflammatory response, in this chapter we examine the molecular mechanisms driving circadian oscillations at the cell level and explore the flow of circadian information from the environmental light/dark cycles ultimately to circadian variation of inflammatory parameters by also putting weight into the mathematical modeling approaches that have been used in order to explore these networks.

3.1: Introduction

In order to cope with environmental challenges and optimize biological fitness, organisms adopt rhythmic variations in their physiological functions. In mammals, this intrinsic timing system is organized in a hierarchical manner where a light sensitive master pacemaker synchronizes a bodywide web of cell autonomous and self-sustained subsidiary clocks that are present in nearly every tissue of the body. The focal point of this system which is commonly referred as the master clock is located in the suprachiasmatic nuclei (SCN) of the anterior hypothalamus of the brain. SCN neurons translate the photic signal of daily cycles to chemical information by altering the expression of various genes. Although SCN neurons adopt oscillatory behavior even in *in vitro* conditions independent of any external cues, the exogenous input of

light-dark information ensures its synchronization to a 24 hour period. Similar behavior is observed in peripheral clocks which, in the absence of an entrainer, oscillate freely while falling out of sync, yet are synchronized *in vivo* by periodic physiological cues. Therefore, even considering the interactions between the central and peripheral clocks in isolation, requires a systems-level approach in order to gain understanding of the internal properties of the network. Obtaining fundamental and useful knowledge about these systems is even more difficult when one considers that the physiological systems regulated by circadian clocks also have their own complex internal dynamics.

One reason that understanding circadian rhythms is important is because they are associated with disease. Environmental desynchronization either by external stressors (e.g. shift work and jet lag) or by other genetic disorders may lead to vulnerabilities to infection and disease both in humans and in rodents. Abolishing master's clock rhythmicity in mice by surgical ablation of the SCN seriously alters the daily rhythms of corticosterone, disturbs the rest-activity cycles, and ultimately leads to accelerated tumor growth. Furthermore, the LPS-induced inflammatory response is magnified in jet-lagged mice relative to control animals, further leading to hypothermia and death after a certain period of time (Castanon-Cervantes, Wu et al. 2010). On the other hand, disease itself can impact circadian rhythmicity. In particular, current experimental data show that systemic inflammatory diseases are associated with blunted rhythmicity of numerous intrinsic signals. For instance, sepsis has been associated with loss of diurnal rhythms of leptin and cortisol (Bornstein, Licinio et al. 1998), and circadian rhythmicity of cortisol has been

shown to be prognostic of longer survival in patients with metastatic breast cancer (Sephton, Sapolsky et al. 2000).

The intersection between circadian rhythms and the inflammatory response, both governed by complex signaling networks, truly necessitates systems biology-based investigation if we are to understand the relationships between these systems and leverage this knowledge towards practical ends. This requires both experimental and computational approaches aimed at understanding circadian rhythms, inflammation, and their interactions. In this review, we discuss knowledge acquired in recent years relative to the bidirectional links between circadian and immune response and the occasions where their rhythmic orchestration is disrupted, as well as current knowledge relative to the reprogramming of endogenous rhythms. We present system biology approaches that have been leveraged in order to gain insight in these networks.

3.2: Mechanistic insight to circadian entrainment of central and peripheral clocks

The core clock elements that give rise to circadian timekeeping in mammalian SCN and found in most, if not all peripheral cells, are a group of so-called clock genes. Mouse SCN involves three period genes (*Per1*, *Per2*, and *Per3*), two cryptochrome genes (*Cry1* and *Cry2*), two basic helix-loop-helix transcription factors (CLOCK and BMAL1), and two orphan nuclear hormone receptors (REV-ERBα and RORα). Negative and positive feedback interactions among these clock genes lead to transcriptional oscillations that retain an approximate 24-h periodicity independent of any external entrainer.

In order to stay in harmony with environmental changes, clock gene oscillations must be corrected on a daily basis by entraining signals. As such, SCN neurons after receiving the environmental input from light/dark cycles, deliver photic information to the periphery of the body via direct routes such as the circadian secretion of hormones and the neuronal activity of the autonomic nervous system, and indirect routes such as the daily rest/activity cycles that further control the feeding time. This network of interactions among SCN and peripheral tissues reveals a nested level of biological organization where circadian information is retained in various levels of mammalian physiology from rhythmic patterns of clock gene expression to behavioral rhythms of sleep/wake cycles. Systemic integrity is largely dependent on the coherent function of the sub-systems composing the network. Their circadian rhythmicity is further related to the integrity of humoral and neuronal entraining signals, further underscoring the need of a system-level approach in order understand the underlying properties and design principles.

Quantitative mathematical models have been applied to gain mechanistic insights into clock gene network function (Leloup and Goldbeter 2003; Becker-Weimann, Wolf et al. 2004; Gallego, Eide et al. 2006; Mirsky, Liu et al. 2009; Westermark, Welsh et al. 2009; Relogio, Westermark et al. 2011) (Table 3.1). Among them, Becker-Weinmann *et al.* using a reduced model to simulate clock genes network, denoted that the negative feedback loop among *Per* and *Cry* genes is critically important for the maintenance of clock gene oscillations. They showed that even if the positive feedback loop among *Bmal*, *Ror* and *Rev-erbα* genes is substituted by a constantly expressed activator,

oscillations can still occur. These modeling results were supported by the experimental evidence showing that *Rev-erbα* $^{-/-}$ mutant mice have rhythmic behavior even though their positive feedback mechanism is not functional. More recently, Mirsky *et al.* used a detailed model to predict the phenotype of 7 knockout and 2 double knockout mutations as well as concentration variations in clock genes in the respective scenarios. However, as it was noted in the work of Mirsky *et al.*, in order to describe phenotypes observed in tissue or organ levels, additional dynamics such as entrainment and synchronization must be taken into consideration.

Recently, the mechanism of peripheral entrainment by systemic cues has been further elucidated. Single cell experiments of Nagoshi *et al.* in rat and mouse fibroblasts showed that single peripheral cells even in *in vitro* conditions independent of any entraining cue retain robust rhythmicity similar to SCN cells (Nagoshi, Saini et al. 2004). As a result, the dampening rhythms they observed *in vitro* at the population level emerge from robust single cell oscillations that fall out of phase and desynchronize in the absence of an entraining force. Based on this, in the following Chapter 4 we study the synchronization properties of cortisol in a population of peripheral clock genes. Furthermore, Abraham *et al.* showed that the oscillator qualities that greatly determine entrainment efficiency, are the ratio between entrainer coupling strength and oscillator amplitude, and the rigidity of the oscillatory system as defined by the relaxation rate upon perturbation (Abraham, Granada et al. 2010) (Table 3.1). This result can explain the evidence that peripheral tissues such as lung, can be entrained by a wider range of entrainer's

frequencies whereas SCN do not, since SCN neurons due to their intercellular coupling retain characteristics of rigid oscillators.

Additionally, there has been a lot of interest relative to entrainment of central and peripheral clocks and several mathematical models have been constructed in order to characterize their underline dynamics (Antle, Foley et al. 2003; Geier, Becker-Weimann et al. 2005; Gonze, Bernard et al. 2005; Antle, Foley et al. 2007; Bernard, Gonze et al. 2007; Abraham, Granada et al. 2010) (Table 3.1). In particular, Abraham *et al.* showed that the oscillator qualities that greatly determine entrainment efficiency, are the ratio between entrainer coupling strength and oscillator amplitude, and the rigidity of the oscillatory system as defined by the relaxation rate upon perturbation (Abraham, Granada et al. 2010) (Table 1). This result can explain the evidence that peripheral tissues such as lung, retain significantly different entrainment characteristics than the SCN since SCN neurons due to their intercellular coupling retain characteristics of rigid oscillatory dynamics.

Deciphering entrainment dynamics of peripheral cells is very important since several genes that are critically involved in the immune function are regulated by peripheral clock genes. These genes are commonly referred as clock controlled genes (CCGs). Transcription factors such as signal transducer and activator of transcription 3 and 5 (STAT3 and STAT5), as well as nuclear factor kappa B (NF-κB) are directly regulated by the molecular clock and exhibit circadian rhythmicity in humans and rodents. Further, these transcription factors participate in cytokine signaling pathways and as such they indirectly regulate innate and adaptive immune responses. As a result, a robust circadian signal of clock genes implies the efficient delivery of

circadian information to the immune response of the body. In addition, circadian information through metabolic, neuronal, and humoral entraining signals reaches organs of the immune system such as lymph nodes and spleen. Outputs of this entrainment among others are the rhythmic variation of critical immune components such as natural killer cell (NK) levels, and cytokine expression that ultimately control critical immune responses such NK cytotoxicity, phagocytosis, and the inflammatory response (Arjona and Sarkar 2008). On the other hand, the temporal variations of immune mediators tune the central clock by affecting critical behavioral rhythms such as sleep/wake patterns forming a feedback interaction between circadian and immune systems.

3.3: Bidirectional communication between circadian clock and immune system

The complexity inherent in both the inflammatory response and the hierarchical system of circadian clocks necessitates a systems biology view to study how these systems interact. One useful experimental technique to study systemic inflammation is the human endotoxemia model that we have extensively discussed in Chapter 1 and Chapter 2. Furthermore, circadian properties of the endotoxemia response have been studied both experimentally (Haimovich, Calvano et al. 2010) and computationally (Scheff, Calvano et al. 2010).

3.3.1: Neuro-endocrine and autonomic circadian regulation of the immune response

The master clock in the SCN governs the central release of circadian hormones and signals which travel throughout the body and entrain the peripheral oscillators to a consistent phase. Interestingly, as summarized in Figure 3.1, many of these circadian signal transduction mediators also play roles in regulating the immune response, such as cortisol, melatonin, and the autonomic nervous system.

One of the direct routes through which the central clock entrains peripheral tissues is by the production of glucocorticoids (cortisol, in humans) in the adrenal gland. Further details about this pathway are given in Chapter 4. The circadian secretion of melatonin may also regulate the expression of immune mediators such as cytokines. The primary mechanism of melatonin production is by the pineal gland of the brain, which is tightly regulated by the SCN. In addition to operating as a circadian entraining hormone, melatonin conveys a significant immunomodulatory effect. For instance, the peak of melatonin circadian rhythm at night has been correlated with the nocturnal rise of blood T lymphocytes. Pinealectomy on the other hand, is followed by an overall immunosuppression, likely mediated by the reduction in lymphocytes and other cytokines such as IL-2, IL-12, and TNF-α that naturally assist the host to mount humoral responses (Reiter 1993). Furthermore, in murine bone marrow cells, administration of melatonin appears to induce immunity by inhibiting apoptosis during early B cell development (Logan and Sarkar 2012). Melatonin plays also a role in the development and growth of cancer since its

production is correlated both with a reduction of IL-10 anti-inflammatory cytokine that has cancer growth promoting-activity and with an increase of human monocytes to produce IL-6 cytokine that has cancer-stimulatory activity.

The autonomic nervous system, through both its sympathetic and parasympathetic efferent arms, also conveys circadian information to the immune system. Light/dark information reaches autonomic system through inhibitory and excitatory inputs from the SCN to the paraventricular nucleus (PVN) that control pre-autonomic neurons and ultimately regulate sympathetic and parasympathetic activity. Autonomic activity is then mediated to the periphery of the body through autonomic innervation of various peripheral organs. The adrenal and pineal glands are innervated by autonomic projections and as such there is an indirect autonomic regulation of immunity embedded in the secretion of cortisol and melatonin respectively. Additionally, primary and secondary lymphoid organs such as the spleen, and liver receive extensive autonomic input. Upon stimulation, sympathetic nerve terminals in the spleen secrete norepinephrine (NE) that ultimately mediates activity of NK cells, and macrophages. It has been recently shown that the NE input to the spleen retains diurnal rhythmicity further illustrating the role of autonomic nervous system as a conveyor of photic information (Logan and Sarkar 2012). Interestingly, in the same experiment, sympathetic denervation disrupted the diurnal variations of splenocyte cytokines and NK cells. Similarly, hepatic NK cells are also regulated by the circadian sympathetic input of the liver. The autonomic nervous system also mediates immunomodulatory effects by the cholinergic anti-inflammatory pathway through the release of acetylcholine

(ACh) from reticuloendothelial organs such as the spleen, liver, and heart that further interact with ACh receptors on tissues macrophages and ultimately inhibit the release of TNF, IL-1, and other cytokines (Tracey 2002). This, combined with the autonomic innervation of critical lymphoid and reticuloendothelial organs, allows for autonomic regulation of the inflammatory response.

These and other centrally-mediated dual circadian and inflammatory signals, impose a circadian character on the inflammatory response. Blood stimulated *ex vivo* with LPS at different times throughout the circadian cycle, results in significant circadian rhythms in the peak responsiveness of cytokines. *In vivo* human endotoxemia experiments showed that, when LPS is injected into healthy volunteers in the evening (when cortisol levels are low) versus in the morning (when cortisol levels are high), there is a significantly larger increase cortisol levels as well as in body temperature (Pollmacher, Mullington et al. 1996).

Herman *et al.* developed a mathematical model to evaluate the neuroendocrine-immune system interactions specifically in the context of rheumatoid arthritis (Meyer-Hermann, Figge et al. 2009) (Table 3.1). This model describes mainly the measured circadian responses of plasma levels of TNF, noradrenaline (NA), and cortisol, making use of a set of ordinary differential equations. The model was calibrated with experimental data of healthy subjects and rheumatoid arthritis (RA) patients. Importantly, they predicted through mathematical modeling that treatment with glucocorticoids between 00:00 and 02:00 am induced the strongest inhibitory effect on TNF secretion. In chronic inflammatory diseases such as RA where patients are

characterized by an overexpressed inflammatory response, reduce of pro-inflammatory mediators such as TNF is often a clinical target. Similary, Scheff *et al.* incorporated a mutli-level mathematical modeling scope based on which evaluated the interplay between inflammation and circadian rhythms (Scheff, Calvano et al. 2010) (Table 3.1). This model predicted that LPS administration during the night induces larger increases in inflammatory mediators and larger reductions in the heart rate variability (HRV) relative to administration in the morning. The modeling results of Scheff *et al.* lie in accordance with experimental data showing that septic patients have a significantly increased risk of mortality at night (Hrushesky and Wood 1997). Extension of this model which was also discussed in Chapter 2, further incorporated a mathematical description of the sympathovagal signals that give rise to heart beats and ultimately to heart rate variability (Scheff, Mavroudis et al. 2011) (Table 3.1), allowed for further investigation of the mechanistic underpinnings of the inflammatory response that ultimately lead to changes in HRV. The importance of this model lies in the fact that it incorporates a semi-mechanistic based representation of circadian heart rate dynamics that includes their derivation from cellular, molecular, and neural signals enabling the evaluation of multiple *in silico* scenarios relative to physiology underpinning changes in HRV.

3.3.2: Immune mediators regulate circadian clock

Just as the mechanisms described above convey circadian information to the immune system, mediators produced in the inflammatory response can in turn modulate the function of circadian clocks. It is well established *in vitro* that LPS-induced responses can exert significant effects on the circadian clock

mechanism. Administration of LPS to SCN slices increases the secretion of arginine-vasopressin (AVP) neuropeptide. Originally, the rhythmic expression of AVP is directly regulated by SCN (Nava, Carta et al. 2000). This suggests that the neuroendocrine output of SCN can be also modified by immune challenge and ultimately influence the behavioral rhythms of the host. In accordance with this, Marpegan *et al.* showed that intraperitoneal injection of LPS in mice induced phase delays to their locomotor activity (Marpegan, Leone et al. 2009). These phase shifts to rodent's activity were present only if LPS was administered specific times of day illustrating a time of day dependency of inflammatory outcome. As it can be implied by the experiment of Marpegan *et al.*, inflammatory stimulus even at the periphery of the body can trigger alteration in the circadian clock of the organism. In particular, Okada *et al.* showed that intravenous injection of LPS to rats results in significant suppression of the clock gene *Per2* and the clock-controlled gene *Dbp* in the SCN underlining a direct effect of a peripheral inflammatory stimulus on the central circadian clock of the body (Okada, Yano et al. 2008).

It is likely that the precise mechanism through which LPS mediates its downstream effects on the SCN and peripheral tissues involves cytokines which are released in response to inflammatory stimuli (Figure 3.1). Relative to the interactions of cytokines and the central clock, Kwak *et al.* found that long term treatment of rat SCN cultures with interferon gamma (IFN-γ) blunts the diurnal rhythmicity of *Per1* even at the level of single cells (Kwak, Lundkvist et al. 2008). Similarly, a cocktail of TNF-α, LPS and IFN-γ caused a decrease in the SCN neuronal firing rhythmicity. Beynon *et al.* further showed that in rodent's SCN, the interleukin-1β (IL-1β) proinflammatory

cytokine receptor (IL-1R1) is rhythmically expressed. In addition, a peripheral immune challenge by a large dose of LPS significantly up-regulated IL-1R1 along with critical components of IL-1β signaling pathway such as c-Fos and p65-NF-κB (Beynon and Coogan 2010). This suggests that the central clock is directly sensitive to immune challenge from peripheral tissues. Numerous experiments have shown that the brain receives inflammatory signals from the periphery of the body in response to injury/infection. This signaling has been implicated to exacerbate sickness, develop symptoms like depression, and impair numerous diurnal rhythms such as temperature and melatonin.

As it is the case for LPS, cytokines cause also alterations in the peripheral clock function. Treatment of human hepatocytes with IFN-α induces a downregulation in the expression of *CLOCK* and *BMAL1* genes in a STAT1 transcription factor dependent manner (Koyanagi and Ohdo 2002). Furthermore, through both *in vitro* and *in vivo* studies, Cavadini *et al.* showed that TNF-α and Il-1β downregulated the expression of mouse *Per1-3,* and *Dbp* (Cavadini, Petrzilka et al. 2007), clearly illustrating that also the output of the clock network is regulated by the cytokine signaling. However, our current mechanistic understanding of these interactions is not sufficient to explain the temporal dynamics observed in endotoxemia experiments, suggesting that there are likely more undiscovered links between circadian rhythms and the inflammatory response (Haimovich, Calvano et al. 2010).

The extent by which LPS injection modulates the central clock *in vivo* in humans is still a topic of debate. An endotoxemia study done in humans (Haimovich, Calvano et al. 2010) found that melatonin levels, a proxy for the function of the circadian clock, did not change in response to endotoxemia.

However, unlike the rat endotoxemia study which directly analyzed gene expression in the SCN, transcriptional analysis was only done in peripheral blood leukocytes, which exhibited similar regulation of clock genes. Thus, it could be that like the effect of feeding on the central clock but unlike the effect of light, endotoxemia primarily effects peripheral clock function. Further studies, including injections at more time points, will be required to further investigate the issue of central clock regulation by LPS, but it is clear that peripheral circadian clocks can be significantly perturbed in endotoxemia. This could indicate a loss of coupling between the central and peripheral clocks under stress.

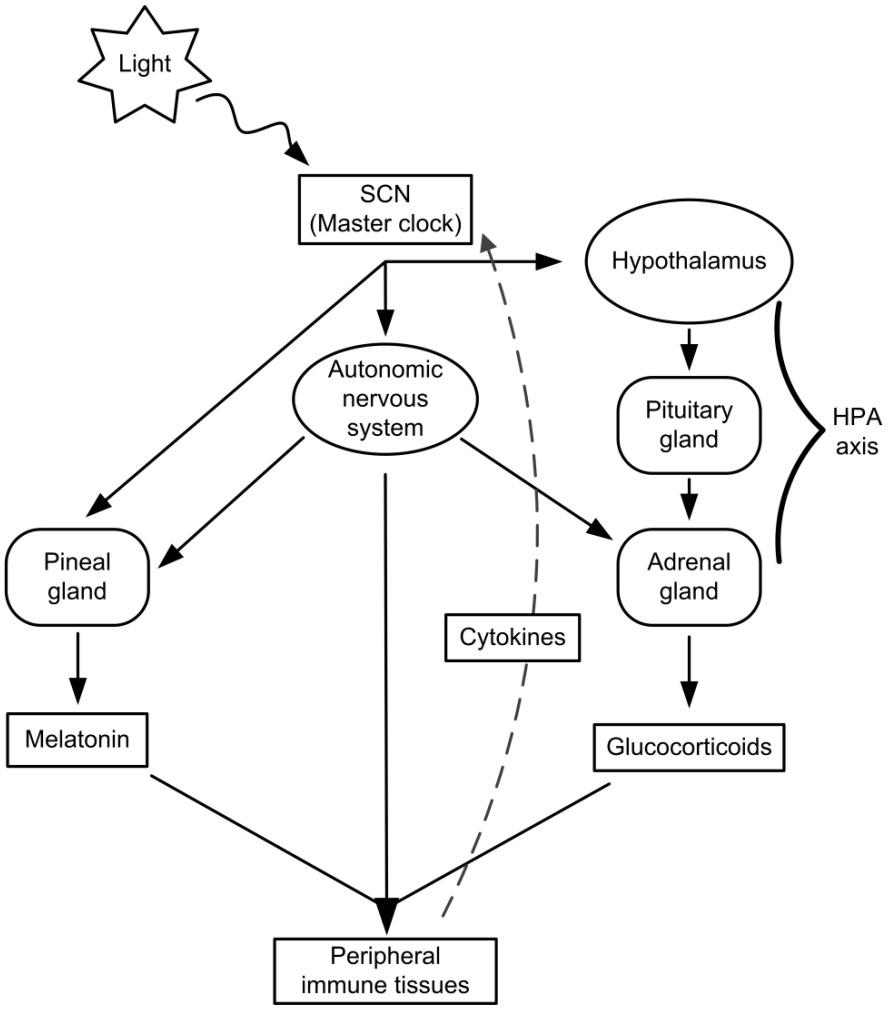

Figure 3. 1: Schematic review of some components of the bidirectional communication between circadian clocks and inflammatory mediators.

Table 3. 1: Mathematical models relative to clock gene, entrainment of clock gene, and immune/clock dynamics. ODE=Ordinary Differential Equations, SDE=Stochastic Differential Equations.

Author / Ref.	**Dynamics of interest**	**Mathematical formulation**	**Findings**
Leloup and Golbeter / (Leloup and Goldbeter 2003)		ODE	Autonomous oscillations with adverse phase of *Per* and *Bmal1* mRNAs in dark period.
		ODE	Predicts phenotypes of 7

Misrky *et al.* / (Mirsky, Liu et al. 2009)			single knockouts and 2 double knockout mutations of clock genes.
Relogio *et al.* / (Relogio, Westermark et al. 2011)		ODE	Dependence of clock gene periodicity on *Per* mRNA degradation rate.
Weinmann *et al.* / (Becker-Weimann, Wolf et al. 2004)		ODE	Retaining of clock gene oscillatory behavior even when the positive feedback is replaced by a constant term (Rev-Erbα mutant).
Gallego *et al.* / (Gallego, Eide et al. 2006)		ODE	The casein kinase mutant (CKI_{ε}^{tau}) increases kinase activity.
Westermark *et al.* / (Westermark, Welsh et al. 2009)		SDE	Predicts that robust oscillations in peripheral cells found experimentally may be in reality damped oscillations driven by noise.
Abraham *et al.* / (Abraham, Granada et al. 2010)		ODE	Entrainment is regulated by i) the ratio between entrainment strength and oscillator amplitude ii) the rigidity of the oscillatory system.
Antle *et al.* / (Antle, Foley et al. 2003)		ODE	Rhythmic regulation in region of SCN involves arrhythmic (gate) and oscillatory cells.
Antle *et al.* / (Antle, Foley et al. 2007)		ODE	Reveals that the previous model

			(Antle, Foley et al. 2003) can be entrained by a circadian input and maintain phase response curve (PRC) similar to what observed experimentally.
Bernard *et al.* / (Bernard, Gonze et al. 2007)	Entrainment of clock gene dynamics	ODE	The number of oscillators and their connectivity are important for synchronization dynamics as well as their periodic behavior.
Geier *et al.* / (Geier, Becker-Weimann et al. 2005)		ODE	Importance of PRC shape for entrainment dynamics.
Gonze *et al.* / (Gonze, Bernard et al. 2005)		ODE	Efficient synchronization of SCN cells is achieved when intracellular coupling dampens the individual cell oscillations.
Mavroudis *et al.* /(Mavroudis, Scheff et al. 2012)		SDE	Cortisol synchronizes peripheral clock genes in an amplitude and frequency dependent manner.
Meyer-Hermann *et al.* / (Meyer-Hermann, Figge et al. 2009)	Immune/clock dynamics	ODE	Treatment with glucocorticoids between 00:00 and 02:00 am was found to have the strongest inhibitory effect on TNF secretion
Scheff *et al.* / (Scheff, Calvano et al. 2010)		ODE	LPS administration at night induces higher reductions in

			HRV
Scheff *et al.* / (Scheff, Mavroudis et al. 2011)		ODE	Semi-mechanistic link between generation of heart beats and immune compartments.

3.4: Disruption of circadian rhythmicity of the body – Reprogramming of biological rhythms

There is a fair amount of evidence indicating that several chronically stressed conditions are correlated with disruption of biological rhythms such as sleep/wake cycles, immune mediators circadian rhythms, and hormone diurnal oscillations (Sephton, Sapolsky et al. 2000). Chrousos *et al.* further showed that a chronically stressed HPA axis is characterized by a decreased variance of cortisol both due to evening nadir elevation and to morning zenith decreases (Chrousos and Gold 1998). In critical illness, this has been hypothesized to be driven by elevated levels of inflammatory mediators, as well as neural input to the adrenal, directly stimulating glucocorticoid secretion. Circadian rhythms in melatonin were observed to be suppressed in septic patients indicating a loss of central clock rhythmicity due to the tight link between SCN function and melatonin secretion (Mundigler, Delle-Karth et al. 2002). However, non-septic patients in the ICU still had circadian rhythms in melatonin suggesting that there may be subtle disease-specific mechanisms driving the specific characteristics of the loss of circadian rhythmicity in critical illness.

Disruption of circadian rhythmicity may be also presented as a phase delay or advance in diurnal rhythmicity. In particular, Alesci *et al.* showed that patients suffering from major depression syndrome (MDD) exhibited a phase shifted profile of IL-6 expression by 12-h compared to non-depressed healthy subjects (Alesci, Martinez et al. 2005). Circadian disruption is also occasionally seen in cancer patients. Among patients with different cancer diseases, disruption of circadian rhythm has been noted in endocrine (e.g. cortisol, melatonin) metabolic (e.g. proteins and enzymes) and immunological components (e.g. cytokines) (Sephton and Spiegel 2003). Whether the circadian dysregulation is a cause or a consequence of a stressful condition is a topic of ongoing research.

As was noted earlier in this review, disrupted biological rhythms are often associated with negative clinical outcomes. Studies in shift workers showed that night working is a risk factor in several types of cancers such as prostate, breast, endometrial, and colon. Furthermore, other diseases such as obesity, diabetes, and cardiovascular seem to be more common among shift workers. Mormont *et al.* showed that patients with poor circadian rhythmicity of sleep/activity cycles had a 5-fold higher risk of dying within 2 years than the patients with a better circadian rhythmicity (Mormont, Waterhouse et al. 2000). As a result, there may be a relationship between circadian rhythmicity and disease development. This notion raises the possibility that reinforcement of disrupted biological rhythms may reset the circadian clock and further improve outcome.

Significant progress has been made through studying mathematical models that elucidate the properties of circadian clocks relative to its entrainment

dynamics and interactions with inflammatory mediators. These models illustrate the predictive power of mathematical approaches that also enable broader comprehensiveness of the biological system. In addition, their application in the context of the immune response based on current *in silico* studies seems promising. Further steps forward will continue to narrow the gap between scientific knowledge and clinical practice by incorporating system biology approaches in real clinical intervention scenarios.

Chapter 4: In-silico models of light mediated entrainment of HPA axis, and its forward effect on synchronization of peripheral clock genes (PCGs)

This chapter contains two primary sections. First section 4.1 discusses the use of a semi-mechanistic model in order to gain insight into the cortisol mediated synchronization of a population of peripheral immune cells. Next, in section 4.2 we elaborate on this model by further considering the secretion of cortisol by hypothalamic pituitary adrenal (HPA) axis, and its entrainment by light/dark cycles. In doing so, we aim to explore the flow of circadian information from the environment to the systemic level of cortisol secretion, and ultimately to peripheral cells.

4.1: Entrainment of peripheral clock genes (PCGs) by cortisol

4.1.1: Introduction

Exogenous daily signals (light, feeding, temperature) give rise to endogenous circadian rhythms in virtually all physiological functions. Chapter 3 discusses a number of bidirectional pathways through which the central pacemaker of SCN entrains peripheral clocks and peripheral clocks regulate the sensitivity of SCN. As was also discussed, independent of the central pacemaker, peripheral tissues exhibit circadian rhythmicity through the oscillations of clock genes (Balsalobre 2002). These peripheral circadian oscillations have profound physiological importance in regulating the circadian functions of numerous tissues such as heart, liver, and blood. (Hastings, Reddy et al. 2003; Reilly, Westgate et al. 2007; Cuninkova and Brown 2008). *In vitro*, peripheral cells initially retain circadian rhythmicity (Balsalobre, Damiola et al. 1998; Yamazaki, Numano et al. 2000), but eventually rhythmicity in the ensemble averages disappears. Experiments in rat-1 fibroblasts revealed that the observed dampening of clock gene expression in tissue explants is not the result of lost rhythmicity in individual cells; rather, circadian rhythms are lost as the individual oscillators fall out of sync in the absence of an entrainer, resulting in a blunted ensemble average (Nagoshi, Saini et al. 2004; Welsh, Yoo et al. 2004). Therefore, the characteristics of endogenous entraining signals and their mechanisms of action on peripheral tissues are of critical importance in understanding the dynamics of circadian rhythms.

Although there are many endogenous signals that may be responsible for the circadian entrainment of peripheral oscillators (Stratmann and Schibler 2006), glucocorticoids (cortisol in humans) are particularly interesting as putative entrainers. Cortisol secretion from the adrenal glands is regulated by the hypothalamic-pituitary-adrenal (HPA) axis and it follows a circadian pattern with a zenith in the early morning and a nadir late at night. Circadian rhythms of glucocorticoids regulate expression of peripheral genes through gene/receptor binding to a specific DNA sequence at the promoter region of target genes named the glucocorticoid response element (GRE) (Ramakrishnan, DuBois et al. 2002). Particularly for clock genes, experiments in human peripheral blood mononuclear cells (PBMCs) and fibroblasts (Balsalobre 2002; Burioka, Takata et al. 2005) established that glucocorticoids, after binding to glucocorticoid receptors, induce the expression of the clock gene *Per1* through a GRE in the *Per1* genome sequence (Yamamoto, Nakahata et al. 2005). Further experiments in mesenchymal stem cells (MSC) revealed the presence of GRE elements in *Per2* and *E4bp4* clock gene locus that were continuously occupied with glucocorticoid receptor upon treatment of cells with the synthetic glucocorticoid dexamethasone (So, Bernal et al. 2009). In addition, genomic deletion of the GRE in *Per2* resulted not only in the failure of glucocorticoids to stimulate *Per2* response, but also in dampened expression of other clock genes (i.e. *Rev-Erbα*), illustrating the downstream regulation of the circadian clock network through glucocorticoid receptor binding to GRE. Collectively, these experiments confirm that glucocorticoids, through glucocorticoid receptor signaling directly stimulate the synchronized rhythmicity of *Per1*,

Per2, and *E4bp4* in peripheral cells, further regulating the peripheral clock gene network. Therefore, although there may be multiple systemic circadian signals that entrain peripheral clock genes, one of our underlying hypotheses is that we can use cortisol as a representative entrainer of peripheral cells in order to explore the dynamics of clock gene synchronization and entrainment by systemic cues. Cortisol is also intriguing as a circadian entrainer given its central role in the inflammatory response and the recent observation that acute changes in both cortisol and clock gene expression occur in peripheral blood leukocytes in response to endotoxemia (Haimovich, Calvano et al. 2010). The disruption of circadian rhythms in cortisol is associated with fatigue, weight loss, insomnia, coronary heart disease and tumor progression (Sephton, Sapolsky et al. 2000; Filipski, King et al. 2002; Fu and Lee 2003; Lipiner-Friedman, Sprung et al. 2007). There has also been interest in cortisol circadian rhythmicity as a predictor of breast cancer survivor (Sephton and Spiegel 2003).

The importance of deciphering clock gene dynamics due to their role in regulating the circadian function of numerous tissues, such as heart, liver, and blood, as well as the complexity of clock gene network and entrainment characteristics, motivates the need for mathematical modeling of the peripheral clock network. Mathematical approaches can be of great help in understanding the underlying dynamics and also predicting clinical outcomes and intervention strategies. Several mathematical models have been proposed to investigate and describe the dynamics of clock genes (Antle, Foley et al. 2003; Leloup and Goldbeter 2003; Becker-Weimann, Wolf et al. 2004; Forger and Peskin 2005; Geier, Becker-Weimann et al. 2005; Gonze, Bernard et al.

2005; Antle, Foley et al. 2007; Bernard, Gonze et al. 2007; Mirsky, Liu et al. 2009). These models, while varying considerably in their underlying assumptions, their degree of complexity, and their method of implementation, all converge to the inclusion of a negative feedback loop that represents the *Per*/*Cry* genes and the CLOCK/BMAL1 heterodimer. In line with the experimental evidence described above, we propose a mathematical model of peripheral clock genes that incorporates cortisol as a systemic entrainer. This computational representation linking central and peripheral oscillators is leveraged to study the entraining properties of a central circadian signal on a population of peripheral cells by integrating models of circadian cortisol production (Chakraborty, Krzyzanski et al. 1999), glucocorticoid pharmacodynamics (Ramakrishnan, DuBois et al. 2002; Jin, Almon et al. 2003), and peripheral clock genes (Becker-Weimann, Wolf et al. 2004). To account for heterogeneity between individual peripheral cells, the model is formulated as a system of stochastic differential equations (SDEs).

We observe that cortisol rhythmicity induces peripheral clock gene entrainment and synchronization in an amplitude and frequency-dependent manner. While homeostatic entraining rhythms stimulate a homogeneous circadian pattern to the population of peripheral cells, the loss of circadian amplitude provokes a desynchronization among the population of cell phases. This biological shift from synchronization to desynchronization progresses through a dynamical state where the individual cells retain a relative phase coherency but are phase shifted relative to the entrainer. Concerning entrainer frequency, peripheral cells remain synchronized only for cortisol frequencies relatively close to the individual cell frequencies. In addition, we observe that

even when cells are totally entrained by cortisol, synchronization varies during the day pointing its lowest values when cells are near their nadir or zenith level.

4.1.2: Material and Methods

4.1.2.1: Models

4.1.2.1.1: Cortisol production and signal transduction

Peripheral circadian clocks are entrained by systemic cues, such as the circadian release of cortisol. The circadian production of cortisol is modeled based on the "two rates" model (Chakraborty, Krzyzanski et al. 1999) where a zero order production term (*RF*) switches between two different values representing a high production rate of cortisol in the morning and a low production rate the rest of the day (Eq. 4.1.1). We have previously used this model due to its simplicity while still retaining the ability to fit experimental data (Scheff, Calvano et al. 2010). Due to the physiological importance of glucocorticoids, there has been much interest in the pharmacokinetics and pharmacodynamics of glucocorticoids in order to understand their behavior in response to endogenous glucocorticoid production by the HPA axis or exogenous treatment. Here, we apply a glucocorticoid pharmacodynamic model which incorporates the steps of the glucocorticoid signal transduction pathway (Eq. 4.1.2-5) (Ramakrishnan, DuBois et al. 2002), culminating in transcriptional regulation of clock genes. In order to ultimately regulate the transcription of glucocorticoid responsive genes, cortisol diffuses in the cytoplasm of the target cells and binds with free glucocorticoid receptors (*R*) forming a glucocorticoid–receptor complex (*FR*), which eventually

translocates to the nucleus (*FR(N)*) where it dimerizes and binds to GRE. This binding leads to decreased levels of glucocorticoid receptor mRNA ($mRNA_R$, Eq. 4.1-2), through a process known as homologous downregulation (Oakley and Cidlowski 1993). Then, part of the receptor is recycled back to the cytoplasm and is used anew to bind to glucocorticoids.

$$\frac{dF}{dt} = RF + k_{in,F_{en}} - k_{out,F} \cdot F \qquad (4.1.1)$$

$$RF = \begin{cases} k_{in,RF1,} & \mathrm{t_{F1}} < \mathrm{mod}(t,24) < t_{F2} \\ 0 & \mathrm{t_{F2}} < \mathrm{mod}(t,24) < t_{F1} \end{cases}$$

$$\frac{dmRNA_R}{dt} = k_{s\_Rm} \cdot \left(1 - \frac{FR(N)}{IC_{50\_Rm} + FR(N)}\right) - k_{d\_Rm} \cdot mRNA_R \qquad (4.1.2)$$

$$\frac{dR}{dt} = k_{s\_R} \cdot mRNA_R + R_f \cdot k_{re} \cdot FR(N) - k_{on} \cdot F \cdot R - k_{d\_R} \cdot R \qquad (4.1.3)$$

$$\frac{dFR}{dt} = k_{on} \cdot F \cdot R - k_T \cdot FR \qquad (4.1.4)$$

$$\frac{dFR(N)}{dt} = k_T \cdot FR - k_{re} \cdot FR(N) \qquad (4.1.5)$$

It is also known that glucocorticoid receptor binding to GRE elements is inhibited by the action of the CLOCK/BMAL1(y_7) heterodimer that acetylizes glucocorticoid receptor nuclear complex (*FR(N)*) in its hinge region and blocks its forward action (Nader, Chrousos et al. 2009). This is modeled by incorporating an inhibitory term based on *FR(N)* and y_7 in the equation $mRNA_R$ (Eq. 4.1.2). k_{ac} parameter that represents the acetylation rate has been chosen adaptively so as not to change the expression levels of the model compartments that were fitted to experimental data. Other parameters were the

same as the original models (Ramakrishnan, DuBois et al. 2002; Scheff, Calvano et al. 2010).

Chronic emotional or physical stress can manifest itself through flattened cortisol rhythmicity (Chrousos and Gold 1998; Lipiner-Friedman, Sprung et al. 2007). Whether this blunted cortisol rhythm is followed by increased (hypercortisolemia) or decreased (hypocortisolemia) levels of cortisol is highly dependent on the various pathologies (Chrousos and Gold 1998; Sephton, Sapolsky et al. 2000; Miller, Chen et al. 2007). Particularly, in a study investigating cortisol rhythms in severely burned adults and children, stressed patients exhibited a blunted cortisol rhythmicity due to higher values of cortisol nadir levels (Hobson, Havel et al. 2004). In line with this experimental evidence, we explored the effects of the loss of circadian amplitude in cortisol by increasing cortisol's nadir values (*Fmin*) and holding cortisol's zenith (*Fmax*) constant. To do this, we increased the lower value of the zero order production term of cortisol, *RF* (Eq. 4.1.1), while holding the higher value constant. In addition, we explored the behavior of our model as cortisol loses its homeostatic frequency pattern while holding its amplitude constant. We further did this by changing the modulus term (mod(t,24)) of Eq. 4.1.1. This provides a consistent way to evaluate the effects of decreased cortisol rhythmicity, in line with experimental evidence.

4.1.2.1.2: Peripheral clock gene regulation by cortisol

We model the interaction between peripheral circadian clocks and cortisol by considering the transcriptional effect of activated glucocorticoid receptor on components of the clock gene network. This peripheral network

incorporates a positive and a negative feedback interaction through which peripheral clock genes exhibit oscillatory activity (Becker-Weimann, Wolf et al. 2004). In particular, the periodic expression of clock genes is driven by *Per* and *Cry* inhibiting the activity of the CLOCK/BMAL1 dimer (negative feedback) and stimulating *Bmal*1 gene transcription (positive feedback).Through the negative feedback loop, the heterocomplex CLOCK/BMAL1 activates the transcription of period (*Per*) and cryptochrome (*Cry*) genes (y_1) upon binding to the E-box promoter region. After the expression of PER/CRY proteins (y_2) in the cytoplasm, they translocate to the nucleus (y_3) where they inhibit their own transcription by shutting off the transcriptional activity of the CLOCK/BMAL1 heterocomplex (y_7). Through the positive feedback loop the nuclear compartment of PER/CRY protein (y_3) activates indirectly *Bmal1* mRNA (y_4) transcription, which after its translation to BMAL1 protein (y_5) and its translocation to the nucleus (y_6) increases the expression of CLOCK/BMAL1 heterodimer. In reality, PER/CRY proteins regulate *Bmal1* transcription through inhibiting the CLOCK/BMAL1 mediated expression of *Ror* (α, β, and γ) and *Rev-Erb* (α and β) genes (Dickmeis 2009; Mirsky, Liu et al. 2009; Relogio, Westermark et al. 2011). While both simpler and more complex models of the circadian network exist, this system represents a good intermediate level of complexity. This network of interactions, without the entraining effect of cortisol, produces the rhythmic expression of clock genes with a period of 23.4hr. Similar periods have been shown to be adopted by peripheral clock genes oscillators in human fibroblasts (24.5hr with standard deviation of 45min among individuals) (Brown, Fleury-Olela et al. 2005) and in human peripheral blood mononuclear cells (23.91hr

to 24.45hr) (Boivin, James et al. 2003). The activated nuclear glucocorticoid receptor complex directly regulates the expression of clock genes by binding to GRE. Similar to the glucocorticoid pharmacodynamic signal transduction pathway described above, CLOCK/BMAL (y_7) antagonizes this binding to GRE, that based on experimental data (Yamamoto, Nakahata et al. 2005; So, Bernal et al. 2009), is present in the promoter region of *Per1* and *Per*2. As such, glucocorticoids, inhibited by CLOCK/BMAL, entrain the local network of clock genes by regulating the transcription of *Per1-2*. This circadian regulation then propagates through to the other model variables, imposing a constant phase on the peripheral oscillators based on the circadian rhythm of cortisol. The behavior of these core circadian components of the peripheral cells is described by Eq. 4.1.6-12.

$$\frac{dy_1}{dt} = \frac{v_{1b} \cdot (y_7 + c)}{k_{1b} \cdot \left(1 + \left(\frac{y_3}{k_{1i}}\right)^p\right) + (y_7 + c)} - k_{1d} \cdot y_1 + k_c \cdot \mathrm{FR(N)} \qquad (4.1.6)$$

$$\frac{dy_2}{dt} = k_{2b} \cdot y_1^{\,q} - k_{2d} \cdot y_2 - k_{2t} \cdot y_2 + k_{3t} \cdot y_3 \qquad (4.1.7)$$

$$\frac{dy_3}{dt} = k_{2t} \cdot y_2 - k_{3t} \cdot y_3 - k_{3d} \cdot y_3 \qquad (4.1.8)$$

$$\frac{dy_4}{dt} = \frac{v_{4b} \cdot y_3^{\,r}}{k_{4b}^r + y_3^{\,r}} - k_{4d} \cdot y_4 \qquad (4.1.9)$$

$$\frac{dy_5}{dt} = k_{5b} \cdot y_4 - k_{5d} \cdot y_5 - k_{5t} \cdot y_5 + k_{6t} \cdot y_6 \qquad (4.1.10)$$

$$\frac{dy_6}{dt} = k_{5t} \cdot y_5 - k_{6t} \cdot y_6 - k_{6d} \cdot y_6 + k_{7a} \cdot y_7 - k_{6a} \cdot y_6 \qquad (4.1.11)$$

$$\frac{dy_7}{dt} = k_{6a} \cdot y_6 - k_{7a} \cdot y_7 - k_{7d} \cdot y_7 \qquad (4.1.12)$$

The entraining effect of cortisol nuclear complex that takes into account receptor's acetylation by CLOCK/BMAL1 (y_7) is modeled similar to other pharmacodynamic models simulating GRE binding (Yao, DuBois et al. 2006)

as an additive term ($k_c * FR(N)/k_{ac} y_7$) on the equation of *Per/Cry* mRNA (y_1), (Eq. 4.1.6). An additive term in the equation for *Per/Cry* mRNA was also used by Geier *et al*. (Geier, Becker-Weimann et al. 2005) to simulate the light entrainment of clock genes in the SCN, given that light differentially regulates the individual mRNAs that comprise the lumped variable (*Per/Cry* mRNA, y_1). A similar phenomenon is hypothesized to occur with clock gene responses to glucocorticoids, as only *Per1* and *Per2* have active GREs (Yamamoto, Nakahata et al. 2005; So, Bernal et al. 2009). Although in reality *Bmal1* transcription (positive feedback) is indirectly regulated by PER/CRY proteins through the antagonistic effects of ROR (α, β, and γ) and REV-ERB (α and β) transcription factors on the retinoic acid related orphan receptor response element (RORE) in the promoter region of *Bmal1* gene (Dickmeis 2009; Mirsky, Liu et al. 2009; Relogio, Westermark et al. 2011), it is not the scope of our work to fully describe the components of this network, but rather to use a fairly simple representation based on which we can investigate the dynamics of clock gene entrainment by an entraining signal (cortisol).

Thus, leverage this relatively simple mathematical model of the central pacemaker as a representative peripheral framework in order to test and explore the dynamics of entrainment of peripheral clocks by a centrally regulated entrainer. The network diagram of the integrated model (Eq. 4.1.1-12) is displayed in Figure 4.1.1 and the parameters used in Table 4.1.1.

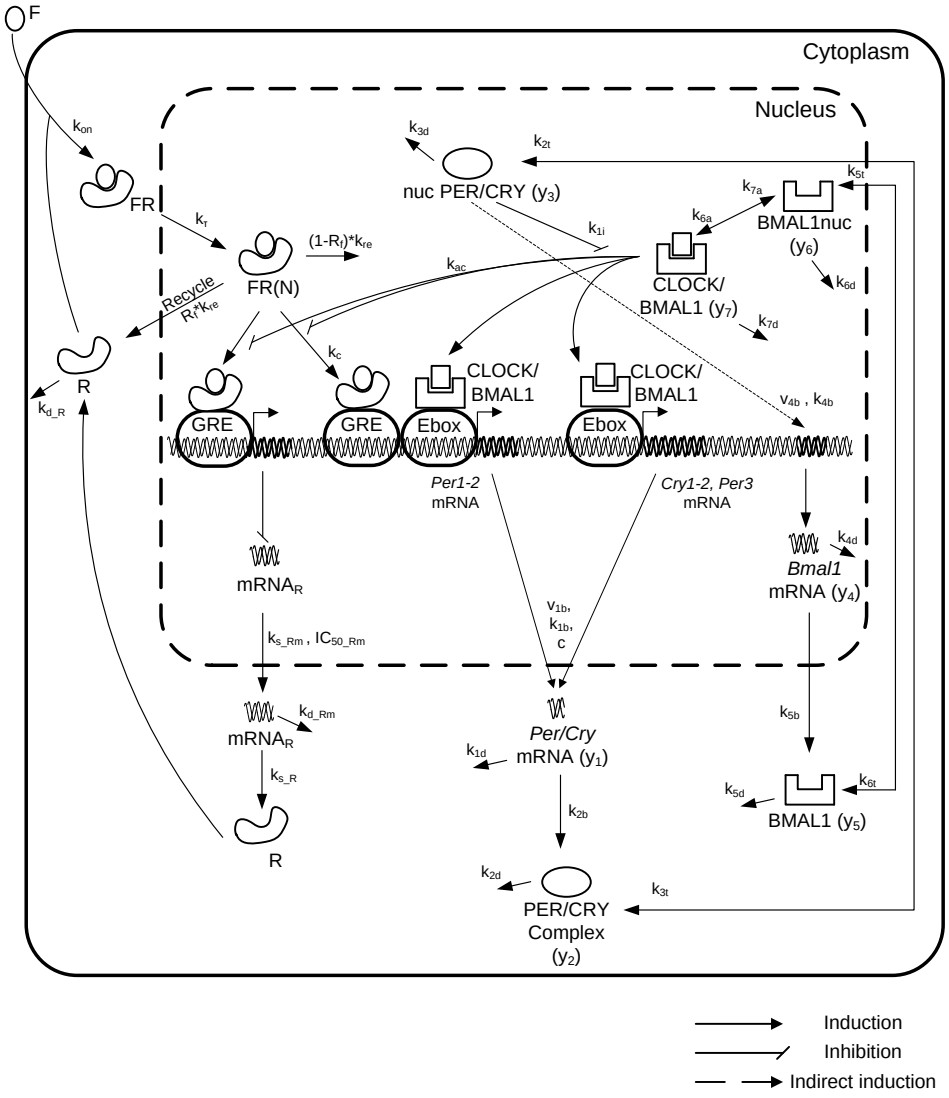

Figure 4.1. 1: Schematic figure of the model. Two components formulate the framework of the model. The first is a pharmacodynamic compartment through which cortisol F diffuses to cytoplasm, binds the glucocorticoid receptor (R) forming the complex FR, translocates to the nucleus FR(N), and regulates the translation of mRNAR and Per/Cry mRNA, and the second includes the clock gene regulatory positive and negative feedback loops (y1- y7)./Cry mRNA and the second includes the clock gene regulatory positive and negative feedback loops (y1- y7).

Table 4.1. 1: List of parameters used in the model (Eq. 4.1.1-12).

#	Parameter	Value	Units	Description
1	$k_{in,Fen}$	0.843	ng/mL/hr	Base production rate of cortisol (Scheff, Calvano et al. 2010)
2	$k_{out,F}$	1.06	1/hr	Clearance rate of cortisol (Scheff, Calvano et al. 2010)
3	$k_{in,RF1}$	0.7346	ng/ml/hr	Circadian production rate of cortisol (Scheff, Calvano et al. 2010)
4	t_{F1}	4.62	hr	Start time for when cortisol production is heightened (Scheff, Calvano et al. 2010)
5	t_{F2}	12.1	hr	End time for when cortisol production is heightened (Scheff, Calvano et al. 2010)
6	k_{syn_Rm}	2.9	fmol/g/hr	Synthesis rate or glucocorticoid receptor mRNA (Ramakrishnan, DuBois et al. 2002)
7	IC_{50_Rm}	26.2	nmol/L/mg	Concentration of FR(N) at which $mRNA_{,R}$ synthesis drops to its half (Ramakrishnan, DuBois et al. 2002)
8	R_0	540.7	nM/L/mg	Baseline value of free cytosolic glucocorticoid receptor (Ramakrishnan, DuBois et al. 2002)
9	R_{m0}	25.8	fmole/gr	Baseline value of glucocorticoid receptor mRNA (Ramakrishnan, DuBois et al. 2002)
10	k_{dgr_Rm}	k_{syn_Rm}/Rm0		Degradation rate of glucocorticoid receptor mRNA (Ramakrishnan, DuBois et al. 2002)
11	k_{dgr_R}	0.0572	1/hr	Degradation rate of cytosolic glucocorticoid

				receptor (Ramakrishnan, DuBois et al. 2002)
12	k_{syn_R}	$(R_0/R_{m0})*k_{dgr\_R}$		Synthesis rate of free cytosolic receptor (Ramakrishnan, DuBois et al. 2002)
13	R_f	0.49		Fraction of cortisol recycled (Ramakrishnan, DuBois et al. 2002)
14	k_{re}	0.57	1/hr	Rate of receptor recycling from nucleus to cytoplasm (Ramakrishnan, DuBois et al. 2002)
15	k_{on}	0.00329	L/nmole/hr	Second order rate constant of glucocorticoid receptor binding (Ramakrishnan, DuBois et al. 2002)
16	k_t	0.63	1/hr	Rate of receptor translocation to the nucleus (Ramakrishnan, DuBois et al. 2002)
17	k_c	0.009	1/hr	Coupling strength
18	v_{1b}	9	nM/hr	Maximal rate of *Per/Cry* transcription (Becker-Weimann, Wolf et al. 2004)
19	k_{1b}	1	nM	Michaelis constant of *Per/Cry* transcription (Becker-Weimann, Wolf et al. 2004)
20	k_{1i}	0.56	nM	Inhibition constant of *Per/Cry* transcription (Becker-Weimann, Wolf et al. 2004)
21	c	0.01	nM	Concentration of constitutive activator (Becker-Weimann, Wolf et al. 2004)
22	p	8		Hill coefficient of inhibition of *Per/Cry* transcription (Becker-Weimann, Wolf et al. 2004)

23	k_{1d}	0.12	1/hr	Degradation rate of *Per/Cry* mRNA (Becker-Weimann, Wolf et al. 2004)
24	k_{ac}	1	nM/hr	Acetylation rate
25	k_c	0.0016	1/hr	Coupling constant (Becker-Weimann, Wolf et al. 2004)
26	k_{2b}	0.3	1/nM/hr	Complex formation rate of *Per/Cry* mRNA (Becker-Weimann, Wolf et al. 2004)
27	q	2		No. of PER/CRY complex forming subunits (Becker-Weimann, Wolf et al. 2004)
28	k_{2d}	0.05	1/hr	Degradation rate of cytoplasmatic PER/CRY (Becker-Weimann, Wolf et al. 2004)
29	k_{2t}	0.24	1/hr	Nuclear import rate of the PER/CRY complex (Becker-Weimann, Wolf et al. 2004)
30	k_{3t}	0.02	1/hr.	Nuclear export rate of PER/CRY complex (Becker-Weimann, Wolf et al. 2004)
31	k_{3d}	0.12	1/hr.	Degradation rate of the nuclear PER/CRY complex (Becker-Weimann, Wolf et al. 2004)
32	v_{4b}	3.6	nM/hr	Maximal rate of *Bmal1* transcription (Becker-Weimann, Wolf et al. 2004)
33	k_{4b}	2.16	nM	Michaelis constant of *Bmal1* transcription (Becker-Weimann, Wolf et al. 2004)
34	r	3		Hill coefficient of activation of *Bmal1* transcription (Becker-Weimann, Wolf et al. 2004)

35	k_{4d}	0.75	1/hr	Degradation rate of *Bmal1* mRNA (Becker-Weimann, Wolf et al. 2004)
36	k_{5b}	0.24	1/hr	Translation rate of BMAL1 (Becker-Weimann, Wolf et al. 2004)
37	k_{5d}	0.06	1/hr	Degradation rate of cytoplasmatic BMAL1 (Becker-Weimann, Wolf et al. 2004)
38	k_{5t}	0.45	1/hr	Nuclear import rate of BMAL1 (Becker-Weimann, Wolf et al. 2004)
39	k_{6t}	0.06	1/hr	Nuclear export rate of BMAL1 (Becker-Weimann, Wolf et al. 2004)
40	k_{6d}	0.12	1/hr	Degradation rate of nuclear BMAL1 (Becker-Weimann, Wolf et al. 2004)
41	k_{6a}	0.09	1/hr	Activation rate of nuclear CLOCK/BMAL1 (Becker-Weimann, Wolf et al. 2004)
42	k_{7a}	0.003	1/hr	Deactivation rate of CLOCK/BMAL1 (Becker-Weimann, Wolf et al. 2004)
43	k_{7d}	0.09	1/hr	Degradation rate of CLOCK/BMAL1 (Becker-Weimann, Wolf et al. 2004)

4.1.2.2: Methods

4.1.2.2.1: Stochastic differential equation formulation

All biological processes (*e.g.* protein folding (Dobson, Šali et al. 1998), gene expression (Kaern, Elston et al. 2005), protein-protein interaction

(Batada, Shepp et al. 2004)) proceed with some level of uncertainty. Relevant to the transcription of clock genes, the binding of a transcription factor such as CLOCK/BMAL1 to a small number of discrete regions to modulate transcription is a highly stochastic process (Kaern, Elston et al. 2005). Furthermore, cortisol secretion as well as its signaling pathways contain stochasticity (Kino, De Martino et al. 2003; Chrousos and Kino 2005), which has been modeled from both the perspectives of hormone release (Brown, Meehan et al. 2001) and downstream transcriptional regulatory effects (An 2004; Mi, Riviere et al. 2007; An 2008). Our model incorporates stochastic expressions for cortisol and clock genes. This uncertainty leads the individual cells, in absence of an entraining signal, to adopt stochastic phases and periods and thus fall out of sync.

The system of ordinary differential equations (ODEs) defined in Eq. 4.1.1-12 was translated to chemical Langevin stochastic differential equations (CLEs) (Gillespie 2000). Generally, this formulation assumes that molecules of the reacting species interact through a number of chemical reactions, each one having a probability of occurrence in an infinitesimal time interval proportional to the rate constant of the reaction. This probability is referred as the propensity of the reaction (Table 4.1.2). The CLE recurrence formula used in this work is defined as:

$$x_i(t+\tau) = x_i(t) + \sum_{j=1}^{M} v_{ji} \cdot a_j\left(x_i(t)\right) \cdot \tau + \sum_{j=1}^{M} v_{ji} \cdot \sqrt{a_j\left(x_i(t)\right) \cdot \tau} \cdot N_j(0,1) \qquad (4.1.13)$$

Where $x_i\,(t)$ are the molecules of the i reacting species (Equation 4.1.1-12) at time t,τ is the fixed time interval length, j is the different type of the total M=31 chemical reactions (Table 4.1.2), v_{ji} is the change in the number of the i

molecules caused by the *j* reaction, and a_j is the propensity of the *j* reaction. N_j are statistically independent, normal (0,1) random variables. The time interval length (τ) has been chosen adaptively so that the propensity of reactions in each time step is slightly changed. In order to translate the determinist model into stochastic, we needed to know the volume of the cell. Similar to Forger and Peskin (Forger and Peskin 2005), this volume was chosen so that the peak of PER/CRY protein molecule count (y_2, Eq. 4.1.7) is nearly 5000 molecules, in accordance with experimental evidence from liver cells.

Table 4.1. 2: Elementary reactions and reaction propensities involved in the model. Where Ω=Cell volume*Avogadro number (N_A).

React. No.	Reaction	Propensity of Reaction (a_j)	Transition
1	$\longrightarrow F$	$a_1=k_{in\_F1}\cdot\Omega$ for $t_{F1}<\mathrm{mod}(t,24)<t_{F2}$ $a_1=k_{in\_F2}\cdot\Omega$ for $t_{F2}<\mathrm{mod}(t,24)<t_{F1}$	$F\longrightarrow F+1$
2	$\longrightarrow F$	$a_2=k_{in\_Fen}\cdot\Omega$	$F\longrightarrow F+1$
3	$F\longrightarrow$	$a_3=k_{out\_F}\cdot F$	$F\longrightarrow F-1$
4	$\longrightarrow mRNA_R$	$a_4=k_{s\_m}\cdot\Omega$	$mRNA_R\longrightarrow mRNA_R+1$
5	$mRNA_R\longrightarrow$	$a_5=k_{s\_m}\cdot\Omega\cdot\frac{\frac{FR(N)}{k_{ac}\cdot\Omega\cdot y_7}}{IC_{50}\cdot\Omega+\frac{FR(N)}{k_{ac}\cdot\Omega}}$	$mRNA_R\longrightarrow mRNA_R-1$
6	$mRNA_R\longrightarrow$	$a_6=k_{d\_m}\cdot mRNA_R$	$mRNA_R\longrightarrow mRNA_R-1$
7	$\longrightarrow R$	$a_7=k_{s\_R}\cdot mRNA_R$	$R\longrightarrow R+1$
8	$\longrightarrow R$	$a_8=R_f\cdot k_{re}\cdot FR(N)$	$R\longrightarrow R+1$
9	$R\longrightarrow FR$	$a_9=\frac{k_{on}\cdot F\cdot R}{\Omega}$	$R\longrightarrow R-1$ $FR\longrightarrow FR+1$

0	**1**	$R \longrightarrow$	$a_{10} = k_{d\_R} \cdot R$	$R \longrightarrow$ R-1
1	**1**	$FR \longrightarrow FR(1$	$a_{11} = k_T \cdot FR$	$FR \longrightarrow$ FR-1 $FR(N) \longrightarrow$ FR(N)+1
2	**1**	$FR(N) \longrightarrow$	$a_{12} = k_{re} \cdot FR(N)$	$FR(N) \longrightarrow$ FR(N)-1
3	**1**	$\longrightarrow y_1$	$a_{13} = \frac{v_{1b} \cdot \Omega \cdot (y_7 + c \cdot \Omega)}{k_{1b} \cdot \Omega \cdot \left(1 + \left(\frac{y_3}{k_{1i} \cdot \Omega}\right)^p\right)}$	$y_1 \longrightarrow y_1$+1
4	**1**	$y_1 \longrightarrow$	$a_{14} = k_{1d} \cdot y_1$	$y_1 \longrightarrow y_1$-1
5	**1**	$\longrightarrow y_1$	$a_{15} = k_c \cdot \frac{FR(N)}{k_{ac} \cdot \Omega \cdot y_7}$	$y_1 \longrightarrow y_1$+1
6	**1**	$\longrightarrow y_2$	$a_{16} = \frac{k_{2b} \cdot y_1^q}{\Omega}$	$y_2 \longrightarrow y_2$+1
7	**1**	$y_3 \longrightarrow y_2$	$a_{17} = k_{3t} \cdot y_3$	$y_2 \longrightarrow y_2$+1 $y_3 \longrightarrow y_3$-1
8	**1**	$y_2 \longrightarrow$	$a_{18} = k_{2d} \cdot y_2$	$y_2 \longrightarrow y_2$-1
9	**1**	$y_2 \longrightarrow y_3$	$a_{19} = k_{2t} \cdot y_2$	$y_2 \longrightarrow y_2$-1 $y_3 \longrightarrow y_3$+1
0	**2**	$y_3 \longrightarrow$	$a_{20} = k_{3d} \cdot y_3$	$y_3 \longrightarrow y_3$-1
1	**2**	$y_3 \longrightarrow$	$a_{21} = k_{3t} \cdot y_3$	$y_3 \longrightarrow y_3$-1
2	**2**	$\longrightarrow y_4$	$a_{22} = \frac{v_{4b} \cdot \Omega \cdot y_3^r}{\left(k_{4b} \cdot \Omega\right)^r + y_3^r}$	$y_4 \longrightarrow y_4$+1
3	**2**	$y_4 \longrightarrow$	$a_{23} = k_{4d} \cdot y_3$	$y_4 \longrightarrow y_4$-1
4	**2**	$\longrightarrow y_5$	$a_{24} = k_{5b} \cdot y_4$	$y_5 \longrightarrow y_5$+1
5	**2**	$y_6 \longrightarrow y_5$	$a_{25} = k_{6t} \cdot y_6$	$y_5 \longrightarrow y_5$+1 $y_6 \longrightarrow y_6$-1
6	**2**	$y_5 \longrightarrow$	$a_{26} = k_{5d} \cdot y_5$	$y_5 \longrightarrow y_5$-1
7	**2**	$y_5 \longrightarrow y_6$	$a_{27} = k_{5t} \cdot y_5$	$y_5 \longrightarrow y_5$-1

				$y_6 \longrightarrow y_6+1$
8	**2**	$y_7 \longrightarrow y_6$	$a_{28}=k_{7a} \cdot y_7$	$y_7 \longrightarrow y_7-1$ $y_6 \longrightarrow y_6+1$
9	**2**	$y_6 \longrightarrow$	$a_{29}=k_{6d} \cdot y_6$	$y_6 \longrightarrow y_6-1$
0	**3**	$y_6 \longrightarrow y_7$	$a_{30}=k_{6a} \cdot y_6$	$y_6 \longrightarrow y_6-1$ $y_7 \longrightarrow y_7+1$
1	**3**	$y_7 \longrightarrow$	$a_{31}=k_{7d} \cdot y_7$	$y_7 \longrightarrow y_7-1$

4.1.2.2.2: Quantification of synchronicity, entrainment and periodicity

In order to study how circadian rhythms in cortisol affect the state of clock genes, we evaluate metrics of both synchronicity (*i.e.* how similar are different cells) and entrainment (*i.e.* how similar cell periods and phases are to the entrainer). To assess synchronization of clock genes, we measure the deviation of *Per/Cry* mRNA levels from their mean value. Therefore, in our analysis we incorporated the degree of synchronization for the variable y_k, $R_{syn,k}$ (Garcia-Ojalvo, Elowitz et al. 2004; Ullner, Buceta et al. 2009) (Eq. 4.1.14), which represents the ratio of the variance of the mean field over the mean variance of each oscillator.

$$R_{syn,k} = \frac{\left\langle \bar{y}_k^{\,2} \right\rangle - \left\langle \bar{y}_k \right\rangle^2}{\frac{1}{N} \cdot \sum_{j=1}^{N} \left(\left\langle y_{k,j}^{\,2} \right\rangle - \left\langle y_{k,j} \right\rangle^2 \right)} \qquad (4.1.14)$$

In Equation 14, $y_{k,j}$ is the timecourse vector output generated by Eq. 4.1.6-12, where the first index k represents the variable, and the second index j represents the cell (N total). Overbar variables ($\bar{y}_k$) are timecourse vectors of

averages over the population of *N* cells (Eq. 4.1.15) and brackets represent time averages (Eq. 4.1.16).

$$\bar{y}_k = \frac{1}{N} \cdot \sum_{j=1}^{N} y_{k,j} \qquad (4.1.15)$$

$$\langle \bar{y}_k \rangle = \frac{1}{T} \cdot \sum_{t=t_1}^{T} \bar{y}_k(t) \qquad (4.1.16)$$

$R_{syn,k}$ is calculated for the *Per/Cry* mRNA variable (k=1) for a time span of 500hr except for the in-silico experiments evaluating circadian variation of synchronization where it was calculated for a period of 2hr. $R_{syn,k}$ has a minimum value of zero when the cells are completely desynchronized and a maximum value of 1 when cells are fully synchronized.

In addition to intercellular synchronization, we evaluate the level of entrainment of peripheral cells by cortisol's rhythmic pattern. For this reason we quantify the degree of phase locking of *Per/Cry* mRNA. Accordingly, we calculate the entrainment index "ρ_1", which is an entropy based metric that takes into consideration the individual cell period distribution (Tass, Rosenblum et al. 1998). The entrainment index for any variable k of the model is defined as:

$$\rho_k = 1 - \frac{S_k}{S_{k,\max}} \qquad (4.1.17)$$

Where $S_k = -\sum_{l=1}^{N} P_{k,l} \cdot \ln(P_{k,l})$ is the entropy of the discrete period distribution for the variable k, l is the number of total N bins, $P_{k,l}$ is the normalized occupancy of the l^{th} bin for the k^{th} variable , and $S_{k,\max} = \ln(N)$.

Lastly, we evaluated the phase coherence of the population of cells as the cortisol amplitude was varied by calculating the standard deviation of the cell phases again for the variable *Per/Cry* mRNA ($\sigma_{\Phi_{Per/Cry mRNA}}$). This was accomplished by using the Fast Fourier Transformation (FFT) (Cooley and Tukey 1965) and then finding the phase angles ($\Phi_{\text{Per/Cry mRNA}}$) over the same time span that were used to calculate $R_{syn,1}$ and ρ_1(500hr). Phase angles were found relative to 0^o of the trigonometric cycle, which can be translated to a constant external time point in the time domain. Because the phase of cortisol is held constant throughout all simulations, these phase angles can be also considered to be relative to the phase of cortisol. Incorporating this frequency domain metric facilitated not only a check on the validity of the two aforementioned metrics, but also the calculation of the phase shift between the entrainer and the population. This procedure was repeated for every amplitude of cortisol tested. The standard deviation of cell phases is expected to change in the opposite direction of $R_{syn,k}$ and ρ_k, taking a value of zero when cells are perfectly entrained and increasing as the cells become desynchronized. We also use the FFT to find the frequency and period of each cell's oscillations. In the results shown below, all of the aforementioned metrics are applied after time t~800hr.

4.1.3 Results

A population of 1000 cells is used in all of *in silico* experiments performed in this work. Initially, in order to understand how the stochastic nature of the system impacts the population characteristics independent of entrainment, we investigate the distribution of single cell phases and periods in absence of

cortisol. In Figure 4.1.2A we examine single cell phases as the coupling strength (k_c) is set to zero. Phases of single cells adopt a uniform distribution as they maintain values through the entire regime from 0 to 2π. Relative to individual cell periods, the stochastic dynamics induce a normally distributed pattern with a mean period of 23.4hr (Figure 4.1.2B).

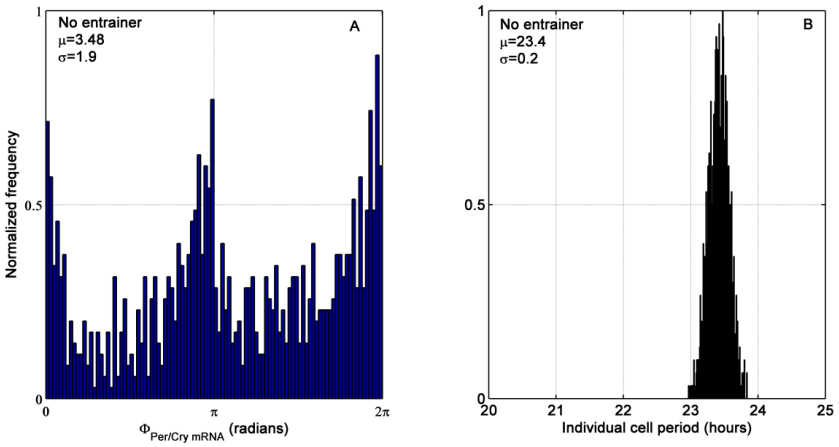

Figure 4.1. 2: Distribution of single cell phases and periods when no entrainer is present. A: Unentrained single cell phases adopt a uniform distribution possessing values through the entire regime from 0 to 2π. B: Individual cell periods adopt a normally distributed pattern with mean period equal to 23.4hr.

In Figure 4.1.3, we explore the synchronization that cortisol imposes on the ensemble average of the population. From time t=0hr until time t=200hr, cells are independent from cortisol regulation as k_c is set to zero. This causes the average to have a very low rhythmicity due to the incoherent rhythms in the single cell level. At time t=200hr, k_c is set to its nonzero value, imposing entrainment by cortisol on the peripheral oscillators. Cortisol affects the ensemble of cells in two ways. First, it stimulates a robust pattern with large amplitude; and second, it imposes its frequency on the peripheral clocks so

that the population average has a 24hr period. At time t=1000hr, cortisol's effect is again removed by setting k_c to zero and the ensemble progressively loses its rhythmicity. Thus, Figure 4.1.3 shows both the synchronization and desynchronization that occur as an entrainer is added and then removed from the system.

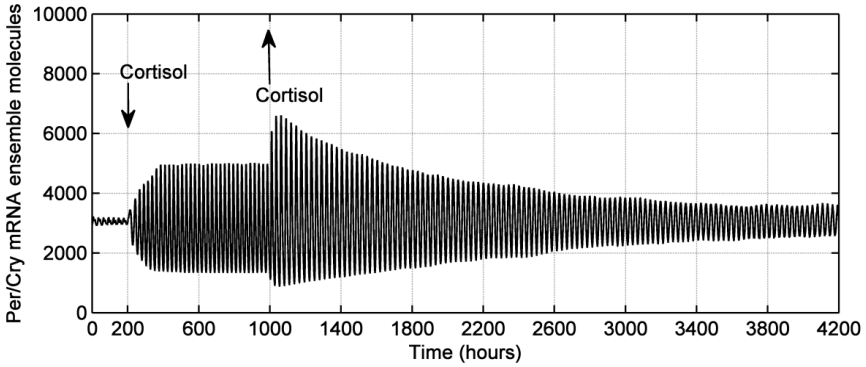

Figure 4.1. 3: Cortisol entrainment to *Per/Cry* mRNA (y_1) compartment (1000 cells). Ensemble average profile of *Per/Cry* mRNA (y1) before and after the presence of cortisol. Cortisol entrainment (200< t <1000hr) results in a robust expression signal at the population level in contrast with desynchronized states (t < 200 and t > 1000hr) where the population signal is weaker.

4.1.3.1: Amplitude dependent synchronization

The impact of cortisol's amplitude on the synchronization of peripheral genes is depicted in Figure 4.1.4. As the amplitude of cortisol increases, moving rightwards on the x-axis, the cell synchronization increases as denoted by the gradually increasing $R_{syn,1}$ and ρ_1 metrics and the decreasing standard deviation of cell phases. In particular, our model reveals three qualitative regimes of synchronization. In the first regime (I), individual cells are nearly fully desynchronized shown by the small values of the $R_{syn,1}$ and ρ_1 entrainment metrics and the high standard deviation of cell phases. As

cortisol's amplitude increases to reach its homeostatic value, individual cells gradually become entrained. The second regime (II) is an intermediate state in which some of the individual cells begin to fall in sync. In the third regime (III), individual cell maintain a high degree of synchronization and the standard deviation of cell phases is small.

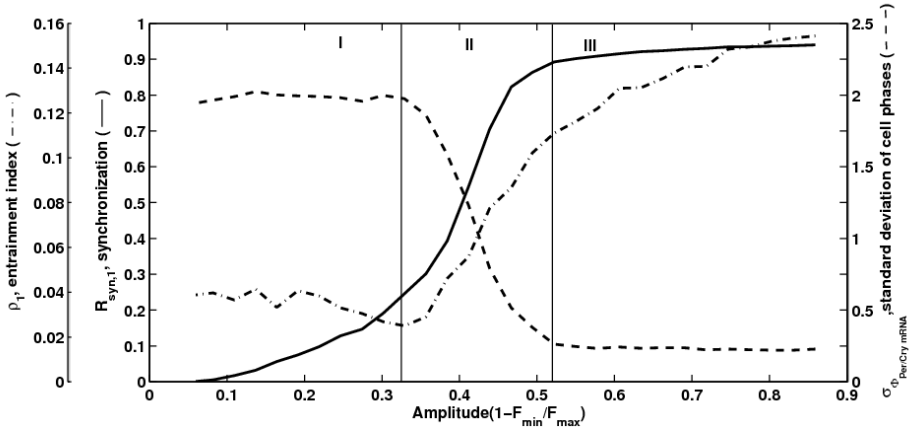

Figure 4.1. 4: Cortisol's amplitude dependent synchronization of peripheral cells (1000 cells). In small cortisol amplitudes (I) individual cells are desynchronized as it is denoted by the small values of $R_{syn,1}$, ρ_1 and the high standard deviation of cell phases ($\sigma_{\Phi Per/Cry\ mRNA}$). As cortisol amplitude approaches its homeostatic value, individual cells pass through an intermediate regime of synchronization (II) where some of the cells are gradually becoming synchronized. Regime III corresponds to the entrained state of the population where the cells are nearly fully synchronized as it is denoted by the high values of $R_{syn,1}$ and ρ_1 metrics and the low value of $\sigma_{\Phi Per/Cry\ mRNA}$.

In order to explore the single cell dynamics when changing the entrainer's amplitude, we further examine single cell phases ($\Phi_{Per/Cry\ mRNA}$) and periods for different cortisol amplitudes. Figure 4.1.5 shows the distribution of cell phases ($\Phi_{Per/Cry\ mRNA}$) as the amplitude of cortisol decreases. We perform eight *in silico* experiments for different ratios of cortisol amplitudes. At the homeostatic level of cortisol, where amplitude (amp=1-F_{min}/F_{max}) is 0.85

(Figure 4.1.5A), the population of cells approximates a normal distribution. As cortisol gradually loses its rhythmicity, although the distribution of cell phases retains its normally distributed pattern, the population mean drifts to higher values (Figure 4.1.5B-5D). As the phase of cortisol remains constant, a change in the mean peripheral circadian phase denotes a phase shift relative to the entrainer. At the same time, the standard deviation slowly increases. In Figure 4.1.5E and 4.1.5F, the population reaches the second regime (II) of synchronization and some cells gradually adopt different phases. Further decreasing cortisol's amplitude the standard deviation increases, culminating in a uniform distribution when cortisol amplitude has become almost constant (Regime I, Figure 4.1.5G and 4.1.5H).

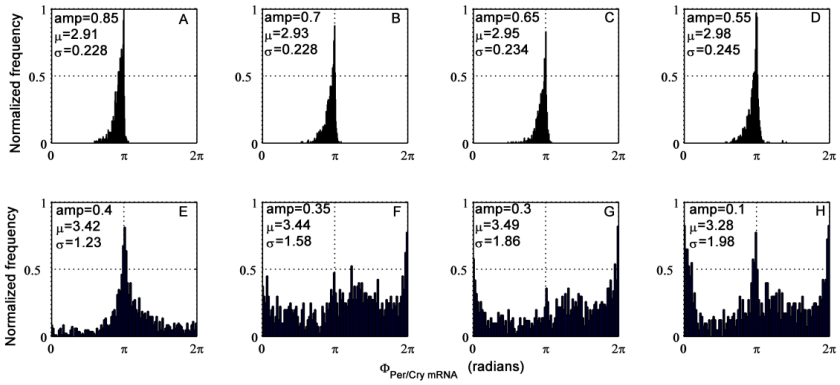

Figure 4.1. 5: Distribution of individual cell phases ($\Phi_{Per/CrymRNA}$) for eight cortisol amplitudes (1000 cells). While in large cortisol amplitudes (amp=1-F_{min}/F_{max}) distribution of single cell phases adopt a normally distributed pattern, as the amplitude of cortisol decreases, the normal distribution becomes gradually uniform. From A to H cortisol amplitude is decreasing. μ and σ are the mean and standard deviation of population phases respectively.

In Figure 4.1.6 we evaluate single cell periods for different cortisol amplitudes. When cortisol's amplitude results in the third regime of synchronization (III, Figure 4.1.4), the single cell periods are narrowly distributed with mean values equal to the circadian period of the entrainer (Figure 4.1.6A-6D). Further decrease of cortisol's amplitude induces the emergence of a second distribution (Figure 4.1.6E) that indicates that cells are beginning to fall out of sync since they adopt periods different from that of the entrainer. This state is gradually reached by the majority of the cells (Figure 4.1.6F and 4.1.6G) until it becomes the sole distribution of the population (Figure 4.1.6H) when all of the cells become unentrained.

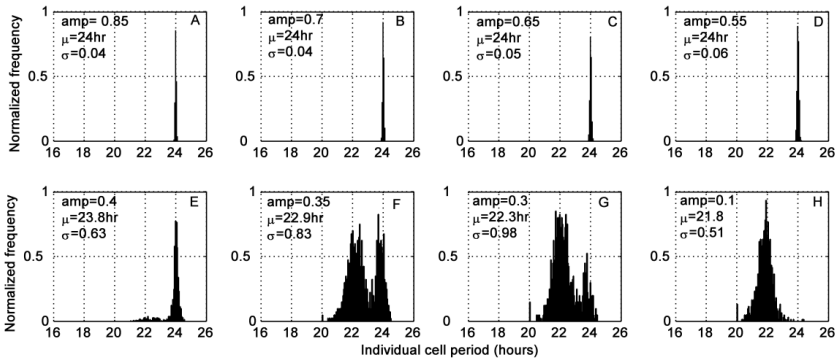

Figure 4.1. 6: Distribution of individual cell periods for eight cortisol amplitudes (1000 cells). In large cortisol amplitudes (amp=1-F_{min}/F_{max}), distribution of cell periods adopt a narrow distribution centered around the circadian period of the entrainer (24hr.). As the amplitude decreases, a second distribution of cell periods surges that ultimately becomes the solely distribution of the population. From A to H cortisol amplitude is decreasing. μ and σ are the mean and standard deviation of population periods respectively.

4.1.3.2: Frequency dependent synchronization

In addition to assessing entrainment properties as the amplitude of the entrainer changes, we examine the synchronization of the cell population upon changing the period of the entrainer (Figure 4.1.7). High levels of

synchronization are observed only for a certain range of cortisol periods near the period of the free-running peripheral circadian oscillator (23.4hr).

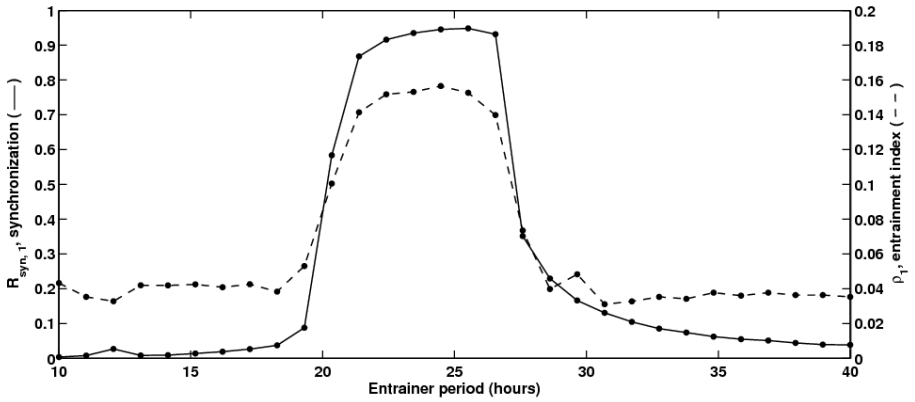

Figure 4.1. 7: Cortisol's frequency dependent synchronization of peripheral cells (1000 cells). Synchronization as calculated with $R_{syn,1}$ and ρ_1 metrics is observed only for entrainer periods relatively close to the individual cell period (23.4hr).

In Figure 4.1.8 and Figure 4.1.9 we evaluate the impact of changing cortisol's period on the single cell level. In particular, Figure 4.1.8 shows individual cell phases for 6 values of entrainer's period. When cortisol's period is very different from that of a single cell (Figures 4.1.8A and 4.1.8B), cell phases adopt a uniform distribution with high standard deviation. As cortisol's period approaches the period of individual cells, their individual phases gradually converge and the standard deviation decreases (Figure 4.1.8C) until the point where the distribution becomes normally shaped (Figure 4.1.8D). For greater period values, individual cells fall out of sync and the population again adopts a uniform distribution (Figures 4.1.8E and 4.1.8F).

We further examine individual cell periods (Figure 4.1.9) upon changing cortisol's period. In response to setting cortisol's period to 10hr, individual

cell periods are concentrated in a normal distribution (Figure 4.1.9A). As the entrainer period approaches the regime of high synchronization (Figure 4.1.7 regime of high values of $R_{syn,1}$ and ρ_1), we observe again the rise of a second distribution (Figure 4.1.9B) that gradually becomes the dominant state of the population (Figure 4.1.9C). This narrow distribution increases in prominence with higher entraining periods (Figure 4.1.9D). Finally, as cortisol's period moves away of the synchronization regime, it induces the appearance of a new distribution (Figure 4.1.9E). As we further increase the period of cortisol, the majority of the cells go to this new distribution until it eventually becomes the sole distribution of the population for a cortisol period equal to 39hr (Figure 4.1.9F).

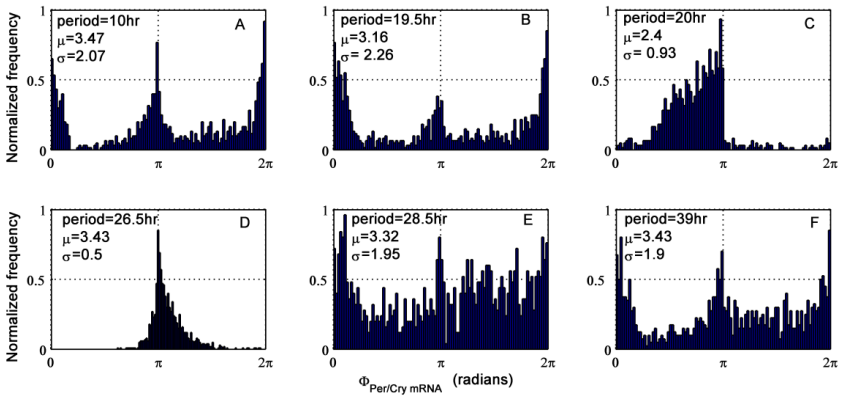

Figure 4.1. 8: Distribution of individual cell's phases for several cortisol periods (1000 cells). As entrainer period remain highly different than that of individual cells (23.4hr), the cell phases adopt a uniform distribution. For cortisol periods close to that of individual cells, there is a gradual concentration of phases under a normal distribution. From A to F cortisol period is increasing. μ and σ are the mean and standard deviation of population periods respectively.

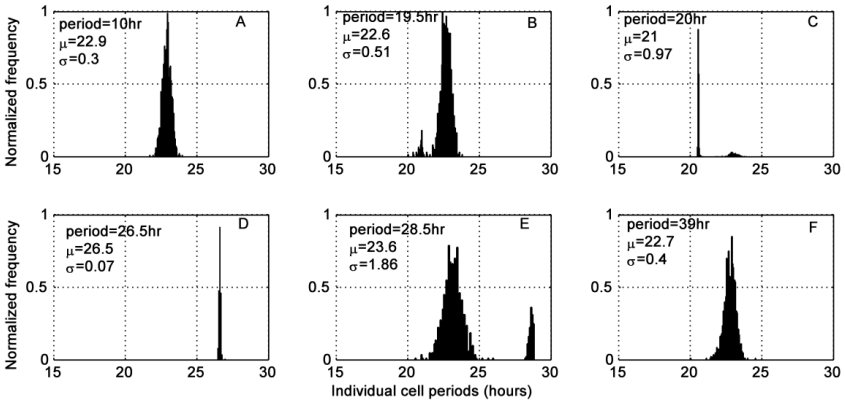

Figure 4.1. 9: Distribution of individual cell periods for several cortisol periods (1000 cells). As cortisol period approaches or departs from the period of individual cells (23.4hr) we see the rise of a second distribution denoting that cells are gradually becoming synchronized or desynchronized respectively. From A to F cortisol period is increasing. μ and σ are the mean and standard deviation of population periods respectively.

4.1.3.3: Circadian variation of clock gene synchronization

Lastly, we investigated variation in clock gene synchronization throughout a 24hr period. Figure 4.1.10A shows single cell profiles of *Per/Cry* mRNA in response to homeostatic cortisol rhythms that cause peripheral cells to retain a high level of entrainment. During the 24hr period, we calculate the $R_{syn,1}$ synchronization metric for successive time windows of 2hr and observe that synchronization varies in a circadian manner, reaching lower values when *Per/Cry* mRNA approaches its nadir or zenith levels ($R_{syn,1}$=0.64 or 0.13 respectively). Focusing on these regions of low synchronization, Figures 4.1.10B and 4.1.10C reveal that single cells have uncorrelated expression profiles with high variances in cell patterns. In contrast, in regions of high synchronization (Figure 4.1.10C), cells adopt coherent profiles with highly correlated dynamics, leading to high values of $R_{syn,1}$.

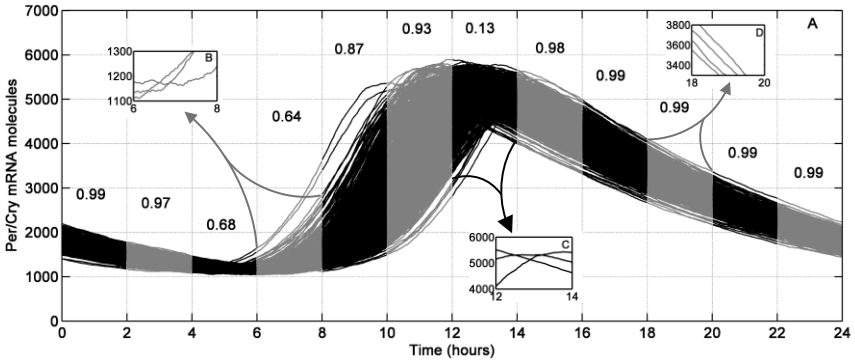

Figure 4.1. 10: Circadian variation of clock gene synchronization throughout a 24hr period. A: Individual cell *Per/Cry* mRNA expression for homeostatic cortisol rhythms. The synchronization metric ($R_{syn,1}$) has been calculated for consecutive time windows of 2hr and has been placed over each time interval. Different colors denote different windows where the metric has been calculated. B: Representation of a small number of cells for the 6hr-8hr window that indicates the highly uncorrelated profiles of single cells. C: A small number of cell profiles for the regime of maximum desynchronization (12hr-14hr). D: A small number of cells for a regime of high synchronization (18hr-20hr). The x and y axes of the inset plots are same to these of the main figure A.

4.1.4: Discussion

The synchronization of endogenous rhythms to external commanding zeitgebers is crucial for the maintenance of biological fitness. In this paper we studied the underlying dynamics of the entrainment of peripheral clocks by a single entrainer (cortisol), focusing on the dependency of cell synchronization on the characteristics of the entraining rhythmic cortisol pattern.

Introducing an external rhythmic force such as cortisol circadian secretion to an oscillating variable such as *Per/Cry* mRNA (at t=200hr in Figure 4.1.3) produces a system equivalent to a forced oscillator (Strogatz and Stewart

1993). The effect of cortisol on the peripheral clock is dependent on two characteristics: the frequency and the amplitude of the entrainer. Experiments in chronically jet lagged and SCN ablated mice indicated that the loss of glucocorticoid circadian frequency was associated with accelerated tumor growth (Filipski, King et al. 2002; Filipski, Delaunay et al. 2004). Also, in humans, cortisol circadian frequency has been found to be disrupted in breast and ovarian cancer patients (Touitou, Bogdan et al. 1996). Heterogeneity in cortisol amplitudes arise due to HPA dysregulation in chronic stress (Nader, Chrousos et al. 2010). The effective amplitude sensed by the peripheral circadian module in our model is largely dependent on the choice of the parameter k_c, which is multiplied with *FR(N)* in Eq. 4.1.6, thus representing the coupling strength between central and peripheral circadian systems (Gonze, Bernard et al. 2005; Bernard, Gonze et al. 2007). In the simulations performed here, this parameter was fixed to a value that was chosen relative to the following qualitative limitations. Firstly, in response to normal cortisol rhythms, the body is at its homeostatic state and peripheral clock gene responses are entrained to cortisol's frequency. Secondly, when cortisol has completely lost its amplitude variability (F_{min}~$F_{max)}$, the individual oscillators lose synchronization and individual cells adopt random phases and periods. This latter modeling constraint is supported by experiments on SCN ablated animals (Reppert, Perlow et al. 1981; Yoo, Yamazaki et al. 2004) that show the loss of circadian rhythmicity in cortisol along with desynchronization in peripheral cells. These limits define a small range of parameters ($0.005<k_c<0.013$) inside of which we chose the k_c value (k_c=0.009). However,

the qualitative results of the model would not be different if we had chosen any other value within that range.

The absence of an entrainer induced a dispersed distribution of single cell phases (Figure 4.1.2A) and a normally distributed pattern in cell periods (Figure 4.1.2B). In particular, unentrained oscillators ($t < 200hr$ and $t>1000hr$, Figure 4.1.3) have a blunted ensemble average similar to the experimentally observed flattening of clock gene rhythmicity when cells are in *in vitro* unentrained conditions (Kino, De Martino et al. 2003), while entrained states lead to a robust rhythm. As was theoretically hypothesized by Balsalobre *et al*. (Balsalobre, Damiola et al. 1998) and experimentally tested by Nagoshi *et al*. (Nagoshi, Saini et al. 2004) and Welsh *et al*. (Welsh, Yoo et al. 2004), this flattening of population-level rhythmicity we observed is an outcome of phase drifting between robust oscillators rather than the loss of individual cellular rhythms. In the *in silico* experiment of Figure 4.1.4, our model predicts the desynchronization of peripheral cells when cortisol's amplitude fall below a critical value (regime **I** and **II**). Given the relationship between circadian rhythms and recovery from critical illness (Chrousos and Gold 1998; Carlson and Chiu 2008), effects of perturbations to cortisol's circadian rhythmicity are particularly interesting because, in addition to its role as a circadian entrainer described here, cortisol plays a critical role as an anti-inflammatory hormone. Furthermore, experimental evidence from severely burned adults indicates that the amplitude of cortisol in stressed patients is diminished, corresponding to our second regime of synchronization (Amplitude $=1-F_{min}/F_{max} \sim 0.38$) (Hobson, Havel et al. 2004). Recently, human endotoxemia experiments showed that there is both an acute increase in cortisol and a time-of-day-

independent resetting of clock gene expression in response to endotoxin treatment (Haimovich, Calvano et al. 2010), which further points to an interaction between cortisol, circadian rhythmicity, and inflammation. Godin and Buchman (Godin and Buchman 1996) hypothesized that systemic inflammation might lead to uncoupling between biological oscillators and that this loss of inter-organ communication may be important in the progression and recovery of critically ill patients. In this context, the loss of central diurnal signals, leading to the desynchronization of peripheral clocks manifested as greater signal regularity in the ensemble level (Figure 4.1.3), can be viewed as a loss of communication between the SCN and peripheral tissues. Thus, a chronically stressed patient might not retain the beneficial properties of circadian rhythms in peripheral tissues (Gachon, Nagoshi et al. 2004).

Given the presence of stochastic noise in our system and that there is no intercellular coupling among the peripheral cells in our model, it is not surprising that cells fall out of phase as the rhythmic entraining input decreases. While it is known that the entrainment of SCN neurons depends on intercellular coupling, cells in peripheral tissues display different entrainment dynamics that can generally be explained by their lack of strong coupling (Yamazaki, Straume et al. 2002; Liu, Welsh et al. 2007; Abraham, Granada et al. 2010). As a result, the degree and rapidity with which the individual cells fall out of phase depends upon the amount of stochastic noise, which in our case is determined by the formulation of the CLE algorithm and the reaction propensities, and the amplitude of the entraining signal. However, Figure 4.1.4 reveals an unintuitive dynamic of peripheral cell entrainment, where

individual cells maintain relative synchronicity as they drift away from their cortisol-entrained phases. Evidence supporting this finding comes from feeding experiments (Zvonic, Ptitsyn et al. 2006), where temporally restricted feeding induces not only a phase shift in the expression of clock genes but also flattened cortisol rhythmicity. Furthermore, it has been observed that peripheral blood mononuclear cells of cancer patients, under exposure to a blunted systemic cortisol rhythm, maintain a phase shifted profile (Azama, Yano et al. 2007). Our model predicts this phase shifting regime when cortisol has slightly lost its amplitude rhythmicity (Figures 4.1.5A-5D, μ value). In this regime, individual cells are normally distributed and the standard deviation is low, denoting the high level of synchronization in the population of cells. For further decreases of cortisol's amplitude, individual cells become desynchronized and adopt phases through the entire range from 0 to 2π (Figure 4.1.5E), culminating in a uniform distribution where cells are fully desynchronized (Figures 4.1.5G-5H).

In our model, we consider the transcriptional effects of glucocorticoids on peripheral clock genes using a fairly simple mathematical model that incorporates negative and positive feedback loops mediated by the PER/CRY protein complex. Additionally, our model takes into account important non-transcriptional effects of glucocorticoids. Recent experiments of Nader *et al.* and Charmandari *et al.* (Nader, Chrousos et al. 2009; Charmandari, Chrousos et al. 2011) show a direct linkage between clock gene rhythmicity and glucocorticoid effects both in HeLa and HCT116 cell lines as well as in peripheral blood mononuclear cells. Specifically, the CLOCK/BMAL1 transcription factor acetylizes the glucocorticoid-receptor complex at a

multiple lysine cluster in its hinge region, producing inefficient binding of the complex to GRE in a time dependent manner. These two signals (CLOCK/BMAL1 production and glucocorticoid/receptor binding to GRE) are in rhythmic synchrony, resulting in decreased tissue sensitivity to cortisol in the morning when cortisol levels are high, and increased sensitivity at night when cortisol reaches its nadir. Consequently, a phase shift in CLOCK/BMAL1 clock gene rhythmicity may indirectly affect the impact of glucocorticoids in peripheral tissues through altering the tissue's sensitivity to glucocorticoids.

Our simulations show that even when the cells are phase shifted relative to the entrainer, their individual period remains equal to that of the entrainer (Figures 4.1.6A-6D). In particular, cortisol imposes its period for all the amplitudes of the third regime (III) of Figure 4. In contrast with the corresponding individual phases (Figures 4.1.5A-D), the deviation of cell periods for the third regime of entrainment is very small. This is an outcome of entrainment dynamics. Generally, a population of cells (oscillators) that is synchronized by an entrainer retains two characteristics. Firstly, all individual cells adopt the period of the entrainer (Figures 4.1.6A-D) and secondly, the individual cell phases are phase locked relative to the entrainer. This is also true for our model in the regime of synchronization (Figures 4.1.5A-5D and Figures 4.1.6A-6D). However, the stochastic nature of cell dynamics leads different cellular oscillators to adopt slightly different periods and phases (Figure 4.1.2B). Consequently, while the individual cell periods can only slightly deviate from the circadian period, there is a wider regime of individual cell phases that retain the phase locking characteristic. For the case where

cortisol has nearly no rhythmicity (Figures 4.1.5H and 4.1.6H), individual cell phases are uniformly distributed (Figure 4.1.6H) while individual cell periods adopt a normal distribution due to the absence of an entraining rhythm (Figure 4.1.5H). At this point, it is interesting to note that our model predicts that the presence of even a very small amplitude entraining signal induces a reduction in the mean period of the population relative to unentrained cells (Figure 4.1.2B versus Figure 4.1.5H). Changes in population periodicity relative to entrainer concentration has also been observed in synthetic oscillators (Stricker, Cookson et al. 2008)

As cortisol's amplitude decreases, cells gradually fall out of sync. In particular, we observe the increasing prominence of a second distribution of individual cell periods (Figure 4.1.6E) that further increases (Figures 4.1.6F and 4.1.6G) and finally becomes the only period distribution of the population (Figure 4.1.6H). This dynamic denotes the "movement" of the population from the regime of synchronization to the regime of desynchronization. This transition happens in a gradual manner. Similar to what was observed for cell phases (Figure 4.1.5E), where we see a gradual dispersion of cell phases that corresponds to the second regime of synchronization (Figure 4.1.4, II), for cell periods we see a transition of cell periods from a regime where they are distributed narrowly around the circadian period of cortisol to a regime where they are distributed with a different mean period.

It is well established that disruption of cortisol circadian periodicity is associated with detrimental outcomes (Filipski, Delaunay et al. 2004). Whether the disruption of cortisol rhythm is a cause or a consequence is an ongoing research problem. In our model we approached this issue by

examining the consequence of a disrupted central systemic entrainment on the expression of peripheral circadian clocks.

Figure 4.1.7 shows that high levels of synchronization are achieved only for cortisol periods close to the individual cell period (23.4hr). In particular, although individual cell phases adopt a nearly uniform distribution for cortisol periods far from the individual cell frequency (Figures 4.1.8A-4.1.8B), as cortisol's period approaches that of individual cells, we see a gradual concentration of cell phases around a mean value and a concurrent reduction of standard deviation (Figure 4.1.8C) until the regime of entrainment (Figure 4.1.8D). The dynamics of our model lie in qualitative accordance with the experimental results of Palomino *et al*. (Mondragon-Palomino, Danino et al. 2011). In their experiment, they used a synthetic genetic oscillator with arabinose as the entraining signal and observed that for entrainer periods near the free synthetic oscillator period, oscillators' phases adopt a dense distribution whereas for periods away of this regime the synthetic oscillators adopt a "double trough" uniform distribution. In the same experiment they also observed the formation of a bimodal distribution similar to what we observed (Figures 4.1.9B and 4.1.9E) as the entrainer period approaches and departs from values that induce the entraining regime.

Both Figure 4.1.6 and Figure 4.1.9, in accordance with experimental evidence (Mondragon-Palomino, Danino et al. 2011), reveal the existence of two distinct dynamic states. Disruption of cortisol rhythms, either by flattening its amplitude or by changing its circadian period, leads the peripheral clock genes to a new non-homeostatic steady state where individual cells have lost their entraining characteristics both respective to their individual cell periods

and individual cell phases. However, our model predicts that even for homeostatic cortisol amplitudes and frequencies, individual cells retain a dynamically varying level of synchronization throughout the day.

There is a circadian time structure associated with many diseases. For example, patients suffering from cardiovascular diseases are at a higher risk of cardiac death (30%) in the morning (Cohen, Rohtla et al. 1997; Hastings, Reddy et al. 2003). Peripheral clocks may play a crucial role in this context since their rhythmic output directly regulate circadian generation of heart beat rhythms (Jeyaraj, Haldar et al. 2012). In addition, the experiments of Balsalobre *et al*. (Balsalobre, Brown et al. 2000) showed that liver's clock genes profiles after injection of dexamethasone produces different phase shifting behavior in the population depending to the time that dexamethasone is administered, further illustrating the dynamic nature of peripheral clock gene behavior. Our modeling effort revealed that the level of synchronization, even at states of high entrainment (homeostatic cortisol amplitude and frequency), is dynamic. When calculating the $R_{syn,1}$ metric in consecutive 2hr time windows for a period of 24hr, we see that synchronization fluctuates, with minimum values at *Per/Cry* mRNA's nadir and zenith (Figure 4.1.10A). In these regions, single cell profiles follow uncorrelated dynamics leading the denominator of the $R_{syn,1}$ formula (mean variance of each oscillator) to increase (Figures 4.1.10B and 4.1.10C). In contrast, at other times, cells adopt highly coherent profiles (Figure 4.1.10D). This more local analysis reveals that, although in macroscale cells are highly entrained by cortisol's rhythmic pattern, there are certain periods of the day where cell oscillators are desynchronized (nadir and zenith levels, Figures 10B and 10C). This further

implies that there are certain times throughout the day when the host may be more vulnerable to external stimuli leading to desynchronization.

In summary, our model is able to predict and evaluate a number of experimental observations, including the necessity of a significant systemic rhythm for the synchronization of the peripheral clocks (Figures 4.1.3 and 4.1.4) and that even mild changes in the amplitude pattern of the entrainer can have indirect effects through altering the orchestration of local networks (*e.g.* acetylization induced by CLOCK/BMAL1) (Figures 4.1.5 and 4.1.6). Furthermore, upon changing either the amplitude or frequency of the entrainer, the transition from the unentrained to entrained state and vice versa happens in a gradual manner, as can be observed in the bimodal distributions of Figure 6 and Figure 9. Our results show that dysregulated cortisol rhythmicity can induce desynchronization of peripheral clock genes, uncoupling them from the systemic circadian network.

4.2: Mathematical modeling of light mediated HPA axis activity and downstream implications on the entrainment of peripheral clock genes.

4.2.1: Introduction

Physiologically, secretion of glucocorticoids is regulated in the paraventricular nucleus (PVN) of the hypothalamus, where corticotropin releasing hormone (CRH) functions as the principal hypothalamic stimulus for the production of adrenocorticotropic hormone (ACTH) from the anterior pituitary, which in turn drives the secretion of cortisol by the adrenal cortex

(Antoni 1986). Eventually, cortisol feeds back in a negative manner to both the PVN and the anterior pituitary to inhibit the release of CRH and ACTH respectively, forming a negative feedback loop that enables the hypothalamic–pituitary–adrenal (HPA) axis and ultimately cortisol to maintain circadian oscillations (Chrousos 1995; Buckley and Schatzberg 2005; Sriram, Rodriguez-Fernandez et al. 2012).

In diurnal species (such as human) the autonomous circadian activity of HPA axis is entrained to the 24hr light/dark cycles so as to maintain an increased cortisol secretion in the morning hours as the organism is anticipating the impending activity phase, and a reduced production at night as the organism enters its rest phase (Chrousos 1995). However, when light perception is partially or totally absent, the host is uncoupled from the environment and adopts its free-running (intrinsic) rhythms that can have slightly greater or smaller periods than 24hr (Campbell, Dawson et al. 1993; Duffy, Cain et al. 2011). The majority of evidence indicate that free-running HPA axis maintains autonomous rhythmicity where cortisol exhibits circadian rhythm albeit of increased, i.e., greater than 24 hr, period (Miles, Raynal et al. 1977; Orth, Besser et al. 1979; Sack, Lewy et al. 1992). Generally, cortisol rhythmicity that deviates from the homeostatic 24hr may denote the loss of entrainment between the body's internal clock and environmental light/dark cycles, and is related with recurrent insomnia and daytime sleepiness in blind individuals (Nakagawa, Sack et al. 1992). Changes in cortisol's rhythmic patterns have been also documented in chronically jet-lagged subjects or shift workers (Sack, Auckley et al. 2007) and have been associated with a number of comorbidities such as cardiovascular disease, gastrointestinal discomfort,

and cancer (Hampton, Morgan et al. 1996; Knutsson, Hallquist et al. 1999; Stevens, Blask et al. 2007). On the other hand, light treatment has been shown to realign and entrain the rhythm of cortisol as well as melatonin, promoting the adaptation of individuals to environmental cycles (Boivin and Czeisler 1998; James, Walker et al. 2004). Therefore, a systematic analysis of the dynamic interactions between light and the HPA axis would reveal characteristics mediating successful entrainment resulting in robust cortisol amplitudes, and likely identify parameters that regulate the adaptation strategy. Numerous studies have shown that light can phase shift the circadian rhythms of cortisol and melatonin in human subjects (Czeisler, Kronauer et al. 1989; Shanahan and Czeisler 1991; Touitou, Benoit et al. 1992; Van Cauter, Sturis et al. 1994). Despite the critical importance of melatonin and its use as a target hormone to reset body rhythms (Shanahan, Kronauer et al. 1999; Lewy, Emens et al. 2006), our work currently focuses on cortisol as a prototypical regulatory hormone and reliable circadian markers of human body (Boivin and Czeisler 1998).

As was discussed in Chapter 3 and 4.1, peripheral tissues also maintain circadian rhythmicity mediated by the cell based machinery of clock genes (CGs) which through transcriptional, and translational negative and positive feedback loops maintain circadian activity. The light mediated HPA axis activity makes cortisol a putative systemic entrainer of the circadian function of the periphery of the body (Stratmann and Schibler 2006). Given the central role of PCGs in coordinating circadian physiology (Hastings, O'Neill et al. 2007), this work aims to elucidate the dynamics of light mediated HPA axis activity that ultimately lead to entrainment of PCGs..

The importance a) of light regulated cortisol secretion and b) of PCGs as the basic cellular machinery for peripheral circadian timekeeping motivates the need for a quantitative characterization of the interactions between the two. In that respect, mathematical modeling is a critical enabler towards developing a better understanding of the underlying dynamics. Although there is considerable prior work focusing on mathematical modeling of the circadian and ultradian dynamics of the HPA axis (Scheff, Calvano et al. 2010; Walker, Terry et al. 2010; Sriram, Rodriguez-Fernandez et al. 2012) as well as models incorporating HPA interaction with light (Jelic, Cupic et al. 2005; Kyrylov, Severyanova et al. 2005; Vinther, Andersen et al. 2011) in the present work we extend the work of the previous section (4.1) by exploring the ability of light's rhythmic characteristics to entrain the HPA's autonomous clock thus adjusting cortisol's period and phase relative to light/dark cycles (Czeisler, Duffy et al. 1999).

By taking into consideration the autonomous oscillations of the HPA axis, we aim to investigate the entrainment of different light schedules and their ultimate effects on the cortisol's rhythmic characteristics. Expanding on our previous work (Mavroudis, Scheff et al. 2012), we propose a two level model that simulates the HPA axis as the central component entrained by light/dark cycles and a population of PCGs as the peripheral component synchronized by cortisol. This two level model is leveraged to understand the ultimate effects of photoperiod characteristics on the synchronization of PCGs which are mediated by changes in the rhythmic patterns of cortisol secretion.

Our integrated model enabled us to reveal time-of-day characteristics of the HPA responsiveness, and in particular, the increased sensitivity to light

during cortisol's rising phase as well as the dependence of cortisol's rhythmic dynamics on light's intensity. Importantly, our model uncovered a sensitivity of the HPA axis amplitude to different photoperiods which denotes the functional relationship between light/dark schedules and cortisol rhythm. Furthermore, we demonstrate that high cortisol amplitudes mediated through a balanced light/dark ratio lead to high level of synchronization of the population of PCGs, whereas light schedules of either very long or very short photoperiods induce higher desynchronization that lead to lower PCGs ensemble amplitude which further indicates a loss of transmission of circadian information to the periphery of the body.

4.2.2: Materials and Methods

In the present work we accounted for the circadian variability present in the light schedule as well as the central and peripheral levels of the body. Each of the levels maintains autonomous oscillations of constant period. At the central level we consider the release of cortisol, originated by the negative feedback in the HPA axis between CRH, ACTH, and cortisol (F), ultimately entrained by the light/dark cycles (environmental cues), while at the peripheral level we describe the network of clock genes at peripheral cells entrained by F (Figure 4.2.1).

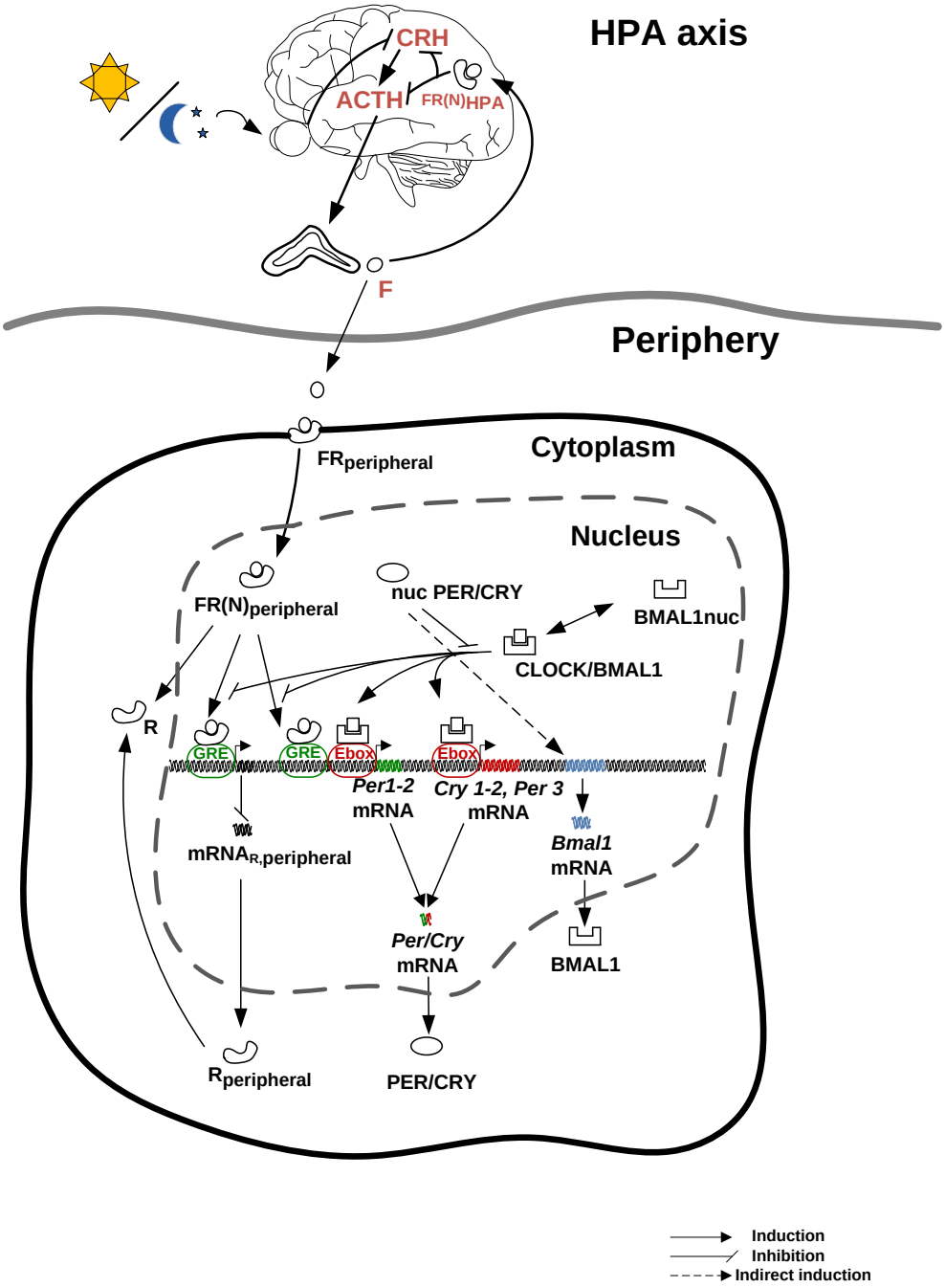

Figure 4.2 1: Schematic representation of the multi-level model. The hypothalamic pituitary adrenal (HPA) axis is entrained to the light/dark cycles. Downstream, the positive and negative feedback of the peripheral clock genes (PCGs) induce peripheral rhythms entrained to cortisol.

4.2.2.1: HPA axis and cortisol signal transduction in the hypothalamus and the anterior pituitary

The mathematical representation of the HPA axis involves the approximation of the rhythmic response of CRH, ACTH and F (Eq. 4.2.1-3). Its structure is based on the Goodwin oscillator refined further to include Michaelian kinetics for the degradation terms in the hypothalamic, pituitary, and adrenal regions in order to avoid the use of unrealistically high Hill coefficients (Gonze, Bernard et al. 2005) . The CRH production is regulated by a zero order production term (Eq. 4.2.1) and further stimulates the secretion of ACTH (Eq. 4.2.2) which in turn activates the production of F (Eq. 4.2.3). F then feeds back to the hypothalamus where it inhibits the secretion of CRH and ACTH as suggested in (Sriram, Rodriguez-Fernandez et al. 2012). This negative feedback of cortisol has been also assumed to induce ultradian rhythmicity (Walker, Terry et al. 2010) and mathematical models have been constructed in order to take into consideration both the ultradian and the circadian component of the feedback mechanism (Faghih, Savla et al. 2011). However, at the current work we evaluate only the generation of circadian rhythmicity.

The physiological actions of cortisol are mediated through the glucocorticoid receptor. (Boyle, Brewer et al. 2005) have shown that alterations in forebrain glucocorticoid receptor, is a causative effect of major depressive disorders that are highly related with cortisol blunted amplitude (Chrousos and Gold 1998). Therefore, in order for F to feed back to the hypothalamus or anterior pituitary and mediate its inhibiting effects, it needs to bind to its receptor in these brain regions and transduce its signal to the

nucleus of the cells. In order to describe this signal transduction, we explored a glucocorticoid pharmacodynamic model (Ramakrishnan, DuBois et al. 2002) that has been also used in the previous section 4.1 (Eq. 4.2.4-7).

The autonomous oscillations of the HPA axis are entrained by the suprachiasmatic nucleus (SCN), a hypothalamic region above the optic chiasm which senses photic information and functions as the central endogenous pacemaker of the body's internal clock (Dibner, Schibler et al. 2010). In particular, experiments have demonstrated that SCN mediated secretion of arginine vasopressin (AVP), is crucial for the maintenance of PVN neuronal firing (Tousson and Meissl 2004; Kalsbeek, Fliers et al. 2010). Furthermore, microinfusions of AVP to rodent's hypothalamus resulted in significant downregulation of adrenal corticosterone (Kalsbeek, Buijs et al. 1992). (Jung, Khalsa et al. 2010) have also shown that acute photic stimuli in humans, induced a downregulation of their cortisol levels. Therefore, our underlying hypothesis is that light entrains the circadian production of cortisol to a 24hr period by regulating the degradation of the PVN's output, CRH. Light cycles are modeled as a step function (Eq. 4.2.8), active for 12 hours during the light period (i.e. 6am to 6pm) and inactive during the dark period between (i.e. 6pm to 6am). Light response is further modulated through the saturation of photoreceptors (Eq. 4.2.1).

$$\frac{dCRH}{dt} = \frac{k_{p1}}{K_{p1} + FR(N)_{HPA}} - V_{d1} \cdot \frac{CRH \cdot \left(1 + \frac{light}{1 + light}\right)}{K_{d1} + CRH} \quad (4.2.1)$$

$$\frac{dACTH}{dt} = \frac{k_{P2} \cdot CRH}{K_{p1} + FR(N)_{HPA}} - V_{d2} \cdot \frac{ACTH}{K_{d2} + ACTH} \quad (4.2.2)$$

$$\frac{dF_{HPA}}{dt} = k_{P3} \cdot ACTH - V_{d3} \cdot \frac{F_{HPA}}{K_{d3} + F_{HPA}} \quad (4.2.3)$$

$$\frac{dmRNA_{R,HPA}}{dt} = k_{syn\_Rm} \cdot \left(1 - \frac{FR(N)_{HPA}}{IC_{50\_Rm} + FR(N)_{HPA}}\right) - k_{\deg} \cdot mRNA_{R\_HPA} \quad (4.2.4)$$

$$\frac{dR_{HPA}}{dt} = k_{syn\_R} \cdot mRNA_{R\_HPA} + r_f \cdot k_{re} \cdot FR(N)_{HPA} - k_{on} \cdot (F_{HPA} - 1) \cdot R_{HPA} - k_{dgr\_R} \cdot R_{HPA} \quad (4.2.5)$$

$$\frac{dFR_{HPA}}{dt} = k_{on} \cdot (F_{HPA} - 1) \cdot R_F - k_T \cdot FR_{HPA} \quad (4.2.6)$$

$$\frac{dFR(N)_{HPA}}{dt} = k_T \cdot FR_{HPA} - k_{re} \cdot FR(N)_{\mathrm{HPA}} \quad (4.2.7)$$

$$light = \begin{cases} 1\,, & 6am \le t < 6\,pm \\ 0\,, & 6\mathrm{pm} \le t < 6am \end{cases} \quad (4.2.8)$$

The characteristics of the intrinsic cortisol rhythms are inferred from free-running rhythms of individuals living in carefully controlled, mild light conditions (~0.03-150 lux), and indicate an intrinsic period of 24.18 ±0.04 hours (Czeisler, Duffy et al. 1999). Intrinsic period has been calculated after averaging the period estimates of core body temperature, plasma melatonin, and cortisol rhythm. Furthermore, based on the available evidence, we hypothesized that cortisol's rhythmicity in absence of light maintains an amplitude and mean value that are largely within normal limits (Reppert, Perlow et al. 1981; Hermann, von Aulock et al. 2006).The parameters used in the model are taken from our previous work (Scheff, Calvano et al. 2010).

4.2.2.2: Cortisol signal transduction in periphery and PCGs entrainment.

Based on our prior work (Mavroudis, Scheff et al. 2012) (Equations 10-20), we modeled the entrainment dynamics of PCGs by taking into consideration the binding of cortisol receptor nuclear complex to the glucocorticoid responsive element (GRE) at the promoter region of *Per1* and *Per2* clock genes (Eq. 4.2.14) (Yamamoto, Nakahata et al. 2005; So, Bernal et al. 2009). The model of PCGs is same as this used in previous section 4.1 (Eq. 4.2.14-20). In order to further account for the delay present at the transportation of the central cortisol signal to the peripheral cells, we applied a transit compartment model ($F_{periphery}$), by using a mean transient time delay τ=15min which we assumed to be equal with the delay present between ACTH production and F secretion (Papaikonomou 1977; Walker, Terry et al. 2010) (Eq. 4.2-9). Finally, we hypothesized that the glucocorticoid receptors present in the peripheral tissue retain the same physiochemical properties as to that of brain level and as such the parameters of the Eq. 4.2.10-13 were the same as that of the Eq. 4.2.4-7 and same as the original model (Ramakrishnan, DuBois et al. 2002). Similarly, parameters of PCGs network have been based on prior work (Becker-Weimann, Wolf et al. 2004) and can be shown on Table 4.2.1.

$$\frac{dF_{periphery}}{dt} = \frac{1}{\tau}\cdot\left(F_{HPA} - F_{periphery}\right) \tag{4.2.9}$$

$$\frac{dmRNA_{R\_periphery}}{dt} = k_{syn\_Rm}\cdot\left(1-\frac{FR(N)_{periphery}}{IC_{50\_Rm}+FR(N)_{periphery}}\right) - k_{\deg}\cdot mRNA_{R\_periphery} \tag{4.2.10}$$

$$\frac{dR_{periphery}}{dt} = k_{syn\_R}\cdot mRNA_{R\_periphery} + r_f\cdot k_{re}\cdot FR(N)_{periphery} - k_{on}\cdot(F_{periphery}-1)\cdot R_{periphery} - k_{dgr\_R}\cdot R_{periphery} \tag{4.2.11}$$

$$\frac{dFR_{periphery}}{dt} = k_{on}\cdot\left(F_{periphery}-1\right)\cdot R_{periphery} - k_T\cdot FR_{periphery} \tag{4.2.12}$$

$$\frac{dFR(N)_{periphery}}{dt} = k_T\cdot FR_{periphery} - k_{re}\cdot FR(N)_{periphery} \tag{4.2.13}$$

$$\frac{dPer/Cry_{mRNA}}{dt} = \frac{v_{1b}\cdot\left(CLOCK/BMAL1+c\right)}{k_{1b}\cdot\left(1+\left(\frac{nucPER/CRY}{k_{1i}}\right)^p\right)} - k_{1d}\cdot y_1 + k_c\cdot\frac{\mathrm{FR(N)}}{CLOCK/BMAL1} \tag{4.2.14}$$

$$\frac{dPER/CRY}{dt} = k_{2b}\cdot Per/Cry_{mRNA}{}^q - k_{2d}\cdot PER/CRY - k_{2t}\cdot PER/CRY + k_{3t}\cdot nucPER/CRY \tag{4.2.15}$$

$$\frac{dnucPER/CRY}{dt} = k_{2t}\cdot PER/CRY - k_{3t}\cdot nucPER/CRY - k_{3d}\cdot nucPER/CRY \tag{4.2.16}$$

$$\frac{dBmal1_{mRNA}}{dt} = \frac{v_{4b}\cdot nucPER/CRY^r}{k_{4b}^r + nucPER/CRY^r} - k_{4d}\cdot Bmal1_{mRNA} \tag{4.2.17}$$

$$\frac{dBMAL1}{dt} = k_{5b}\cdot Bmal1_{mRNA} - k_{5d}\cdot BMAL1 - k_{5t}\cdot BMAL1 + k_{6t}\cdot nucBMAL1 \tag{4.2.18}$$

$$\frac{dnucBMAL1}{dt} = k_{5t}\cdot BMAL1 - k_{6t}\cdot nucBMAL1 - k_{6d}\cdot nucBMAL1 + k_{7a}\cdot CLOCK/BMAL1 - k_{6a}\cdot nucBMAL1 \tag{4.2.19}$$

$$\frac{dCLOCK/BMAL1}{dt} = k_{6a}\cdot nucBMAL1 - k_{7a}\cdot CLOCK/BMAL1 - k_{7d}\cdot CLOCK/BMAL1 \tag{4.2.20}$$

Table 4.2 1: List of parameters used in the model (Eq. 4.2.1-20).

Parameter	Value	Units	Description/Reference
kp1	0.7965	μM/hr	Rate of CRH production/Estimated
Kp1	1.0577	μM	Dissociation constant for CRH production/Estimated

Vd1	0.5084	μM/hr	Rate of CRH enzymatic degradation /Estimated
Kd1	1.9627	μM	Michaelis constant of CRH enzymatic degradation/Estimated
kp2	0.6857	1/hr	Rate of ACTH production/Estimated
Vd2	0.5129	μM	Rate of ACTH enzymatic degradation /Estimated
Kd2	0.3069	μM/hr	Michaelis constant of ACTH enzymatic degradation/Estimated
kp3	0.7097	1/hr	Rate of $F_{central}$ production/Estimated
Vd3	0.3618	μM/hr	Rate of $F_{central}$ enzymatic degradation /Estimated
Kd3	0.4695	μM	Michaelis constant of $F_{central}$ enzymatic degradation/Estimated
k_{syn_Rm}	2.9	fmol/g/hr	Synthesis rate or glucocorticoid receptor mRNA /(Ramakrishnan, DuBois et al. 2002)
IC_{50_Rm}	26.2	nmol/L/mg protein	Concentration of FR(N) at which $mRNA_{,R}$ synthesis drops to its half/ (Ramakrishnan, DuBois et al. 2002)
R_0	540.7	nM/L/mg protein	Baseline value of free cytosolic glucocorticoid receptor /(Ramakrishnan, DuBois et al.

			2002)
R_{m0}	25.8	fmole/gr	Baseline value of glucocorticoid receptor mRNA/ (Ramakrishnan, DuBois et al. 2002)
k_{dgr_Rm}	k_{syn_Rm}/R_{m0}		Degradation rate of glucocorticoid receptor mRNA/ (Ramakrishnan, DuBois et al. 2002)
k_{dgr_R}	0.0572	1/hr	Degradation rate of cytosolic glucocorticoid receptor /(Ramakrishnan, DuBois et al. 2002)
k_{syn_R}	(R_0/R_{m0}) $*k_{dgr\_R}$		Synthesis rate of free cytosolic receptor/ (Ramakrishnan, DuBois et al. 2002)
R_f	0.49		Fraction of cortisol recycled /(Ramakrishnan, DuBois et al. 2002)
k_{re}	0.57	1/hr	Rate of receptor recycling from nucleus to cytoplasm /(Ramakrishnan, DuBois et al. 2002)
k_{on}	0.00329	L/nmole/hr	Second order rate constant of glucocorticoid receptor binding /(Ramakrishnan, DuBois et al. 2002)

k_t	0.63	1/hr	Rate of receptor translocation to the nucleus/ (Ramakrishnan, DuBois et al. 2002)
k_c	0.004	1/hr	Coupling strength
v_{1b}	9	nM/hr	Maximal rate of Per/Cry transcription/ (Becker-Weimann, Wolf et al. 2004)
k_{1b}	1	nM	Michaelis constant of Per/Cry transcription/ (Becker-Weimann, Wolf et al. 2004)
k_{1i}	0.56	nM	Inhibition constant of Per/Cry transcription/ (Becker-Weimann, Wolf et al. 2004)
c	0.01	nM	Concentration of constitutive activator /(Becker-Weimann, Wolf et al. 2004)
p	8		Hill coefficient of inhibition of Per/Cry transcription/ (Becker-Weimann, Wolf et al. 2004)
k_{1d}	0.12	1/hr	Degradation rate of Per/Cry mRNA/ (Becker-Weimann, Wolf et al. 2004)
k_c	0.0016	1/hr	Coupling constant /(Becker-Weimann, Wolf et al. 2004)
k_{2b}	0.3	1/nM/hr	Complex formation rate of Per/Cry mRNA /(Becker-Weimann, Wolf et al. 2004)

q	2		No. of PER/CRY complex forming subunits /(Becker-Weimann, Wolf et al. 2004)
k_{2d}	0.05	1/hr	Degradation rate of cytoplasmatic PER/CRY/ (Becker-Weimann, Wolf et al. 2004)
k_{2t}	0.24	1/hr	Nuclear import rate of the PER/CRY complex /(Becker-Weimann, Wolf et al. 2004)
k_{3t}	0.02	1/hr	Nuclear export rate of PER/CRY complex /(Becker-Weimann, Wolf et al. 2004)
k_{3d}	0.12	1/hr	Degradation rate of the nuclear PER/CRY complex/ (Becker-Weimann, Wolf et al. 2004)
v_{4b}	3.6	nM/hr	Maximal rate of Bmal1 transcription /(Becker-Weimann, Wolf et al. 2004)
k_{4b}	2.16	nM	Michaelis constant of Bmal1 transcription/ (Becker-Weimann, Wolf et al. 2004)
r	3		Hill coefficient of activation of Bmal1 transcription /(Becker-Weimann, Wolf et al. 2004)
k_{4d}	0.75	1/hr	Degradation rate of Bmal1 mRNA/ (Becker-Weimann, Wolf et al. 2004)

k_{5b}	0.24	1/hr	Translation rate of BMAL1 /(Becker-Weimann, Wolf et al. 2004)
k_{5d}	0.06	1/hr	Degradation rate of cytoplasmatic BMAL1 /(Becker-Weimann, Wolf et al. 2004)
k_{5t}	0.45	1/hr	Nuclear import rate of BMAL1 /(Becker-Weimann, Wolf et al. 2004)
k_{6t}	0.06	1/hr	Nuclear export rate of BMAL1/ (Becker-Weimann, Wolf et al. 2004)
k_{6d}	0.12	1/hr	Degradation rate of nuclear BMAL1/ (Becker-Weimann, Wolf et al. 2004)
k_{6a}	0.09	1/hr	Activation rate of nuclear CLOCK/BMAL1/ (Becker-Weimann, Wolf et al. 2004)
k_{7a}	0.003	1/hr	Deactivation rate of CLOCK/BMAL1 /(Becker-Weimann, Wolf et al. 2004)
k_{7d}	0.09	1/hr	Degradation rate of CLOCK/BMAL1 /(Becker-Weimann, Wolf et al. 2004)

4.2.2.3: Ensemble of cells and calculation of synchronicity, periodicity and phase

We opted to examine cell-cell variability introduced by uniformly sampling (±5%) the parameters of the Eq. 4.2.9-20 that represent the reactions that take place at the level of peripheral cell (Liu, Welsh et al. 2007). Various alternative methods could have been used including solution of the ordinary differential equations (ODEs) stochastically as we previously demonstrated (Mavroudis, Scheff et al. 2012) using the Gillespie or the Chemical Langevin equations (Gillespie 2000). For the purpose of our analysis, the results would not be dependent on the specific method used mainly due to the fact that, as we have already shown in (Mavroudis, Scheff et al. 2012), the entrainment of PCGs by cortisol would force the ensemble of cellsto adopt cortisol's period, and would lock its phase based on the rhythmic characteristics of cortisol. Therefore, we applied the simplest method that could generate a distribution of cell responses.

When the cortisol entrainer is absent (k_c=0, in Eq. 4.2.14), the variation of peripheral cells parameters causes the individual cells to oscillate at their intrinsic period (~23.4hours) but with different phases thus falling out of synch. In contrast, when k_c is set to its non-zero value (k_c= 0.004), cortisol entrains the population of cells imposing its period (either 24hr when HPA axis is entrained by light, or 24.2hr when HPA free-runs according to our inferred frequency to the model) and synchronizing their phases.

Period and phases are determined relative to cortisol's peak time. In particular, cortisol's period was estimated by calculating the time between two

consecutive peaks, and phase by calculating the time between the first peak and 12am which was assumed to be the reference phase. Next we calculated the phase on angular coordinates by $\Phi = \frac{2\pi \cdot \Delta t}{T}$ where T is the period of the cortisol rhythm and Δt the time difference between the peak and 12am.

In order to calculate the level of synchronization among f peripheral cells, similar to the previous section (4.1) we incorporated the degree of synchronization for *Per/Cry* mRNA, R_{syn} (Garcia-Ojalvo, Elowitz et al. 2004; Gonze, Bernard et al. 2005; Ullner, Buceta et al. 2009). R_{syn} has been calculated for a time span of 100hr.

4.2.3: Results

Our *in silico* studies aimed at characterizing the dynamics of interacting rhythms: light, cortisol, and PCGs, deciphering the complexities of their cross-communicating signals.

Figure 4.2.2 depicts the dynamics of the HPA axis hormones (CRH, ACTH, and F) as entrained by a rhythmic light stimulus of 24hr period. Entrainment leads HPA axis autonomous rhythm to adopt the 24hr period of light/dark cycles and as a result the HPA axis compartments to maintain a constant phase relative to light. For the purposes of our study we assume that a "typical" day is represented by a 12 hr Light /12 hr Dark cycle (12L/12D) with light onset at 6am and offset at 6pm. During the course of the day, light intensity is assumed constant. This is a typical way of representing an *in silico* day (Figure 4.2**A**). CRH and ACTH exhibit a small time delay in their peak responses since the secretion of CRH (Figure 4.2B) drives the secretion of

ACTH (Figure 4.2**C**) ultimately leading to the secretion of F (Figure 4.2D). The phase that cortisol adopts after light entrainment closely follows physiological observations (Hermann, von Aulock et al. 2006).

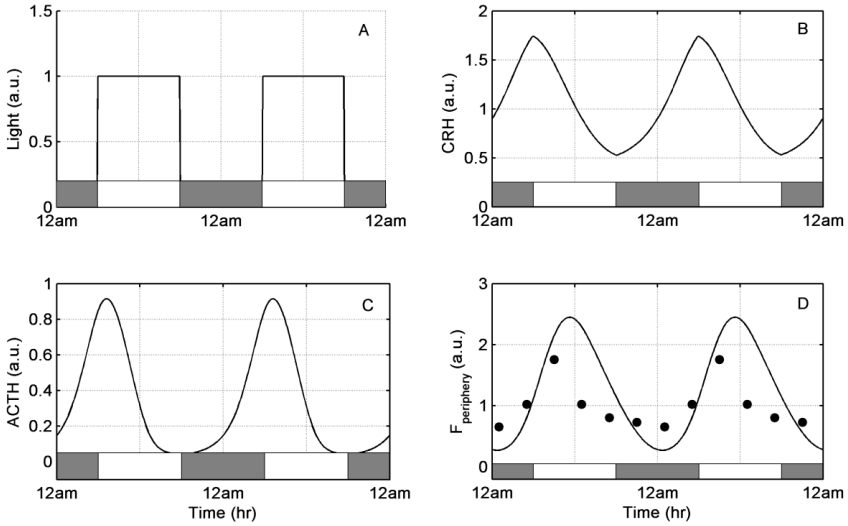

Figure 4.2 2: Responses of the HPA axis compartments under entrainment by periodic light A: Base line light profile is modeled as a step function equal to 1 between 6am and 6pm (light period) and 0 between 6pm and 6am (dark period). B,C: CRH and ACTH responses. D: Cortisol (F) in the periphery along with normalized experimental data (dots) for comparison (Hermann, von Aulock et al. 2006). a.u. stands for arbitrary units.

Initially we explored the effects of light's mean value to cortisol rhythm. Therefore, we compared cortisol's profile resulting from rhythmic light, to profiles resulting from constant light of varying intensities. (Figure 4.2.3A-D). Figure 4.2.3F-H depicts cortisol response corresponding to the various light schedules. Entrainment by rhythmic light induces robust cortisol amplitude that peaks at morning (Figure 4.2.3E, Amplitude (Amp)=2.2). However, constant light induces a blunted cortisol response (Figure 4.2.3F) further down-regulated as the intensity of light increases (Figure 4.2.3G&3H).

Similarly, Figure 4.2.4 illustrates the change in cortisol's period for different intensities of constant light. In the absence of light cortisol adopts the period that in accordance with experimental data (Czeisler, Duffy et al. 1999) we imposed to our model and is slightly greater than 24 hours (24.2 hr) and as the intensity of light increases, the period decreases.

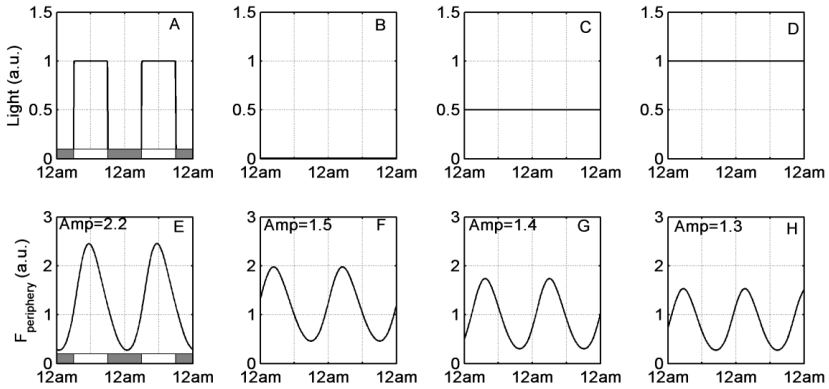

Figure 4.2 3: Cortisol response under rhythmic or constant light of increasing intensity. **A**: Rhythmic light profile. B,C,D: Constant light with intensity equal to the minimum (B), mean (C), and maximum (D) levels of the rhythmic light . E,F,G,H: Corresponding cortisol profiles and their amplitude values (Amp). a.u. stands for arbitrary units.

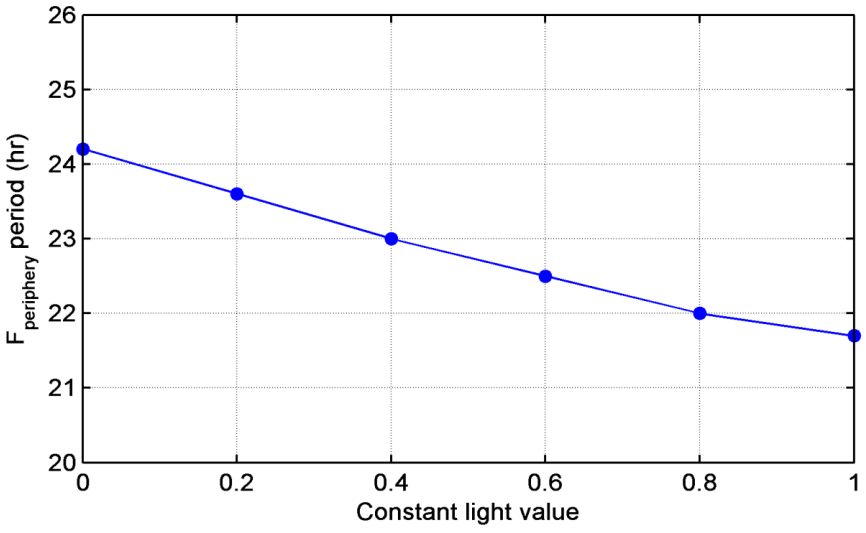

Figure 4.2 4: Cortisol period as a function of intensity of constant light.

In order to evaluate the sensitivity of the autonomous clock of the HPA axis to light, the system was exposed to persistent “dim” light conditions (low light intensity, no rhythmic variability, black line in Figure 4.2.5A) and a 6hr light stimulus nearly 100 times higher than its maximum rhythmic level was introduced at different times of the subjective time (Figure 4.2.5A-5B). Since in dim light conditions there is no rhythmic light entrainment, we assumed that subjective time equals to zero at the point where cortisol peaks in accordance with experiments setting subjective time to zero at the start of the activity period. Light stimuli induced different levels of downregulation to cortisol profile (Figure 4.2.5C) dependent on the phase where the stimulus was applied. Higher downregulation was observed when light was introduced at the increasing phase of cortisol (light blue, pink, brown curves) whereas light at the descending phase of cortisol induced a lower decrease (blue, green, red curves). Next, a phase response curve (PRC) was created by measuring the phase changes between the perturbed and unperturbed cortisol profiles (Figure 4.2.5D-5B). The resulting PRC was of type-1 with a very slight period of time where cortisol was insensitive to light stimulus resulting in a zero phase difference (“dead zone” when light was introduced at subjective time -12 and -4). These results, as further analyzed in the next section, are in agreement with experimental observations (Khalsa, Jewett et al. 2003; Jung, Khalsa et al. 2010).

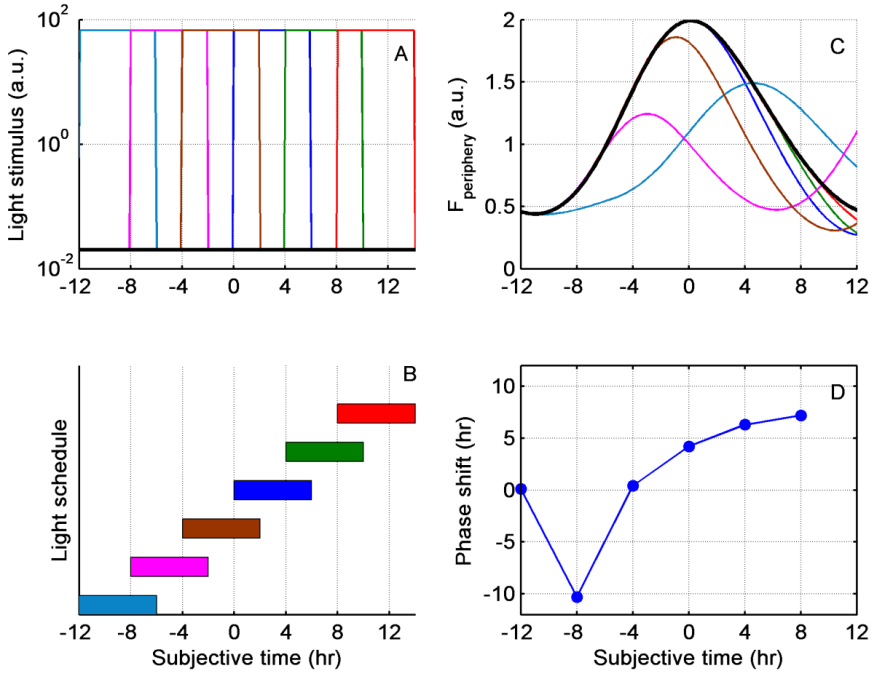

Figure 4.2 5: Effects of light stimulation at different times of cortisol cycle. A: Light stimulus of 6hr duration applied at different times of subjective time. Thick black line represents the "mild light" condistion B: Light schedule shown in caption A. C: Transient effects of light stimuli on cortisol's response immediately after the light perturbation. Thick black line represents the unperturbed cortisol profile under mild light conditions (constant routine) D: Phase response curve resulted from the light stimuli represented in A-B.

We then explored the implications of varying the L/D rhythmic characteristics ranging from very "long" (22L/2D) to very "short" (2L/22D) days in order to quantify how these photoperiod lengths impact the phase and amplitude characteristics of cortisol. Figure 4.2.6A-C depicts three different experiments of various light schedules: (a) the start of the light period is the same but the length of the light period varies (Figure 4.2.6A); (b) the middle of the light period remains the same while the length of the light period changes (Figure 4.2.6B); and (c) the end of the light period remains the same

and length varies (Figure 4.2.6C). Therefore the purpose of the experiment is to assess the interplay between cortisol's and light's entraining rhythmic characteristics.

In Figures 4.2.6D-F the radial dimension represents the amplitude of cortisol profiles and angular displacement cortisol's phase. Based on the results of Figure 4.2.6D we note that although there is a consistent phase shift, where the angle decreases as the photoperiod decreases - decreased angle from light green to yellow arrow, the amplitude initially increases (from photoperiod 22L/2D to 12L/12D) and then decreases (from photoperiod 12L/12D to 2L/22D) . Similarly, in Figure 4.2.6E&6F we observed that there is a peak in cortisol's amplitude near the 12hr Light/12hr Dark photoperiod as the phase is shifted from higher to lower values. However, we observed that decreased photoperiod induces a phase advance instead of a phase delay.

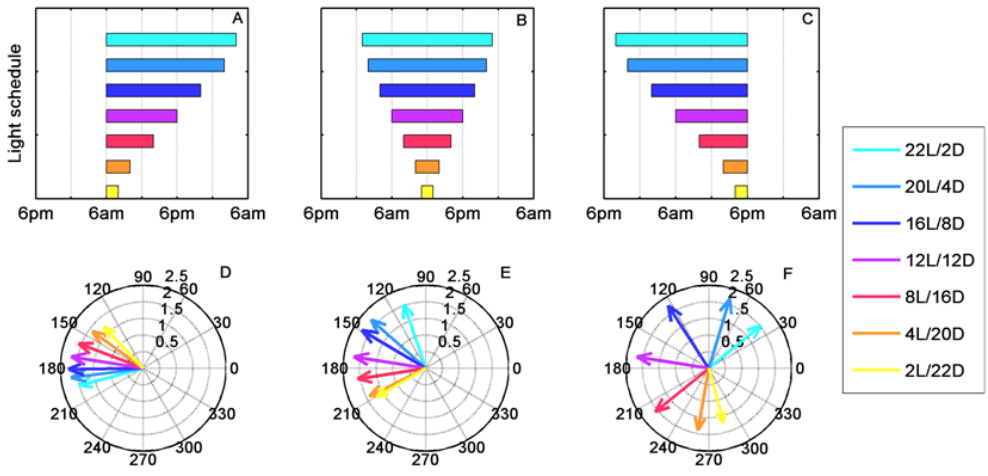

Figure 4.2 6: Cortisol's phase and amplitude for different photoperiods. A: Start of the light period remain constant while its duration is changing (6am) B: The mid-point of the light period remains the same while the photoperiod duration changes (12pm) C: The end of the light period remains constant (6pm) while the photoperiod changes. D-E-F: Compass plot

denoting cortisol's amplitude (radial dimension) and phase (angular dimension) for each of the corresponding light schedules (A-B-C).

To elucidate the effects of rhythmic characteristics of light on the dynamics of peripheral clock genes, we further analyzed the link between the HPA axis and a representative peripheral tissue consisting of 1000 cells. In Figure 4.2.7 we compared the effects of the12hr Light/12hr Dark photoperiod *(*Figure 4.2.7B**)** and the two extremes of 2hr Light/22hr Dark (Figure 4.2.7A) and 22hr Light/2hr Dark (Figure 4.2.7C) while keeping the middle of the light period the same, on the synchronization of PCGs. As our experiment in Figure 6 indicates, in the second row of Figure 4.2.7 denotes that the highly disrupted light schedules (2L/22D and 22L/2D) resulted in reduced cortisol's amplitude (Figure 4.2.7D&7F) compared with its amplitude when 12L/12D schedule is present (Figure 4.2.7E). This reduction in cortisol's amplitude further impacts the synchronization of the population of PCGs as it can be seen in the R_{syn} value of Figures 4.2.7G-I. In particular, compared to the 12L/12D profile of PCGs population that presented a very high synchronization (Figure 4.2.7H), light schedules of very short (2L/22D, Figure 4.2.7G) or very long (22L/2D, Figure 4.2.7I) photoperiod resulted in desynchronized states. Furthermore, we observed that the desynchronization at the single cell level is translated to a reduced ensemble average amplitude (bold line in Figures 4.2.7G-I).

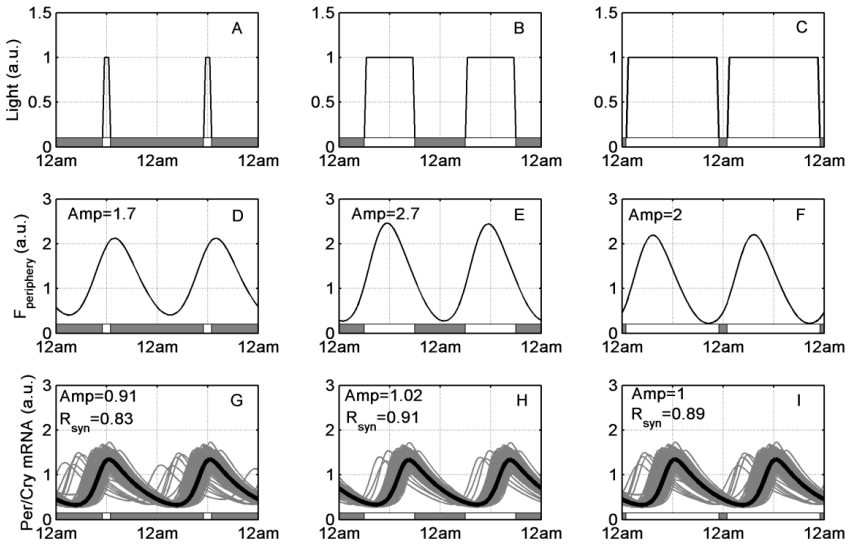

Figure 4.2 7: Effects of different light schedules on the synchronization of peripheral clock genes (PCGs). (A) 2L/22D; (B) 12L/12D; (C) 22L/2D light schedules. (D-F) Corresponding effects of different light schedules on cortisol's rhythm (Fperiphery) - "Amp" denotes amplitude. (G-I) Corresponding implications of different light schedules on the synchronization of *Per*/*Cry* mRNA on a population of cells (*Per/Cry* mRNA). Bold lines indicate ensemble average profiles of *Per/Cry* mRNA. Amp denotes amplitude of the ensemble average. . a.u. stands for arbitrary units.

Finally, we examined how the coupling strength between the HPA axis and periphery, as quantified by the parameter k_c (Eq. 4.2.14), impacts the synchronization of the population of PCGs and ultimately their ensemble phase. The light periods were changed by keeping the middle of the light period the same. Figure 4.2.8A depicts the model predictions while varying the photoperiod of light schedule for varying coupling strength. Low coupling strength (~0.001) results in low synchronization as quantified by R_{syn}. As the coupling strength increases (~0.003), PCGs present higher synchronization near "balanced" light'dark schedules (i.e.12hr photoperiod) compared to either

high or low photoperiods. Finally, for high entrainment strengths the population adopts high R_{syn} values in all photoperiods. In Figure 4.2.8B we observe that for low coupling, the cells are not synchronized and therefore PCGs ensemble phase does not consistently shifts according to different light schedules. For higher coupling strength, population of cells become synchronized and changes its ensemble phase according to photoperiod. In particular, we observe that as the photoperiod increases, ensemble phase delays.

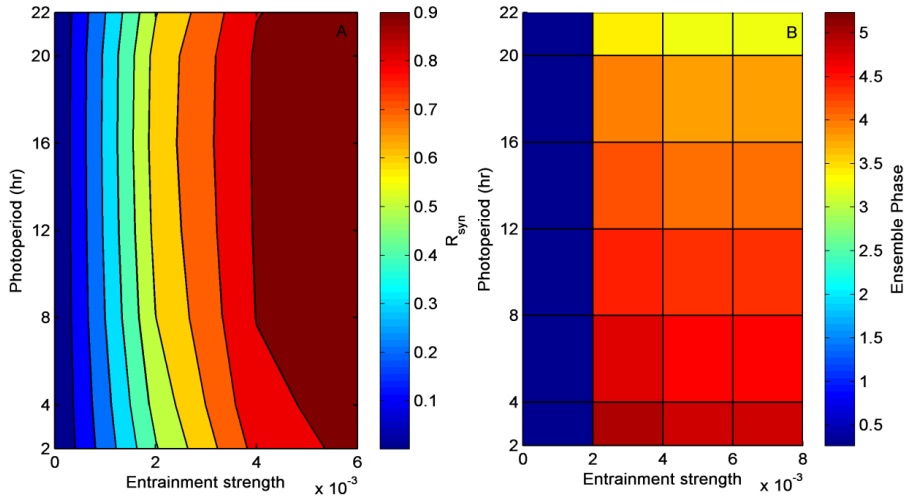

Figure 4.2 8: A: PCGs synchronization level as quantified by R_{syn} metric for different photoperiods and different coupling strengths (k_c, Eq. 4.2.14). B: PCGs ensemble phases for different photoperiods (L/D) and different coupling strengths (k_c, Eq. 4.2.14).

4.2.4: Discussion

Entrainment between the internal body clock and the environment is crucial for the maintenance of biological fitness. In this work, we investigated how the changes in light/dark characteristics impact the HPA-mediated

secretion of cortisol and ultimately the synchronization of a population of PCGs.

Recent evidence suggests that appropriate synchronization between the environment and the internal clock is critical for the recovery in a rodent model of sepsis (Carlson and Chiu 2008). In particular, it was observed that exposure to constant dark conditions following cecal ligation and puncture (CLP), increased mortality compared to exposure to 12hr Light/12hr Dark schedule. In our model, we hypothesized that light entrains the HPA axis via inhibition of the secretion of CRH in the hypothalamus (Figure 4.2.1). The interaction between light and CRH, entrains HPA compartments, namely CRH, ACTH, and F to the 24 hours light/dark period, and to a phase commanded by the phase of the light/dark rhythm. Although there are evidences that light can increase (Scheer and Buijs 1999; Leproult, Colecchia et al. 2001), decrease (Kostoglou-Athanassiou, Treacher et al. 1998; Jung, Khalsa et al. 2010), or has little effect (Leproult, Van Reeth et al. 1997; Lavoie, Paquet et al. 2003) on cortisol levels, our model is assumed to simulate the indirect inhibiting effects of arginine vasopressin (AVP) on the hypothalamus emanating from the central clock of SCN.

Observations in blind individuals (Orth, Besser et al. 1979; Sack, Lewy et al. 1992), as well as experiments investigating endogenous rhythms independent of external zeitgebers (Czeisler, Duffy et al. 1999), reveal that cortisol's autonomous period is slightly greater than 24 hours (24.1-24.5 hours) with robust amplitude. Therefore our HPA axis model (Eq. 4.2.1-3) was calibrated such that the intrinsic cortisol period in the absence of light is 24.2 hours while its amplitude and average levels are similar to those of

normal subjects (parameters shown in Table 4.2.1). Clearly, there are multiple groups of parameters that can be used in Equations 1-3 that can achieve the aforementioned characteristics. However, once the HPA axis is entrained by light, it adopts the 24hr period of light and a phase commanded by the functional form of the interactions with light. Therefore, despite the fact that we only adjusted parameters associated with cortisol's intrinsic rhythms (i.e. in the absence of light rhythmicity, constant dark), the introduction of light results in appropriate cortisol rhythmic patterns leading to morning peak values (Figure 4.2.2D) (Hermann, von Aulock et al. 2006).

Prior studies have examined circadian rhythms in order to discriminate between the internal rhythms and external zeitgebers, such as light/dark cycles or food intake, using experimental protocols that aim to disrupt the synchronization among them in order to focus on the free-run body clock (Duffy and Dijk 2002). These protocols ("constant routines") aim to reveal the endogenous circadian clock of the body by excluding external rhythmic stimulus such as light and sleep. In particular, in the context of light entrainment, these protocols incorporate the introduction of a very mild constant light. In our model, constant mild light enables the HPA compartments to adopt their autonomous rhythmic patterns with period of 24.2 hours similar to the one corresponding to complete lack of any light stimulus, i.e., constant darkness. When HPA axis is uncoupled with the environment, we can test the sensitivity of the autonomous HPA axis rhythm when it is perturbed by light stimuli at different times of subjective day (Figure 4.2.5A-5B). The resulted PRC (Figure 4.2.5D) revealed a characteristic type 1 PRC with significant point-to-trough amplitude with no prolonged "dead zone" of

photic insensitivity. This lies in accordance with the work of (Khalsa, Jewett et al. 2003) where they measured melatonin's PRC. Furthermore, under constant routine protocols CRH and $FRn_{central}$ oscillate in an antiphasic manner. This dynamic further leads to increased CRH/ACTH, and F sensitivity at their rising phase to light perturbations, since the inhibitory action of $FRn_{central}$ due to negative feedback (Eq. 4.2.1-2) is nearing its minimum. Therefore, in accordance with experimental data of (Jung, Khalsa et al. 2010), a bright light stimulus at the rising phase of cortisol, (Figure 4.2.5C light blue, pink and brown curves), due to the reduced intensity of $FRn_{central}$ negative feedback, leads to a more pronounced down-regulation compared to administration of stimulus at the descending phase (Figure 4.2.5B blue, green and red curves).

It is well established that different photoperiods induce different effects both in central hormones and in the periphery of the body especially in components related to immune function (Adams, Castanon-Cervantes et al. 2013). (Vondrasova, Hajek et al. 1997) have shown that exposure of human subjects to "summer" photoperiod (i.e., increased "light" period: 16L/ 8D) induced a 2hr phase advance to cortisol rise. Along similar lines (Laakso, Porkka-Heiskanen et al. 1994) reported that cortisol's peak in human subjects was significantly delayed in mid-winter compared to mid-summer and mid-autumn. In both of these experiments, shorter (winter) days were days where the light was introduced at later times of the day similar to our in-silico experiments of Figure 4.2.6B-C, E- F where shorter days such as 8L/16D, 4L/20D or 2L/22D, correspond to a light schedule where light increases later than the regular time of 6am. Our *in silico* predictions are in agreement with experimental observations predicting a consistent phase advance relative to

cortisol peak, as the photoperiod increases. This is due to interactions between the light and CRH degradation (Eq. 4.2.1) since increased light exposure at specific times of the day differentially affects CRH degradation. Therefore, as we advance or delay the time where light is introduced, relative to the intrinsic CRH rhythm (Figure 4.2.6), we simultaneously advance or delay the peak of CRH and as such its phase since we move forward or backward respectively the time that CRH will start to decrease. However when light was introduced at 6am (Figure 4.2.6A&6D) the difference among the various photoperiods is the time when light decreases that further induce a decreased degradation in CRH and ultimately an increased CRH production. A shorter light period will then signal an increase in CRH at an earlier time and as such a phase advance (Figure 4.2.6D). Recent experiments by (Otsuka, Goto et al. 2012) in rodents have shown that long photoperiods, in addition to phase shifting corticosterone rhythms, also result in an amplitude decrease compared to shorter photoperiods. Our model uncovers this type of response, in accordance with experimental data, characteristic of cortisol's amplitude changes as the photoperiod is changing. We further predict that near a 12 hr photoperiod is required for cortisol to maintain its maximum amplitude. The implication being that the rhythmic characteristics of light affect the amplitude of cortisol oscillation which has also been shown to be a critical downstream regulator (Scheff, Kosmides et al. 2011; Scheff, Calvano et al. 2012). Previous works investigating Chaffinches activity have also demonstrated that 12L/12D cycles represent particularly strong Zeitgebers (West and Pohl 1973).

As the photoperiod changes both the light/dark ratio as well as the mean value or else the area under the curve (AUC) of light exposure, changes.

Longer photoperiods induce a prolonged decrease on the rhythmic characteristics of CRH and as such greater cortisol amplitude. Furthermore, longer photoperiods of more intense light (higher mean value) increase the degradation of CRH ultimately resulting in decreased cortisol amplitude. The latter can be also seen in Figure 4.2.3F-H where as a result of an increased constant light, cortisol's amplitude is reduced. Therefore, longer photoperiods result in opposing forces that control the amplitude in the opposite manner. As the photoperiod changes from short to long, initially there is an increase of cortisol's amplitude due to the elongation of CRH degradation, until a point where the mean value of light schedule is "high enough" and starts to negatively impact cortisol's amplitude. The resulting dynamic indicates that not only the rhythm of the light entrainer but also the balance between its rhythmic characteristics and mean value should be accounted for in order to achieve desired entrainment characteristics. This can be also seen in Figure 4.2.9 where the photoperiods were kept constant but the amplitude (Figure 4.2.9A&B**)** as well as the phase (Figure 4.2.9C&D**)** of the entrainer was varied simulating scenarios of impaired light perception and phase shift respectively. Our model indicates that a reduced entrainer's amplitude (Figure 4.2.9A) mainly impacts cortisol's amplitude (Figure 4.2.9B) and not its phase until a regime where the light amplitude is not high enough to induce entrainment and cortisol oscillates independently (Figure 4.2.9A&B, red line and arrow). This would further implicate that the circadian information is weakened and the body lose its sensitivity relative to its environment. On the other hand, a phase shift of light entrainer (Figure 4.2.9C) will impact solely the phase of cortisol

and not its amplitude (Figure 4.2.9D). In such a case, sensitivity is time-shifted anticipating activity or rest periods at different times of day.

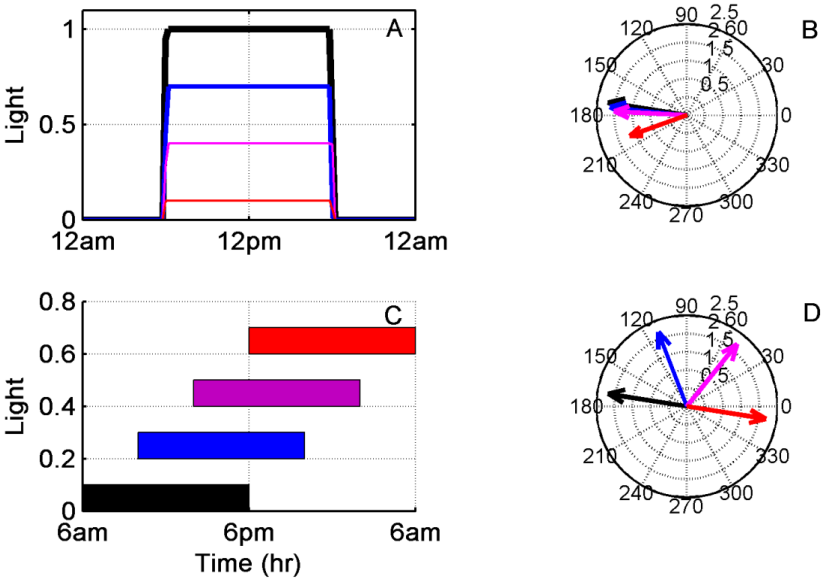

Figure 4.2 9: In silico simulation of impaired light perception and phase shift.A: Light schedules of gradually decreasing amplitude. B: Cortisol phase and amplitude while Light retains gradually decreasing amplitude. C: Light schedules of different phase. D: Cortisol phase and amplitude while Light entrainer maintains different phase.

Our results demonstrate that light can also affect the period of the HPA compartments. Figure 4.2.4 indicates that increased constant light reduces the period of cortisol. Under conditions of constant darkness (*light* = 0) according to our model assumptions that are based in experimental evidence (Czeisler, Duffy et al. 1999), cortisol free runs with the period of 24.2 hours. The observed decrease in frequency with increasing light intensity is the result of a higher CRH degradation rate (Eq. 4.2.1) that accelerates its degradation and as such reduces the time between peaks and troughs. This dynamic is in accordance with *Aschoff's first rule* (Aschoff 1960) stating that diurnal

animals decrease their behavioral period with increasing light intensity, while nocturnal animals tend to increase it. Since our HPA axis model is formed on assumptions based on human's experiments, it can be presumed to be indicative of a diurnal organism.

It is now well established that light/dark information is transduced to the periphery of the body through systemic signals entraining numerous physiological functions (Mavroudis, Scheff et al. 2013), and that disrupted light rhythmicity can result in detrimental outcomes. In particular (Prendergast, Hotchkiss et al. 2003) showed that exposure of rodents to short days was followed by a decreased production of cytokines in response to LPS and a decreased mortality. Along the same lines (Bilbo, Drazen et al. 2002) further observed that short days accompanied a reduction in fever and anorexia and overall attenuation of infection symptoms comparing to long days. There is enough evidence in humans indicating that circadian disruption may implicate immune dysfunction. The review of (Dinges, Douglas et al. 1995) as well as more recent works (Lange, Dimitrov et al. 2010; Faraut, Boudjeltia et al. 2012; Ruiz, Andersen et al. 2012) elucidate the attribution of immune suppression to sleep restriction. Additionally, there are evidences relating shift work to circadian disruption on cytokine rhythms (van Mark, Weiler et al. 2010), and chronic diseases (Wang, Armstrong et al. 2011). Lastly, the work of Keller et al. (Keller, Mazuch et al. 2009), convincingly linked the rhythmic component of the inflammatory response to peripheral clock genes further elucidating the critical role of PCGs to the regulation of immune parameters (Jelic, Cupic et al. 2005).

Our model predicts that high cortisol amplitudes emanating from an appropriate light schedule (i.e. 12hr Light/12hr Dark) induce high synchronization in the peripheral cell population (Figure 4.2.7) in contrast with very short (2hr Light/22hr Dark) or very long photoperiods (22hr Light/2hr Dark). In particular, 12hr Light/12hr Dark light schedules result in cortisol profiles of higher amplitude that successfully entrain the population of PCGs producing high amplitude oscillations (i.e., total mRNA) at the ensemble level (Figure 4.2.7H). Changing the rhythmic patterns of light results in reduction of cortisol's amplitude (Figure 4.2.7D&7F**)** that leads to PCG desynchronization ultimately manifested as increased R_{syn} value and blunted ensemble average rhythmicity. This disrupted rhythm at the ensemble level is signifying loss of circadian information at the periphery. This loss of information may result in increased vulnerability and decreased adaptability to respond to external stressors (Castanon-Cervantes, Wu et al. 2010) .

The *effective* cortisol amplitude "sensed" by the PCGs is dependent on the choice of the parameter k_c (Equation 14) that expresses the regulation of expression of *Per/Cry* by FRN(N) quantifying the coupling strength between HPA axis and PCGs (Mavroudis, Scheff et al. 2012). Based on experimental findings, we wished our population of PCGs to be efficiently synchronized when cortisol maintained its normal rhythmicity, and become desynchronized when cortisol lose its amplitude variability. Our analysis indicated that rhythmicity and synchronization of PCG is very sensitive to the choice of k_c parameter providing a very small regime of k_c values.

We further examined how coupling strength impacts the PCG synchronization in relation to changes in photoperiod. For a given

photoperiod, as the coupling strength k_c increases (Figure 4.2.8A) cells are gradually becoming more synchronized indicated by the gradually increasing R_{syn}. Interestingly, for intermediate levels of coupling (Figure 4.2.8A, $0.003 < k_c < 0.005$) cells are more synchronized at photoperiods near the homeostatic (~12hr). This is a result of the higher cortisol amplitude emanating from balanced light schedules (Figure 4.2.6D-F). Figure 4.2.8 further reveals that for intermediate levels of coupling the observed changes in PCGs synchronization for different photoperiods are relatively low. This is because despite of the different light/dark schedules, cortisol retains its circadian period and its robust amplitude. As it is by now well established (Abraham, Granada et al. 2010; Mavroudis, Scheff et al. 2012), these two characteristics of the entrainer play a major role for circadian entrainment. For high coupling strengths cells are synchronized independent of the photoperiod (Figure 4.2.8A, $k_c>0.005$). Once cells are synchronized, their phase is locked relative to cortisol entrainer with exactly the same manner as cortisol rhythm becomes phase locked to light (Figure 4.2.2). If instead of cortisol phase, we examine how the phase of the ensemble of PCGs advances or delays as function of the photoperiod, we observe a similar phase shift. In particular, for a given coupling strength, as photoperiod increases there is a concurrent delay in the ensemble PCGs phase (Figure 4.2.8B). This phase shift is independent of the coupling strength once cells are synchronized (Figure 4.2.8B). However, for small coupling strengths (Figure 4.2.8B, $k_c < 0.002$) cells are desynchronized and they adopt phases that depend solely on the level of their desynchronization. We therefore observe a consistent phase delay as we increase the photoperiod. This is because light schedule was changed retaining

the middle of the light schedule constant according to Figure 4.2.6B**.** The results would be similar if we would use the light schedules of Figure 4.2.6A&6C but instead of phase delay we would observe a phase advance for the case of 6A similar to what has been observed for cortisol rhythm in Figure 4.2.6E.

In summary our model is able to evaluate a number of experimental observations as well as point towards ways of understanding the signal transduction of photic information from the central clock of SCN and HPA axis to the periphery of the body and PCGs. Through our modeling efforts we showed that light characteristics such as light/dark ratio or light mean value, regulate HPA axis phase (Figure 4.2.6), amplitude (Figure 4.2.3, Figure 4.2.6) or frequency (Figure 4.2.4) and play critical role for the successful delivery of the environmental information to the periphery of the body. In particular, we showed that cortisol's rhythm retained maximum amplitude variability when entrained by light schedules resembling environmental light cycles of 12hr Light/12hr Dark ultimately leading to a successful synchronization of PCGs. On the contrary, loss of light amplitude led to disrupted cortisol profiles that were incapable of synchronizing peripheral cells. Our work denotes the importance of maintenance significant rhythm variability in the hormonal level sourcing from the successful entrainment with the environment.

Chapter 5: Circadian characteristics of permissive and suppressive effects of cortisol and their role in homeostasis and the acute inflammatory response

5.1: Introduction

Inflammation is a critical component of body's response to a variety of harmful stimuli such as infection and trauma. Under normal circumstances, the bi-directional flow of information between immune and neuroendocrine systems removes the pathogen or repairs the damaged tissue and restores homeostasis (Hotchkiss and Karl 2003). The principal peripheral effectors of the neuroendocrine system are glucocorticoids that are regulated by the hypothalamic-pituitary-adrenal (HPA) axis, and the catecholamines norepinephrine/epinephrine which are secreted by the sympathetic nervous system (Chrousos 2009). Mainly due to their immunosuppressive actions, glucocorticoids (cortisol in humans) have been regularly utilized for the treatment of autoimmune diseases and inflammatory disorders (Tsigos and Chrousos 1994; Barnes 1998). Glucocorticoids induce their anti-inflammatory action through suppressing the production of numerous pro-inflammatory mediators (cytokines) such as IL-1 (interleukin-1), IL-2, IL-3, IL-6, and IFN-γ (interferon-γ) which are dangerous in excess (Tracey, Beutler et al. 1986; Tracey, Lowry et al. 1987). Along with their immunosuppressive role, it has long been suggested that they enhance the response to external stressors rather

than solely limiting it (Sapolsky, Romero et al. 2000). Therefore glucocorticoids have been shown to up-regulate the expression of cytokine receptors (Akahoshi, Oppenheim et al. 1988; Snyers, De Wit et al. 1990; Gottschall, Koves et al. 1991; Re, Muzio et al. 1994; Kamisoglu, Sleight et al. 2013) sensitizing the target cells to an upcoming stimulus. Interestingly, these opposing glucocorticoid effects do not cancel each other out, but are rather providing an optimal defense mechanism (Munck and Naray-Fejes-Toth 1992). Investigation of the dynamics giving rise to glucocorticoids permissive and suppressive actions could provide insight into the emergent dynamics of response to stress.

Glucocorticoids exert their genomic effects through two types of receptors: *type I* (mineral corticoid, MR), and *type II* (glucocorticoid, GR) receptors that after binding to glucocorticoid ligand, they translocate to the nucleus where they interact with specific promoter regions named glucocorticoid responsive elements (GREs) to activate appropriate hormone-responsive genes (Pratt 1990; Funder 1993; Ramakrishnan, DuBois et al. 2002). Since the affinity of MR to cortisol is much higher compared to that for GR (Arriza, Weinberger et al. 1987), it has been hypothesized that basal cortisol levels mediate downstream effects mainly through MR while at higher cortisol levels binding to GR dominates (Joels and de Kloet 1994; De Kloet, Vreugdenhil et al. 1998). In the context of immunity and inflammation, basal cortisol levels have been further shown to act proactively, thus enhancing resistance to infection (Jefferies 1991; Jefferies 1994). On the other hand, suppressive actions are a characteristic of higher glucocorticoid levels (Sapolsky, Romero et al. 2000).

We have previously presented a number of *in silico* studies of acute inflammation (Foteinou, Calvano et al. 2009; Foteinou, Calvano et al. 2009; Scheff, Calvano et al. 2010; Scheff, Mavroudis et al. 2011; Scheff, Mavroudis et al. 2013). In the work presented herein we further explore cortisol's dynamic behavior taking into consideration its inducing effect on pro-inflammatory cytokine receptors aiming to elucidate the balance between its immunosuppressive and permissive effects mediated through the inhibition of pro-inflammatory cytokines via GR and regulation of cytokine receptors via MR respectively. Furthermore, we account for circadian rhythmicity present both at the single immune cell level (periphery) by peripheral clock genes (PCGs) as well as at the systemic level of hormonal secretion.

Our model describes cortisol's antagonistic effects during the course of day. Permissive effects are accentuated during the dark (rest) period where the body is building its defense for the impending activity phase whereas during the light (active) period immunosuppressive characteristics of cortisol are denoted (Sapolsky, Romero et al. 2000). Thus we predict that acute LPS administration at night results in higher levels of cytokines compared to LPS administration at morning time. Furthermore, our model indicates that increased cytokine receptor expression during the night, leads to a more potent inflammatory response when acute stimulus is administered at cortisol's rising phase compared to its descending phase even for the same cortisol values. This further illustrates cortisol's preparative role for either sensitizing or desensitizing the body.

5.2: Materials and Methods

5.2.1: Modeling circadian rhythms at the systemic and peripheral level

5.2.1.1: Cortisol and glucocorticoid/mineralococrticoid receptors pharmacodynamics

The overall model is depicted in Figure 5.1.1. At the systemic level we considered the daily secretion of cortisol using the "two rates" model (Chakraborty, Krzyzanski et al. 1999; Scheff, Calvano et al. 2010; Scheff, Mavroudis et al. 2011) that we have already used in section 4.1(Eq. 5.1).

Subsequently cortisol reaches peripheral cells (Eq. 5.2) where it diffuses into their cytoplasm, and binds to the active forms of its two receptors (MR^*_c and GR^*_c). We hypothesize that cortisol activates, though phosphorylation, the two receptors (Sathiyaa and Vijayan 2003; Frey, Odermatt et al. 2004) rendering them active and able to bind cortisol (Eq. 5.3 and 5.6). Following binding the two glucocorticoid complexes (FMR_c Eq. 5.4, and FGR_c Eq. 5.7) translocate into the nucleus ($FMR(N)_c$ Eq. 5.5, and $FGR(N)_c$ Eq. 5.8) and ultimately binds to the GRE at the promoter regions of target genes(Jin, Almon et al. 2003)(*Per/Cry*, cytokine receptors and cytokines) [30].

$$\frac{dF}{dt} = RF + k_{in,F_{en}} \cdot \left(1 + k_{F_{en},P} \cdot P_{ens}\right) - k_{out,F} \cdot F \qquad (5.1)$$

$$RF = \begin{cases} k_{in,RF1,} & t_{F1} < \mathrm{mod}\left(t,24\right) < t_{F2} \\ 0 & t_{F2} < \mathrm{mod}\left(t,24\right) < t_{F1} \end{cases}$$

$$\frac{dF_{per,c}}{dt} = \frac{1}{\tau} \cdot \left(F - F_{per,c}\right) \qquad (5.2)$$

Mineralocorticoid receptor:

$$\frac{dMR^*_c}{dt} = \frac{k_{MR}\cdot(1+\frac{k_{F,MR}\cdot F_{per,c}}{K_{F,MR}+F_{per,c}})\cdot(MR_T - MR^*_c)}{K_{MR}+MR_T-MR^*_c} - \frac{k_{MR,\deg}\cdot MR^*_c}{K_{MR,\deg}+MR^*_c} - k_{b,MR}\cdot F_{per,c}\cdot MR^*_c + k_{r,MR}\cdot FMR(N)_c \quad (5.3)$$

$$\frac{dFMR_c}{dt} = F_{per,c}\cdot MR_c - FMR_c \quad (5.4)$$

$$\frac{dFMR(N)_c}{dt} = FMR_c - FMR(N)_c \quad (5.5)$$

Glucocorticoid receptor:

$$\frac{dGR^*_c}{dt} = \frac{k_{GR}\cdot(1+\frac{k_{F,GR}\cdot F_{per,c}}{K_{F,GR}+F_{per,c}})\cdot(GR_T - GR^*_c)}{K_{GR}+GR_T-GR_c} - \frac{k_{GR,\deg}\cdot GR^*_c}{K_{GR,\deg}+GR^*_c} - k_{b,GR}\cdot F_{per,c}\cdot GR^*_c + k_{r,GR}\cdot FGR(N)_c \quad (5.6)$$

$$\frac{dFGR_c}{dt} = F_{per,c}\cdot GR_c - FGR_c \quad (5.7)$$

$$\frac{dFGR(N)_c}{dt} = FGR_c - FGR(N)_c \quad (5.8)$$

Subscript ***c*** denotes the level of single peripheral cell. In order to account for the delay associated with cortisol's transport, we assumed a transient compartment model (Eq. 5.2) (Sun and Jusko 1998) using a mean transient time delay of τ=15 min (Walker, Terry et al. 2010). We further assumed that the phosphorylation/dephosphorylation reactions of glucocorticoid and mineralocorticoid receptors (Eq. 5.3 and 5.6) are governed by Michaelis-Menten kinetics (Tyson, Chen et al. 2003). Finally, in accordance with the theoretical model of (Munck and Naray-Fejes-Toth 1992; Sapolsky, Romero

et al. 2000) we assumed a dissociation constant of cortisol for GR equal to 30 ($K_{F,GR}$=30) (Eq. 5.6) and for MR equal to 0.5($K_{F,MR}$=0.5) (Eq. 5.3). We further assumed similar reaction kinetics for the two receptors binding and translocation to the nucleus (Eq. 5.4-5, and 5.7-8).

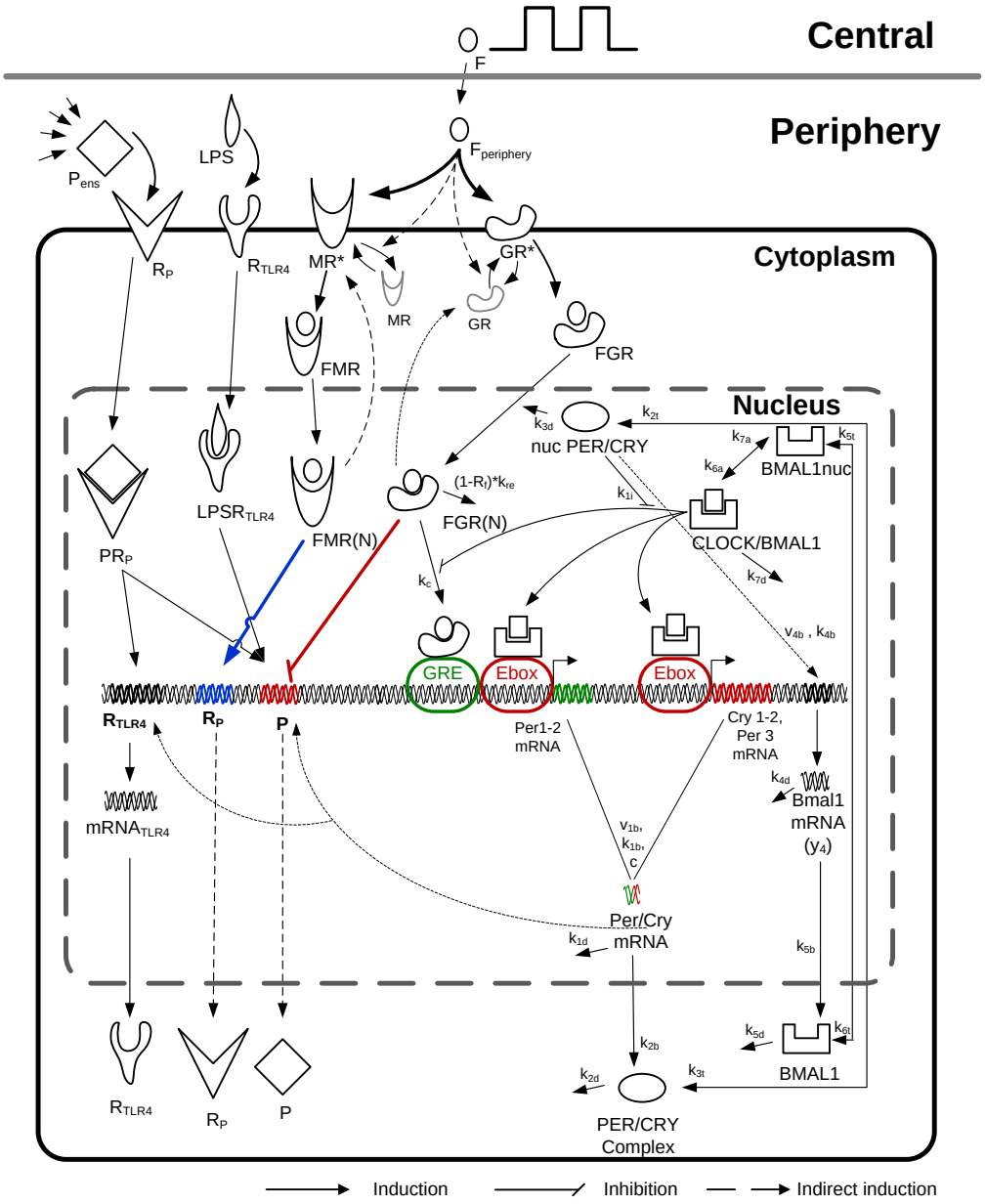

Figure 5. 1: Schematic figure of the model.

5.2.2. Peripheral clock genes dynamics

It is by now well established that rhythmicity in peripheral tissues is originated from the cell autonomous oscillatory activity of peripheral clock genes (PCGs) (Reppert and Weaver 2002). These peripheral oscillators are entrained by systemic signals carrying the photic information and as such they are in synchrony with the environment. In the present work, in accordance with our previous modeling efforts (Mavroudis, Scheff et al. 2012), we incorporate the entrainment of peripheral immune cells by cortisol by considering the binding of glucocorticoid/receptor complex to the GRE present at the promoter region of *Per* and *Cry* clock genes (Yamamoto, Nakahata et al. 2005; So, Bernal et al. 2009). By this we aim to further investigate the translation of PCGs rhythmicity to pro-inflammatory cytokine expression (Keller, Mazuch et al. 2009).

5.2.3. Modeling circadian rhythms of pro-inflammatory cytokines and cytokine receptors

Pro-inflammatory cytokines, such as interferon γ (IFN-γ), interleukin 1 (IL-1), or tumor necrosis factor α (TNF-α), exhibit distinct circadian rhythmicity with peak duringearly morning periods (Petrovsky and Harrison 1997; Petrovsky, McNair et al. 1998). Cortisol has been recognized as a critical driver of circadian cytokine secretion (Petrovsky and Harrison 1998). In particular, experimental evidence suggests that cortisol mediated repression of cytokine expression is reduced by glucocorticoid receptor antagonist (Knudsen, Dinarello et al. 1987; Kutteh, Rainey et al. 1991; Amano, Lee et al. 1993; Paliogianni and Boumpas 1995), further illustrating a GR mediated

cytokine inhibition. Therefore, cortisol's inhibition of the expression of a cytokine's mRNA, ($mRNA_{P,c}$ Eq.*5.9*), is simulated as an indirect response that further considers the saturation of cortisol receptor complex. Cytokine circadian rhythms persist even in absence of systemic cues due to the presence of local peripheral clocks that are mediated by PCGs (Keller, Mazuch et al. 2009) . Therefore, the cytokine production is further regulated by Per/Cry to express the peripheral (autonomous) regulation of cytokine secretion. Finally, we simulate the "autocatalytic" role of proinflammatory cytokines (Akira, Hirano et al. 1990; Chang and Karin 2001; Sommer and Kress 2004) by further considering cytokine mediated induction of expression of $mRNA_P$ (Eq. 5.9).After transcription, $mRNA_{P,c}$ further translates to its corresponding cytokine (P_c, Eq. 5.10).

Cortisol's mediated upregulation of cytokine receptors mRNA ($mRNA_{Rp,c}$, *Equation* 11) was also modeled via an indirect response model where the nuclear component of cortisol/mineralocorticoid receptor complex, FMR(N), regulates the transcription of $mRNA_{Rp.}$ Following translation, the cytokine receptor (R_P, Eq. 5.12) binds to cytokine ligand forming cytokine/cytokine-receptor complex ($PR_{P,c}$) which feeds back to $mRNA_P$. The ensemble cytokine levels, P_{ens}, were assumed to follow dynamics accounting for secretion of cytokines from the ensemble of peripheral immune cells with a simple degradation term (Eq. 5.14).

$$\frac{dmRNA_{P,c}}{dt} = k_{mRNA_{P,in}} \cdot \left(1 + k_{P,LPSR_{TLR4}} \cdot LPSR_c\right) \cdot \left(1 - \frac{k_{fr} \cdot FGR(N)_c}{K_{fr} + FGR(N)_c}\right) \cdot \left(1 + k_{pc} \cdot Per/Cry_{mRNA,c}\right) \cdot \left(1 + PR_{p,c}\right) - k_{mRNA_{P,out}} \cdot mRNA_{P,c} \quad (5.9)$$

$$\frac{dP_c}{dt} = k_{in,P} \cdot mRNA_{P,c} - k_{out,P} \cdot P_c \quad (5.10)$$

$$\frac{dmRNA_{R_P,c}}{dt} = k_{mRNA_{R_P,in}} \cdot \left(1 + \frac{k_{fr,2} \cdot FMR(N)_c}{K_{fr,2} + FMR(N)_c}\right) - k_{mRNA_{R_P,out}} \cdot mRNA_{R_P,c} \quad (5.11)$$

$$\frac{dR_{P,c}}{dt} = k_{in,R_P} \cdot mRNA_{R_P,c} - k_d \cdot P_{ens} \cdot R_{P,c} - k_{out,R_P} \cdot R_{P,c} \quad (5.12)$$

$$\frac{dPR_{P,c}}{dt} = k_d \cdot P_{ens} \cdot R_{P,c} - k_{out,PR_P} \cdot PR_{P,c} \quad (5.13)$$

$$\frac{dP_{ens}}{dt} = mean(P) - P_{ens} \quad (5.14)$$

The response of the system to an acute inflammatory challenge is based on our previously published model of human endotoxemia (Scheff, Mavroudis et al. 2011). Administration of low doses of endotoxin (lipopolysaccharides, LPS) in healthy individuals evokes signs and symptoms characteristic of systemic inflammation, making it a practical experimental model of systemic inflammation in humans (Lowry 2005). LPS regulates the production of inflammatory mediators by binding to its Toll-Like receptor 4 (TLR4). This provides a controlled model of TLR4 agonist-induced systemic inflammation which has been used to study how inflammation activates physiological system (hormonal release, neural activity) as well as how exogenous treatment can modulate inflammation (hormone treatment, vagal stimulation). Based on recent experiments, our current work considers the cell autonomous circadian rhythmicity of TLR4 which is induced indirectly by PCGs (Keller, Mazuch et al. 2009) (Eq. 16).

$$\frac{dLPS}{dt} = k_{LPS,1} \cdot LPS \cdot (1 - LPS) - k_{LPS,2} \cdot LPS \quad (5.15)$$

$$\frac{dmRNA_{TLR4,c}}{dt} = k_{LPS,3} \cdot \left(1 + k_{mRNA_{TLR4}} \cdot PR_{P,c}\right) \cdot \left(1 + Per / Cry_{mRNA,c}\right) - k_{LPS,4} \cdot mRNA_{TLR4,c} \quad (5.16)$$

$$\frac{dR_{TLR4,c}}{dt} = k_{syn} \cdot mRNA_{TLR4,c} + k_2 \cdot \left(LPSR_{TLR4,c}\right) - k_1 \cdot LPS \cdot R_{TLR4,c} - k_{syn} \cdot R_{TLR4,c} \quad (5.17)$$

$$\frac{dLPSR_{TLR4,c}}{dt} = k_1 \cdot LPS \cdot R_{TLR4,c} - k_3 \cdot \left(LPSR_{TLR4,c}\right) - k_2 \cdot \left(LPSR_{TLR4,c}\right) \quad (5.18)$$

The binding of LPS to its receptor, TLR4, (Eq. 5.15-18) induces the indirect transcription of the mRNA of pro-inflammatory cytokines (P) (Eq. 5.9). We simulate the inhomogeneity of the peripheral cells by accounting for a population of (1000) cells. Intercellular variability is introduced by uniformly varying the parameters of single cell variables by 5% of their original value for each cell. All the parameters of the model are presented in Table 5.1.

Table 5. 1: List of parameters used in the model (Eq. 5.9-18).

Parameter	Value	Units	Description/Reference
$k_{in,Fen}$	0.85	ng/mL/hr	Base production rate of F/(Scheff, Calvano et al. 2010)
$k_{Fen,P}$	0.35	1	Strength of indirect stimulus on F by P_{ens}/(Scheff, Calvano et al. 2010)
$k_{out,F}$	2.10	1/hr	Clearance rate of F/(Scheff, Calvano et al. 2010)
$k_{in,RF1}$	2.60	ng/mL/hr	Circadian production rate of F/(Scheff, Calvano et al. 2010)
τ	0.15	hr	Delay for the transportation of cortisol signal to periphery/(Walker, Terry et al. 2010)
$k_{MR,pr}$	0.56	1/hr	Base transcription rate of MR/Estimated
MR_T	1.35	1	Total MR concentration/Estimated
$K_{MR,pr}$	0.13	1	Michaelis constant for MR

			production/Estimated
$k_{MR,deg}$	0.58	1/h	Degradation rate for MR/Estimated
$k_{b,MR}$	0.00329	l/nmol/hr	Degradation rate for cortisol/mineralocorticoid receptor binding/(Ramakrishnan, DuBois et al. 2002)
$k_{r,MR}$	0.001	1/h	Ratio of mineralocorticoid receptor recycled*rate of recycle/Estimated
$k_{b,GR}$	0.00329	l/nmol/hr	Degradation rate for cortisol/mineralocorticoid receptor binding/(Ramakrishnan, DuBois et al. 2002)
$k_{r,GR}$	0.001	1/h	Ratio of mineralocorticoid receptor recycled*rate of recycle/Estimated
$K_{MR,deg}$	1.39	1	Michaelis constant for degradation of MR/Estimated
$k_{GR,pr}$	1.18	1/hr	Base transcription rate of GR/Estimated
GR_T	1.81	1	Total GR concentration/Estimated
$K_{GR,pr}$	0.74	1	Michaelis constant for GR production/Estimated
$k_{GR,deg}$	1.52	1/h	Degradation rate for GR/Estimated
$K_{GR,deg}$	1.05	1	Michaelis constant for degradation of GR/Estimated
k_c	0.004	1/hr	Coupling strength//Estimated
v_{1b}	9	nM/hr	Maximal rate of Per/Cry transcription/ (Becker-Weimann, Wolf et al. 2004)
k_{1b}	1	nM	Michaelis constant of Per/Cry transcription/ (Becker-Weimann, Wolf et al. 2004)
k_{1i}	0.56	nM	Inhibition constant of Per/Cry transcription/ (Becker-Weimann, Wolf et al. 2004)
c	0.01	nM	Concentration of constitutive activator /(Becker-Weimann, Wolf et al. 2004)
p	8		Hill coefficient of inhibition of Per/Cry transcription/ (Becker-Weimann, Wolf et al. 2004)
k_{1d}	0.12	1/hr	Degradation rate of Per/Cry mRNA/ (Becker-Weimann, Wolf et al. 2004)
k_c	0.004	1/hr	Coupling constant /(Becker-Weimann, Wolf et al. 2004)

k_{2b}	0.3	1/nM/hr	Complex formation rate of Per/Cry mRNA /(Becker-Weimann, Wolf et al. 2004)
q	2		No. of PER/CRY complex forming subunits /(Becker-Weimann, Wolf et al. 2004)
k_{2d}	0.05	1/hr	Degradation rate of cytoplasmatic PER/CRY/ (Becker-Weimann, Wolf et al. 2004)
k_{2t}	0.24	1/hr	Nuclear import rate of the PER/CRY complex /(Becker-Weimann, Wolf et al. 2004)
k_{3t}	0.02	1/hr	Nuclear export rate of PER/CRY complex /(Becker-Weimann, Wolf et al. 2004)
k_{3d}	0.12	1/hr	Degradation rate of the nuclear PER/CRY complex/ (Becker-Weimann, Wolf et al. 2004)
v_{4b}	3.6	nM/hr	Maximal rate of Bmal1 transcription /(Becker-Weimann, Wolf et al. 2004)
k_{4b}	2.16	nM	Michaelis constant of Bmal1 transcription/ (Becker-Weimann, Wolf et al. 2004)
r	3		Hill coefficient of activation of Bmal1 transcription /(Becker-Weimann, Wolf et al. 2004)
k_{4d}	0.75	1/hr	Degradation rate of Bmal1 mRNA/ (Becker-Weimann, Wolf et al. 2004)
k_{5b}	0.24	1/hr	Translation rate of BMAL1 /(Becker-Weimann, Wolf et al. 2004)
k_{5d}	0.06	1/hr	Degradation rate of cytoplasmatic BMAL1 /(Becker-Weimann, Wolf et al. 2004)
k_{5t}	0.45	1/hr	Nuclear import rate of BMAL1 /(Becker-Weimann, Wolf et al. 2004)
k_{6t}	0.06	1/hr	Nuclear export rate of BMAL1/ (Becker-Weimann, Wolf et al. 2004)
k_{6d}	0.12	1/hr	Degradation rate of nuclear BMAL1/ (Becker-Weimann, Wolf et al. 2004)
k_{6a}	0.09	1/hr	Activation rate of nuclear CLOCK/BMAL1/ (Becker-Weimann, Wolf et al. 2004)
k_{7a}	0.003	1/hr	Deactivation rate of CLOCK/BMAL1 /(Becker-Weimann, Wolf et al. 2004)

k_{7d}	0.09	1/hr	Degradation rate of CLOCK/BMAL1 /(Becker-Weimann, Wolf et al. 2004)
$k_{mRNAP,in}$	7.3	1/h	Base transcription rate of $mRNA_P$
$k_{P,LPSR_{TLR4}}$	59.81	1	Rate of LPSR mediated transcription of $mRNA_P$/Estimated
k_{fr}	1.07	1	Maximum rate of FGR(N) mediated suppression of $mRNA_P$/Estimated
K_{fr}	1	1	Michaelis constant for FGR(N) mediated suppression of $mRNA_P$/Estimated
k_{pc}	0.35	1	Rate of Per/Cry_{mRNA} mediated transcription of $mRNA_P$/Estimated
$k_{mRNAP,out}$	2.89	1/hr	Degradation rate of $mRNA_P$/Estimated
$k_{in,P}$	0.29	1/hr	Translation rate of P/Estimated
$k_{out,P}$	1.06	1/hr	Degradation rate of P/Estimated
$k_{mRNA_{R_P,in}}$	0.61	1/hr	Base transcription rate of $mRNA_{RP}$/Estimated
$k_{fr,2}$	0.8	1	Maximum rate of FMR(N) mediated transcription of $mRNA_{RP}$/Estimated
$K_{fr,2}$	0.5	1	Michaelis constant for FMR(N) mediated transcription of $mRNA_{RP}$/Estimated
$k_{mRNA_{R_P,out}}$	0.19	1/hr	Degradation rate of $mRNA_{RP}$-/Estimated
$k_{in,Rp}$	1.11	1/hr	Translation rate of R_P/Estimated
k_d	0.14	1/hr	P-R_p binding rate/Estimated
$k_{out,Rp}$	0.26	1/hr	Dissociation rate of R_P/Estimated
$k_{out,PRp}$	1.30	1/hr	Dissociation rate of PR_P/Estimated
$k_{LPS,1}$	4.5	1/hr	Growth rate of LPS/(Scheff, Calvano et al. 2010)
$k_{LPS,2}$	6.79	1/hr	Clearance rate of LPS/(Scheff, Calvano et al. 2010)
$k_{LPS,3}$	0.0914	1	Base transcription rate of $mRNA_{TLR4}$/(Scheff, Calvano et al.

				2010)
	$k_{mRNA,TLR4}$	1.74	1	Rate of PR_p mediated transcription of $mRNA_{TLR4}$/(Scheff, Calvano et al. 2010)
	$k_{LPS,4}$	0.32	1/hr	Decay rate of $mRNA_{TLR4}$/(Scheff, Calvano et al. 2010)
	k_{syn}	0.02	1/hr	Translation rate of TLR4/(Scheff, Calvano et al. 2010)
	k_2	0.04	1/hr	Dissociation rate between LPS and TLR4/(Scheff, Calvano et al. 2010)
	k_1	3	1/hr	Binding rate between LPS and TLR4/(Scheff, Calvano et al. 2010)
	k_3	5	1/hr	Decay rate of LPSR/(Scheff, Calvano et al. 2010)

5.3: Results

Our *in-silico* study aims to investigate the circadian interplay of cortisol's permissive and suppressive balance of effects as well as its implications with respect to acute stress. In order to evaluate cortisol's antagonistic effects we consider the actions of pathway throught the mineralocorticoid and glucocorticoid receptors in the model shown in Figure 5.1.

Figure 5.2 depicts the homeostatic response of our model. In accordance with experimental data, cortisol levels peak at morning (Figure 5.2A) whereas pro-inflammatory cytokines maintain peak values later at night (Figure 5.2B). Grey lines of Figure 5.2B reflect single cell simulations while thick black line their average profile.

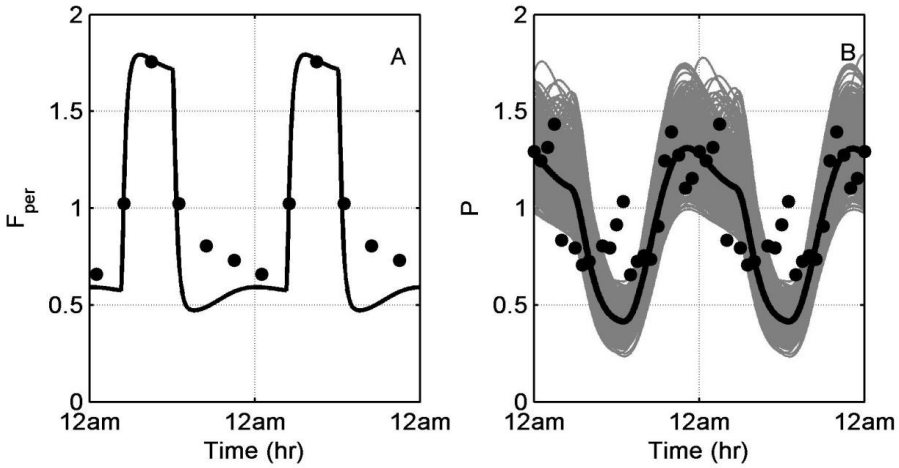

Figure 5. 2: Homeostatic responses of A: cortisol (F_{per}) and B: pro-inflammatory cytokines (P). Grey lines represent single cell profiles and thick black line denotes their average profile. Experimental data have been adopted from (Petrovsky, McNair et al. 1998).

In order to explore the circadian dependence of the sensitivities of our model, we analyzed the response to an acute LPS stimulus at different times of day. We conducted a series of *in silico* experiments where LPS was injected at different times during the day and we recorded the maximum predicted levels of cytokines (denoted as max P_{ens}) during the 24 h period post-injection. The LPS levels were assumed to induce an acute, self-resolving inflammatory response Figure 5.3A depicts homeostatic cortisol rhythm (left panel, solid line) along with the maximum P_{ens} level, while Figure 5.3B expresses a "phase plane"-like plot of the same data. It is important to realize that the figure depicts the level of cortisol at the time of the injection, whereas the maxP_{ens} denotes the maximum cytokine levels at some future time. A superficial reading of the figure may imply that the response is rather expected: the lower the cortisol level at the time of the injection of LPS, the higher the cytokine production, and *vice versa*. Closer examination, however, reveals a far more interesting and complex response.

Cortisol's profile can roughly be separated in four domains. Periods where cortisol remains close to its nadir (n) or zenith (z) levels, and periods where cortisol is at its ascending (a) or descending (d) phase (Figure 5.3A, left panel solid line arrows). Generally, lowest responsiveness, expressed as low maximum P_{ens} value, was observed at times where cortisol was indeed around its zenith (z) levels (Figure 5.3A, roughly from 6am to12pm). Figure 5.3B, however, indicates that even for the same cortisol values the response of the system upon an acute LPS stimulus can be different depending on whether cortisol is at its ascending (a) or descending (d) phases. Evenduring periods where cortisol is close to its zenith (z) or nadir (n) levels, Figure 5.3B also indicates significantly different sensitivities of the response relative to cortisol level.

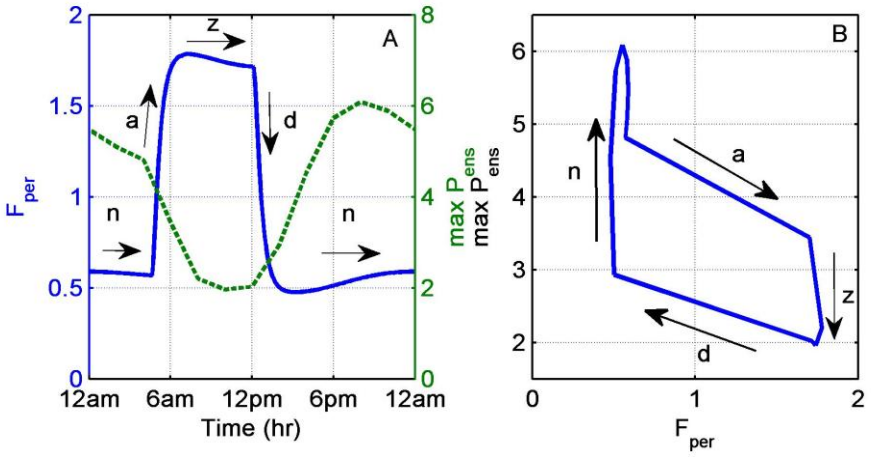

Figure 5. 3: Administration of acute LPS at different times of day (TOD). A: Cortisol (F_{per}, solid line, left axis) and maximum ensemble pro-inflammatory cytokine levels ($maxP_{ens}$, dotted line, left axis) relative to time of day. B: Maximum ensemble pro-inflammatory cytokine levels ($maxP_{ens}$) relative to cortisol cortisol levels. Max P_{ens} was calculated for the 24hr following LPS administration. a, d, z, and n denote cortisol's ascending, descending, zenith and nadir levels respectively.

To further elaborate on the underlying dynamics leading to changes in P_{ens} levels following acute LPS administration, Figure 5.4 depicts the permissive/suppressive effects of cortisol relative to time (Figure 5.4A) and cortisol levels (Figure 5.4B). Cortisol's permissive effects quantify the cortisol mediated induction of cytokine receptor through mineralocorticoid receptor ($\frac{k_{fr,2} \cdot FMR(N)}{K_{fr,2} + FMR(N)}$, Eq. 11) whereas the suppressive effects quantify the cortisol-mediated suppression of cytokine secretion through glucocorticoid receptor ($\frac{k_{fr} \cdot FGR(N)}{K_{fr} + FGR(N)}$, Eq. 9). Figure 5.4A indicates that when cortisol is near its nadir (n) levels, the permissive effects are greater than the suppressive. As cortisol increases, moving to its peak levels (ascending phase), the suppressive effects begin to increase and eventually dominate leading to a switch near the zenith (z) levels where the suppressive effects dominate. On the other hand, as cortisol decreases while moving towards its circadian nadir levels (descending phase) the permissive effects begin to dominate until eventually reaching cortisol's nadir (n) to where permissive effects are in full effect. Figure 5.4B further illustrates the relative impact of cortisol's permissive/suppressive effects as a function to cortisol levels.

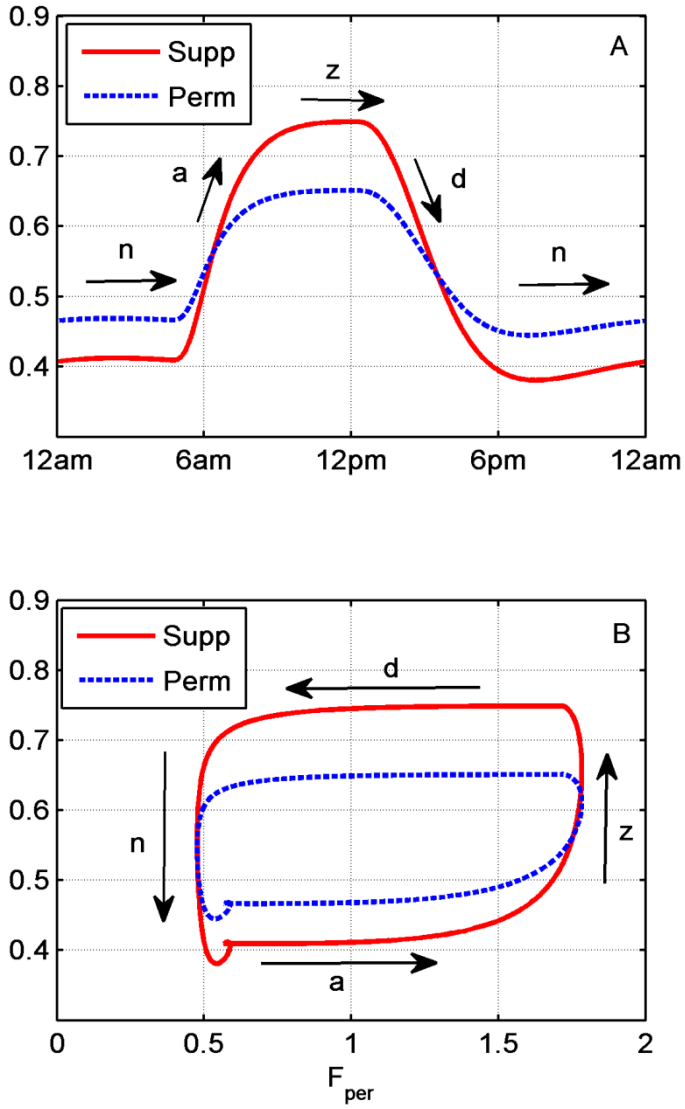

Figure 5. 4: Permissive and suppressive effects of cortisol during the day. A: Cortisol's permissive (perm, dotted line) and suppressive (sup, solid line) effects relative to time. B: Permissive and suppressive effects relative to cortisol levels (F_{per}).Permissive profile represents the cortisol mediated induction of cytokine receptors through mineralocorticoid receptor ($\frac{k_{fr,2}\cdot\langle FMR(N)\rangle}{K_{fr,2}+\langle FMR(N)\rangle}$) whereas suppressive the cortisol mediated inhibition of cytokines through glucocorticoid receptor ($\frac{k_{fr}\cdot\langle FGR(N)\rangle}{K_{fr}+\langle FGR(N)\rangle}$). a, d, z, and n denote

cortisol's ascending, descending, zenith and nadir levels respectively. Angle brackets denote average levels.

5.4: Discussion

The balance between cortisol's immunosuppressive and immunopermissive effects is crucial for the maintenance of homeostasis as well as the response of the body to stress. Rhythmic hormonal and metabolic signaling between organs establishes proper phase relations among the various clocks and these rhythmic signals play a major role in immune (Lee and Edery 2008; Paladino, Leone et al. 2010; Silver, Arjona et al. 2012) and metabolic functions(Feillet, Albrecht et al. 2006) conferring adaptive advantages by means of anticipatory control mechanisms (Edery 2000). In this work, we examined the interplay between cortisol's seemingly, antagonistic effects by investigating cortisol mediated regulation of cytokine receptors and cortisol mediated inhibition of cytokines.

The time of day dependence of the immune response has been extensively studied in animal and human models and appears to be regulated both by central and peripheral circadian clocks that function autonomously (Keller, Mazuch et al. 2009). In our model we considered the existence of circadian oscillation both at the central level of hormone secretion as well as the peripheral level of immune cells. In particular, autonomous oscillations at the central level (cortisol) are described by a "two rates model" (Eq. 1) with a zero-order production term (*RF*) simulating the distinct cortisol production levels during the day (Chakraborty, Krzyzanski et al. 1999). At the level of peripheral immune cells (denoted by the subscript ***c***) autonomous oscillations

are driven by the convolution of positive and negative feedback loops further regulating the rhythm of pro-inflammatory cytokines ($mRNA_p$). In order to further account for rhythmicity at the tissue/organ level, we considered a representative population of 1000 cells where intercellular variability was introduced by varying the parameters of the equations representing peripheral cell level (Eq. 2-13 and 16-18, and those equations of PCGs, 4.2.14-20) by ±5% of their nominal value (Haus and Smolensky 1999).

Figure 5.2 depicts the homeostatic response of our model at the population (thick black lines Figure 5.2A and Figure 5.2B) and single cell level (grey lines, Figure 5.2B) respectively. Introduction of intercellular variability leads to a distribution of phases, amplitudes and periods for each peripheral cell. We have previously (Mavroudis, Scheff et al. 2012) discussed that cortisol's rhythmic secretion synchronize the population of peripheral cells in order to maintain a narrow distribution of periods and phases that is further mediated to cytokine rhythm (Figure 5.2B). The average of single cell responses is optimized in order to be in accordance with available experimental data (Figure 5.2A, 5.2B) (Petrovsky, McNair et al. 1998). In particular, cortisol levels maintain peak values at morning whereas pro-inflammatory cytokines present their zenith levels later at night.

Experimental data suggest that circadian rhythms can influence the human response to an inflammatory challenge (Keller, Mazuch et al. 2009). The work of (Pollmacher, Mullington et al. 1996) further demonstrated that diurnal variation of human's susceptibility to endotoxin may be due to a suppression of the cytokine effects by glucocorticoids.

Our model demonstrates that the time of day dependence of the inflammatory response is a broader function of the relative strength of the pro- and anti-inflammatory characteristics of cortisol and, likely, does not reflect a simple dose-response. Our time of day response to endotoxin dependence results are in agreement with experimental data of human endotoxaemia showing that acute LPS administration at 12am results to a more pronounced inflammatory response and higher cytokine expression compared to LPS administration at 12pm (Alamili, Bendtzen et al. 2014). Furthermore, our predictions lie in close proximity with our own work (unpublished data) showing that healthy volunteers challenged with endotoxin at 9pm present significantly higher secretion of cytokines compared to volunteers challenged with LPS at 9am. Furthermore, ex-vivo studies (Petrovsky and Harrison 1998) also indicate that cytokine peak production occurs at night when cortisol level is lowest. Our model indicates that cortisol manifests a complex regulation of body's response to stress. Figure 5.3B illustrates that acute LPS administration at times when cortisol maintains same levels (i.e. $F_{per}=1$) can result in significantly different cytokine levels (Figure 5.3B) depending on if LPS is administered at cortisol's ascending or descending phase. In particular, administration of LPS stimulus duringcortisol's ascending (a) phase results in higher cytokine secretion compared to LPS administration at cortisol's descending (d) phase. Similar response is observed at cortisol's nadir (n) and zenith (z) levels. Particularly, during the period when cortisol maintains either its peak or nadir values despite cortisol's constant levels, our model present significantly different inflammatory responses. Cortisol's complex dynamics embedded in the ascending and descending phases has also been evaluated in

the context of light induction both experimentally (Jung, Khalsa et al. 2010) as well as *in silico* in our recent work (Mavroudis, Corbett et al. 2014), where we demonstrate that a bright light stimulus at the rising phase of cortisol due to the reduced intensity of $FRn_{central}$ negative feedback, leads to a more pronounced down-regulation compared to a stimulus at the descending phase.

Cortisol's "permissive" effects likely sensitizes immune cells to an upcoming challenge (Ingle 1954) and has been argued that this is mediated through an increase in the number of cytokine receptors (Baker, Barsh et al. 1978; Akahoshi, Oppenheim et al. 1988). Recently, we demonstrated that 24 hr cortisol infusion in healthy individuals, as means to emulate periods of increased stress, enhanced expression of genes encoding for cytokine receptors (Kamisoglu, Sleight et al. 2013). This surge in cytokine and pattern recognition receptors had been further linked with priming effects of cortisol on the immune function. In the model presented herein, we considered the cortisol mediated induction of pro-inflammatory cytokine receptors (Eq. 5.11) as well as the cortisol mediated suppression of cytokines (Eq. 5.9). In accordance with experimental evidence (De Kloet, Vreugdenhil et al. 1998) we investigated the scenario under which permissive cortisol effects are mediated through mineralocorticoid receptors, while suppressive effects by glucocorticoid receptor. Figure 5.4 shows the relative contribution of permissive and suppressive effects of cortisol during the day as quantified by the terms regulating the two effects in Eq. 5.9 and 11($\frac{k_{fr,2}\cdot\langle FMR(N)\rangle}{K_{fr,2}+\langle FMR(N)\rangle}$ (Perm) and $\frac{k_{fr}\cdot\langle FGR(N)\rangle}{K_{fr}+\langle FGR(N)\rangle}$ (Supp) respectively). At times when cortisol

maintains its nadir (n) values, permissive effects are elevated compared to cortisol's suppressive effects (Figure 5.4A). In particular, Figure 5.4B depicts that near cortisol's nadir levels, there is a switch from a state where suppressive effects are greater (activity phase of previous day) to a state where permissive effects are greater. During this time of the day cortisol acts as a priming agent, sensitizing the organism in preparation for the activity phase. This further implies that LPS administration at consecutive times at cortisol nadir (n) levels will result in higher cytokine levels until a point where cortisol reaches nearly the end of its ascending (a) phase (Figure 5.3A right axis dotted line, Figure 5.3B). At cortisol's ascending (a) phase, permissive effects still retain higher values compared to suppressive in contrast with cortisol's descending phase where the adverse is true (Figure 5.4B). This different predominance of permissive and suppressive effects in cortisol's ascending (a) and descending (d) phase leads to a higher response when LPS stimulus is introduced at times when cortisol is at its ascending (a) phase (Figure 5.3B, Figure 5.3A).

The physiological properties of mineralocorticoid/glucocorticoid receptors included in this model are based on the theoretical models of (Munck and Naray-Fejes-Toth 1992; Sapolsky, Romero et al. 2000). Therefore, the mineralocorticoid affinity for cortisol has been modeled by a lower dissociation constant of cortisol/MR complex ($K_{F,MR}$ Eq. 5.3 vs $K_{F,GR}$ Eq. 5.6). Furthermore, in accordance with experimental evidence showing a higher secretion of GR under higher cortisol concentrations (Sapolsky, Romero et al. 2000), we further assumed a higher maximum rate of GR ($k_{F,GR}$ Eq. 5.6 vs $k_{F,MR}$ Eq. 5.3).

The different dissociation constants between the two cortisol receptors results to a faster saturation of mineralocorticoid receptor as cortisol reaches its zenith values (Figure 5.4A). On the other hand, glucocorticoid receptors will saturate slower but to a higher value. Therefore, nearing cortisol's zenith we observe a switch from a state of higher permissive effects (mediated by mineralocorticoid receptor) to a state where suppressive effects (mediated by glucocorticoid receptor) dominates. This further reveals that although cortisol levels are same at its zenith, administration of LPS stimulus to consecutive times at zenith levels, results in lower maximum P_{ens} levels.

5.5: Conclusions

Despite the classical view of glucocorticoids as an endocrine response to stress that generally prevents the stress activated stress reactions from overshooting , their time of day dependent role still remains controversial (Sapolsky, Romero et al. 2000). Through our modeling effort we aimed to explore the convolution of cortisol's permissive and suppressive effects and their role in the body's time of day dependent response to an acute stimulus. In order to investigate these effects, in accordance with experimental data we assumed that mineralocorticoid receptors mediate cortisol's permissive role through regulating cytokine receptors while glucocorticoid receptors mediate cortisol's suppressive role through suppressing cytokine transcription. Our model point towards a non dose dependent cortisol effect. In particular, our results unveil the preparative role of cortisol that sensitizes the organism at times of day less likely to get infected (second half of cortisol's nadir (n) and ascending (a) phase), in order to build an efficient reactive mechanism at the

impending activity phase (second half of cortisol's zenith (z) and descending phase).

Chapter 6: Conclusion and Future Outlook

Homeostasis is maintained in the body through a large number of bidirectional interactions among physiological systems. The circadian and immune systems play leading roles in this dynamic behavior, and their effective regulation is of utmost importance. Due to the highly complex, multi-level network of interactions between the circadian clock and the inflammatory response, a systems-level approach is attractive in order to elucidate the underlying dynamics and design potential clinical interventions. The discussion presented herein aim to shed light in critical dynamics leading to physiologic variability as well as present scenarios where this can be disrupted.

Through the use of quantitative model linking endotoxemia and HRV, Chapter 2 discusses the source of physiologic variability at the systemic level of the heart and investigates a number of scenarios justified by experimental data. Chapter 3, further focus on circadian variability and provides several evidences of the links between circadian and immune interactions in the body. Based on this, Chapter 4 illustrates the use of in-silico models in order to give insight to the entrainment of PCGs to cortisol, and cortisol to environmental light/dark cycles. Finally, Chapter 5 considers the presence of circadian variability at the systemic and peripheral levels of the body and investigates the disparate effects of cortisol under scenarios of acute stress.

In terms of the work presented in Chapters 3 and 4, a direct extension is the consideration of multiple entrainers apart from cortisol. Among others, feeding has shown to be a critical synchronizer of body's rhythms. In particular, Li *et al.* showed that intermittent feeding for 2-h/day induces 24-h rhythmic expression of critical genes in clock-deficient tumors. Further, mice fed intermittently 2-h per day exhibit ~40% less tumor growth than mice fed *ad libitum* emphasizing that meal timing can not only enhance circadian rhythmicity but also improve survival (Li, Delaunay et al. 2010). Similar results have been obtained for mice with Glasgow osteosarcoma, where restricted feeding induced an increase in the amplitude of temperature and activity diurnal rhythms (Wu, Li et al. 2004). Importantly, both of these studies indicated that intermittent feeding reinforced endogenous rhythmicity independent of its caloric composition, which further underlines the specific importance of feeding time. Along the same lines, Filipski *et al.* showed that altering feeding time can counterbalance the detrimental effect of chronic jet lag on tumor growth (Filipski and Levi 2009). In particular, restricted feeding prevented the circadian disruption originally induced by chronic jet lag in the liver and slowed cancer progression. Therefore, a possible next step is to include in addition to cortisol feeding rhythms and explore the dynamics emerging by the convolution of the two entrainers. Initial results indicate that the second entrainer can restore phase changes resulting from dampening of cortisol's rhythm

Chapter 5 investigates the time of day dependent of inflammatory response by using an in-silico model that takes into consideration the immuno-

permissive/suppressive effects of cortisol. These counteractive cortisol's effects have been also correlated with disparate effects of cortisol infusion (Barber, Coyle et al. 1993) and in general with the deleterious effects of continuous low levels of stress (Sapolsky, Romero et al. 2000). The model presented in Chapter 5 and the underlying dynamics that have considered can be elaborated in order to model these scenarios. Furthermore, the model presented in Chapter 5 includes links that can be further explored and investigated. Importantly, how the convolution of systemic and peripheral rhythms can influence the response to a stressor. In the model presented in Chapter 5, PCGs rhythmicity regulate the rhythm of TLR4 and $mRNA_P$. Based on the work of (Keller, Mazuch et al. 2009) that denotes the importance of peripheral clocks in acute inflammatory response, future works can elaborate on these links and investigate scenarios involving administration of LPS stimulus on disrupted peripheral networks (PCGs mutations).

In total, each component of this dissertation can be used as a test-bed for future research, both experimental and computational. Continued work along these lines would likely be fruitful in gaining further insight into the inflammatory response and guiding future investigations.

Appendix A: Multiscale model of human endotoxemia

The model presented in this appendix has been iteratively developed over several publications. Below, the latest form of the model, incorporates circadian rhythms (Scheff, Calvano et al. 2010) and autonomic modulation at the SA node of the heart (Foteinou, Calvano et al. 2011). The unified model combining these two works has not been previously discussed in the literature.

Through the analysis of leukocyte gene expression data, the essential responses characterizing the leukocyte transcriptional dynamics are identified. Specifically, these responses, in the case of transient human endotoxemia, include (1) an early increase in pro-inflammatory signaling molecule production; (2) an anti-inflammatory response to counter pro-inflammatory signaling; and (3) an energetic response representing diminished cellular bio-energetic processes. These transcriptional responses are triggered by the activation of critical signaling cascades as a result of the recognition of the extracellular LPS signal. In the endotoxin injury model, the focus has been on NF-κB as the archetypical signaling module that regulates the expression of pro-inflammatory genes, as provoked by the binding of LPS to its receptor TLR4 (*R*) (Eq. A1.a- A1.d) leading to the activation of the NF-κB, which initiates the transcriptional response to inflammation. NF-κB is normally bound to IκB molecules which inhibit its translocation to the nucleus, thus inactivating its role as a transcription factor. LPS via TLR4 and adapter molecules stimulates the activation of IKK, which phosphorylates IκBα leading, in turn, to ubiquitination and degradation of IκBα in the proteasome.

Then, the free NF-κB can move into the nucleus and stimulate the transcription of a number of genes, including its inhibitor IκBα, thus creating a negative feedback loop. The NF-κB module is based on a reduced model of NF-κB dynamics that includes IKK (Eq. A1.e), nuclear (activated) NF-κB (Eq. A1.f), and IκBα (Eq. A1.g, A1.h) (Ihekwaba, Broomhead et al. 2004) which allows the model to broadly capture the negative feedback regulatory behavior of NF-κB . The fundamental transcriptional processes found in the gene expression data are the pro-inflammatory (Eq. A1.i), anti-inflammatory (Eq. A1.j), and energetic (Eq. A1.k) responses. Circadian production of inflammatory mediators is regulated by melatonin (Eq. A1.l), which has shown to be correlated to a number of cytokines (Petrovsky and Harrison 1998) and thus is used as a proxy for central circadian control of leukocyte transcriptional activity (Scheff, Calvano et al. 2010).

$$\frac{dLPS}{dt} = k_{lps,1} \cdot LPS \cdot (1 - LPS) - k_{lps,2} \cdot LPS \tag{A1.a}$$

$$\frac{dR}{dt} = k_{syn} \cdot mRNA,R + k_2 \cdot (LPSR) - k_1 \cdot LPS \cdot R - k_{syn} \cdot R \tag{A1.b}$$

$$\frac{d(LPSR)}{dt} = k_1 \cdot LPS \cdot R - k_3 \cdot (LPSR) - k_2 \cdot (LPSR) \tag{A1.c}$$

$$\frac{d(mRNA,R)}{dt} = k_{in,mRNA,R} \cdot (1 + H_{mRNA,R,P}) - k_{out,mRNA,R} \cdot mRNA,R \tag{A1.d}$$

$$\frac{dIKK}{dt} = k_3 \cdot (LPSR) / (1 + IkBa) - k_4 \cdot IKK + P \cdot \left(\frac{IKK^2}{1 + IKK^2} \right) \tag{A1.e}$$

$$\frac{dNFkBn}{dt} = \frac{k_{NFkB,1} \cdot IKK \cdot (1 - NFkBn)}{(1 + IkBa)} - k_{NFkB,2} \cdot NFkBn \cdot IkBa \qquad \text{(A1.f)}$$

$$\frac{dmRNA_{IkBa}}{dt} = k_{in,IkBa} \cdot (1 + k_{IkBa,1} \cdot NFkBn) - k_{out,IkBa} \cdot mRNA_{IkBa} \qquad \text{(A1.g)}$$

$$\frac{dIkBa}{dt} = k_{I,1} \cdot mRNA_{IkBa} - k_{I,2} \cdot (1 + IKK) \cdot (1 - NFkBn) \cdot IkBa - k_{I,1} \qquad \text{(A1.h)}$$

$$\frac{dP}{dt} = k_{in,P} \cdot (1 + H_{P,NFkBn}) \cdot (1 + H_{P,E}) \cdot (1 + H_{P,M}) / A - k_{out,P} \cdot P \qquad \text{(A1.i)}$$

$$\frac{dA}{dt} = k_{in,A} \cdot \left(1 + H_{A,cAMP}\right) \cdot \left(1 + H_{A,E}\right) \cdot \left(1 + H_{A,FRN}\right) \cdot (1 + H_{\mathrm{A,M}}) - k_{out,A} \cdot A \qquad \text{(A1.j)}$$

$$\frac{dE}{dt} = k_{in,E} \cdot (1 + H_{E,P}) / A - k_{out,E} \cdot E \qquad \text{(A1.k)}$$

$$\frac{dM}{dt} = RM \cdot \left(1 + \frac{F}{1+F}\right) \cdot \left(1 - \frac{P}{1+P}\right) - k_{out,RM} \cdot M$$
$$RM = \begin{cases} k_{in,RM1}, & t_{M1} < \mathrm{mod}(t, 24) < t_{M2} \\ k_{in,RM2}, & t_{M2} < \mathrm{mod}(t, 24) < t_{M1} \end{cases} \qquad \text{(A1.l)}$$

$$H_{i,j} = k_{i,j} \cdot J$$

The interplay between the NF-κB pathway and the pro- and anti-inflammatory responses normally leads to a self-limited inflammatory response that resolves after LPS has been cleared, but high doses of LPS can lead to a state of persistent inflammation. Additionally, corticosteroids (both endogenous and exogenous) play a critical role in modulating the progression of inflammation and significant prior research has elucidated the mechanisms driving corticosteroid activity (Jusko 1994; DuBois, Xu et al. 1995; Xu, Sun et

al. 1995; Sun, DuBois et al. 1998; Almon, DuBois et al. 2002; Almon, Dubois et al. 2005; Almon, Lai et al. 2005; Almon, DuBois et al. 2007). Such studies simulate the pharmacodynamic action of glucocorticoids at the cellular level and the pharmacogenomic effect of glucocorticoids at the transcriptional level (Ramakrishnan, DuBois et al. 2002; Jin, Almon et al. 2003; Jusko, DuBois et al. 2005). Corticosteroid pharmacodynamics include: (i) the binding of the corticosteroid to its cytosolic receptor; (ii) the subsequent formation of the corticosteroid-receptor complex; and (iii) the translocation of the cytosolic complex to the nucleus that alters the transcriptional machinery, activating or repressing numerous genes. This is modeled by equations governing the inflammation-induced production of cortisol along with the endogenous circadian pattern in cortisol secretion (Eq. A1.m), transcription and translation of cytosolic glucocorticoid receptor (Eq. A1.n, A1.o), and the intracellular dynamics as the signal is transduced from the cytoplasm (Eq. A1.p) to the nucleus (Eq. A1.q).

$$\frac{dF}{dt} = RF + k_{in,F_{en}} \cdot \left(1 + H_{F_{en},P}\right) - k_{out,F} \cdot F$$
$$RF = \begin{cases} k_{in,RF1}, & t_{F1} < \mathrm{mod}(t,24) < t_{F2} \\ 0, & t_{F2} < \mathrm{mod}(t,24) < t_{F1} \end{cases} \qquad \text{(A1.m)}$$

$$\frac{dR_m}{dt} = k_{syn\_Rm} \cdot \left(1 - \frac{FR(N)}{IC_{50\_Rm} + FR(N)}\right) - k_{\deg} \cdot R_m \qquad \text{(A1.n)}$$

$$\frac{dR_F}{dt} = k_{syn\_R} \cdot R_m + r_f \cdot k_{re} \cdot FR(N) - k_{on} \cdot \left(F - 1\right) \cdot R_F - k_{dgr\_R} \cdot R_F \qquad \text{(A1.o)}$$

$$\frac{dFR}{dt} = k_{on} \cdot (F - 1) \cdot R_F - k_T \cdot FR \qquad \text{(A1.p)}$$

$$\frac{dFR(N)}{dt} = k_T \cdot FR - k_{re} \cdot FR(N) \qquad \text{(A1.q)}$$

Pro-inflammatory cytokines interact with neural-based pathways that modulate the progression of the immune response. As a result of the activation of neuroendocrine axis, anti-inflammatory hormones are secreted and recognized by immune cells. In the case of catecholamines, the secretion of catecholamines from SNS and adrenal medulla attenuates the pro-inflammatory manifestations of human endotoxemia, as evidenced by reduced TNF levels (van der Poll, Coyle et al. 1996). The anti-inflammatory influence is mediated by intracellular cAMP signaling potentiating anti-inflammatory (IL-10) signaling (van der Poll, Coyle et al. 1996; van der Poll 2001). Epinephrine is modeled as being secreted in response to stimulation by the pro-inflammatory response (Elenkov, Wilder et al. 2000), and ultimately leads to increased anti-inflammatory signaling, as shown in Eq. A1.r- A1.u. Cortisol produced in the adrenal cortex interacts with the adrenal medulla, ultimately stimulating epinephrine production (Wurtman, Pohorecky et al. 1972). As experimental data shows that plasma epinephrine levels lag cortisol levels (Kronfol, Nair et al. 1997; Dimitrov, Benedict et al. 2009), cortisol is modeled as stimulating epinephrine production, thereby producing a slightly delayed circadian peak in the baseline epinephrine profile.

$$\frac{dEPI}{dt} = k_{in,EPI} \cdot \left(1 + H_{EPI,P}\right) \cdot \left(1 + H_{EPI,FRN}\right) - k_{out,EPI} \cdot EPI \qquad \text{(A1.r)}$$

$$\frac{dR_{EPI}}{dt} = k^0_{R_{EPI}} - \left[k_{1,R_{EPI}} \cdot \left(1 + H_{R_{EPI},EPI}\right) + k_{2,R_{EPI}} \right] \cdot R_{EPI} \qquad \text{(A1.s)}$$

$$\frac{dEPIR}{dt} = k_{1,R_{EPI}} \cdot \left(1 + H_{R_{EPI},EPI}\right) \cdot R_{EPI} - k_{3,EPIR} \cdot \left(EPIR + 1\right) \qquad \text{(A1.t)}$$

$$\frac{dcAMP}{dt} = \frac{1}{\tau} \cdot \left((1 + EPIR)^n - cAMP\right) \qquad \text{(A1.u)}$$

These elements in Eq. A1, and the corresponding parameter values in Table A1, comprise a semi-mechanistic model of human endotoxemia, including physiologic diurnal rhythms (Foteinou, Calvano et al. 2009; Foteinou, Calvano et al. 2009; Scheff, Calvano et al. 2010; Foteinou, Calvano et al. 2011).

Param	Value	Param	Value	Param	Value	Param	Value
$\mathbf{K_{in,RM1}}$	0.406	$K_{A,E}$	0.534	$K_{2,REPI}$	5.465	K_4	2.240
$\mathbf{K_{in,RM2}}$	0.032	$K_{out,A}$	0.810	$K_{3,EPIR}$	5.546	$K_{in,mRNA,R}$	0.091
$\mathbf{K_{out,RM}}$	0.421	$K_{A,FRN}$	0.401	τ	0.053	$K_{mRNA,R,P}$	1.740
$\mathbf{K_{in,F1}}$	0.992	$K_{in,Fen}$	0.843	n	5.509	$K_{out,mRNA,R}$	0.251
$\mathbf{K_{EPI,FRN}}$	0.090	$K_{Fen,P}$	0.256	$K_{in,HRV}$	1.185	$K_{NFkB,1}$	16.294
$\mathbf{K_{P,M}}$	0.973	$K_{out,F}$	1.058	$K_{out,HRV}$	1.045	$K_{NFkB,2}$	1.186
$\mathbf{K_{A,M}}$	1.000	$K_{in,EPI}$	5.921	$K_{Ips,1}$	4.500	$K_{in,IkBa}$	0.463
$\mathbf{T_{F1}}$	12.082	$K_{EPI,P}$	0.231	$K_{Ips,2}$	6.790	$K_{IkBa,1}$	13.273
$\mathbf{T_{F2}}$	16.530	$K_{out,EPI}$	7.286	K_{syn}	0.020	$K_{out,IkBa}$	0.463
$\mathbf{T_{M1}}$	1.732	K_{0REPI}	11.011	K_2	0.040	$K_{I,1}$	1.400
$\mathbf{T_{M2}}$	20.149	$K_{1,REPI}$	3.006	K_1	3.000	$K_{I,2}$	0.870
$\mathbf{K_{in,A}}$	0.461	$K_{REPI,EP}$	0.845	K_3	5.000	$K_{in,P}$	0.033
		I					
$\mathbf{K_{A,cAMP}}$	0.145						

Table A 1: Model parameter values, as set in our previous publications (Foteinou, Calvano et al. 2009; Foteinou, Calvano et al. 2009; Foteinou, Calvano et al. 2010; Scheff, Calvano et al. 2010; Foteinou, Calvano et al. 2011).

Appendix B: Cortisol's immune-permissive/suppressive effects

B.1: Homeostatic responses

Figure B1 depicts our model homeostatic responses. Cortisol secretion after reaching the periphery of the body (F_{per}), mediates the acetylation of MR and GR that further leads to the active form of the receptors MR*,GR*. Higher dissociation constant of GR* leads to a slower saturation compared to MR*. Cortisol ligand, binds to the two receptors forming cortisol receptor complexes and after translocating to the nucleus, FMR(N) mediates the translation of cytokine receptors ($mRNA_{Rp}$) and FGR(N) suppresses the translation of cytokine mRNA ($mRNA_P$). After their expression, cytokines diffuse out of the cell and lead to the formation of cytokine ensemble average (P_{ens}). Lastly, ensemble level of cytokines reach again peripheral cells and bind to cytokine receptors ultimately forming cytokine receptor complexes (PR) that feed-forward to cytokine expression.

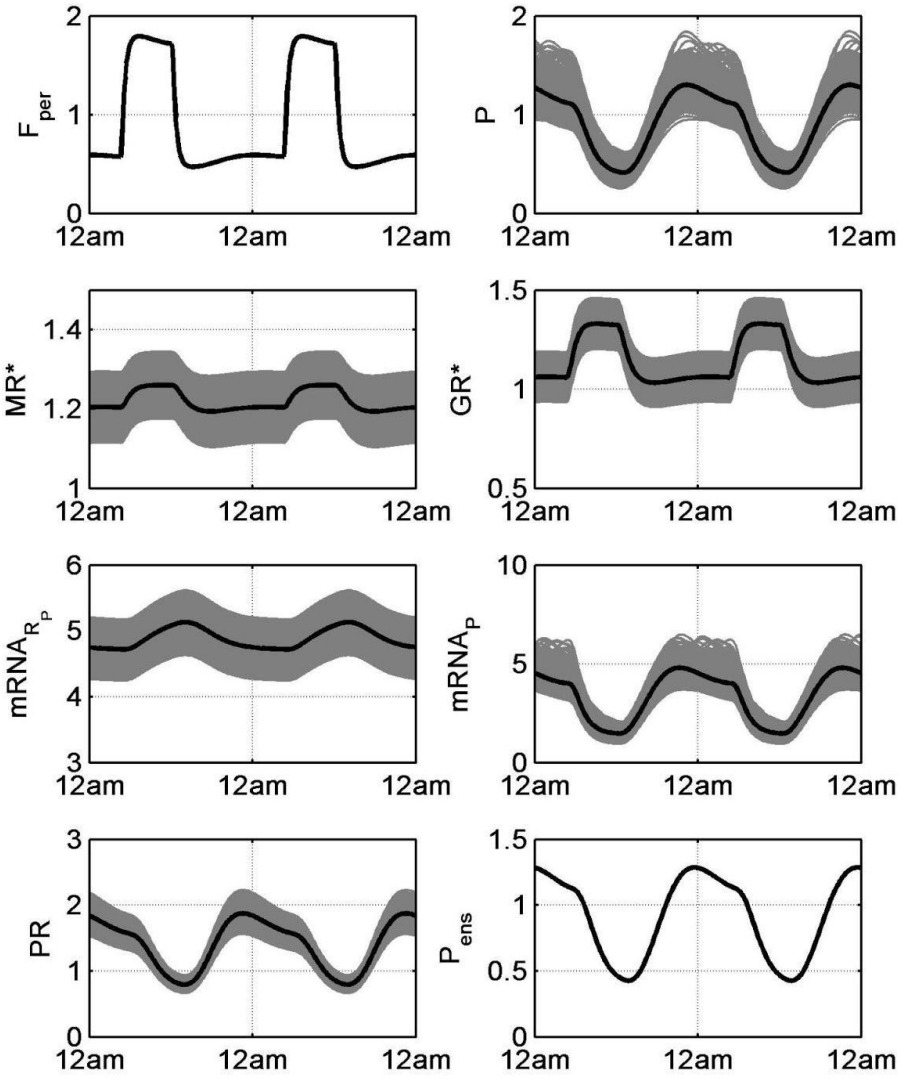

Figure B 1: Homeostatic responses. Grey lines represent single cell profiles and thick black line denotes their average profile.

B.2:Acute LPS administration at cortisol's ascending/descending phase

The analysis presented in the main text indicates that administration of acute LPS dose is not solely dependent on cortisol levels. In particular, Figure

5.3B reveals that LPS introduction at cortisol's ascending (a) phase results in higher cytokine levels compared to LPS administration at cortisol's descending (d) phase. Figure B2 further illustrates the response of our model when LPS is introduced at same cortisol levels (F_{per} = 1.2, black dotted points) in ascending (a) and descending (d) cortisol's phase. Subplot A shows cortisol's response upon LPS administration at ascending (red line) and descending (green line) phase. LPS at ascending phase leads to a higher secretion of cytokines as it is shown in Subplot B, that further feeds-back to cortisol and mediates a higher cortisol's response (Subplot A, red line). Subplots C and D illustrate cortisol's permissive (dotted line) and suppressive (solid line) effects when LPS is introduced at ascending and descending phase respectively. When LPS is introduced at cortisol's ascending phase (Subplot C), permissive effects (blue line) retain higher values than suppressive (red line) and as a result there is a higher response (dotted lines) compared to administration of LPS stimulus at cortisol's descending phase (Subplot D) where suppressive effects predominate.

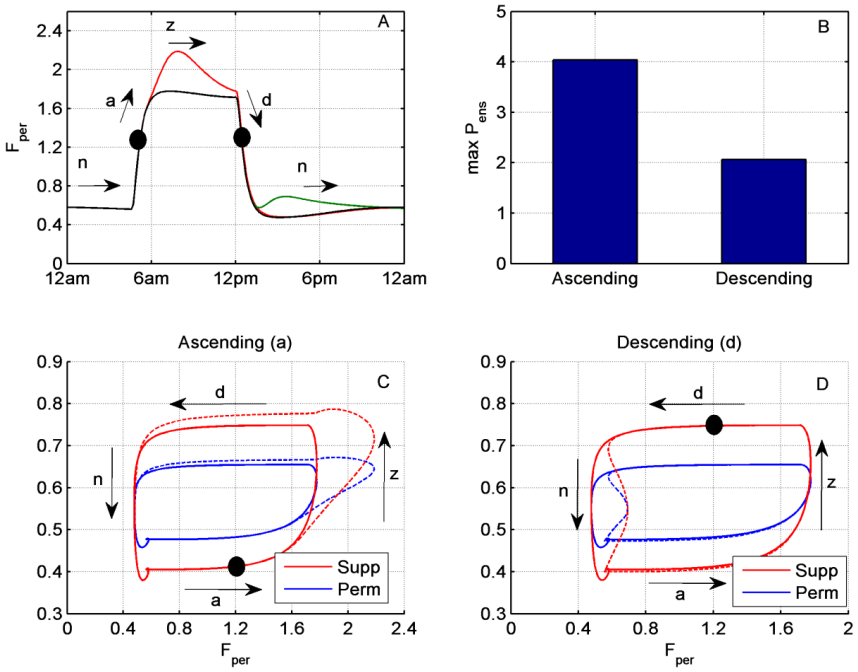

Figure B 2: Administration of LPS stimulus at cortisol's ascending (a) and descending (d) phase. A: Cortisol profile when LPS is introduced at ascending (a) and descending (d) phase. B: Maximum P_{ens} levels calculated for 24hr following LPS introduction at ascending or descending phase. C: Suppressive (Supp, red line) and permissive (perm, blue line) effects in homeostasis (solid lines) and when LPS is introduced at cortisol's ascending phase. Dotted point indicates the time of the stimulus. D: Suppressive (Supp, red line) and permissive (perm, blue line) effects in homeostasis (solid lines) and when LPS is introduced at cortisol's descending phase. Permissive profile represents the cortisol mediated induction of cytokine receptors through mineralocorticoid receptor ($\frac{k_{fr,2} \cdot FMR(N)}{K_{fr,2} + FMR(N)}$) whereas suppressive the cortisol mediated inhibition of cytokines through glucocorticoid receptor ($\frac{k_{fr} \cdot FGR(N)}{K_{fr} + FGR(N)}$). Dotted point indicates the time of the stimulus.

B.3: Acute LPS administration at cortisol's zenith/nadir levels

Figure 5.3B of the main text further indicates that LPS administration at times where cortisol maintain its zenith (z) and nadir (n) levels results in significantly different Pens responses. Figure S2 further illustrates the response of our model when LPS is introduced at cortisol's zenith or nadir levels at times where cortisol's permissive/suppressive effects are equal (i.e. perm=sup=0.55). Subplot A of Figure B3 shows homeostatic cortisol's profile (black line) along with cortisol's profile when LPS is introduced at its zenith (red line) or nadir (blue line) levels. Subplot B further indicates the resulting P_{ens} secretion after LPS stimulus. Administration of LPS at cortisol's nadir levels results in slightly higher cytokine secretion. Subplot C illustrates that at times when cortisol maintain its zenith levels, suppressive effects are shifting to higher than permissive values. Therefore, when LPS is administered at consecutive times at zenith levels where suppressive effects are continuously predominate, secretion of cytokines will be lower. The adverse is true at cortisol's nadir levels. At nadir levels suppressive effects are shifting to lower values than permissive. As such, administration of LPS stimulus at consecutive times of cortisol's nadir levels will ultimately result in increasing Pens values.

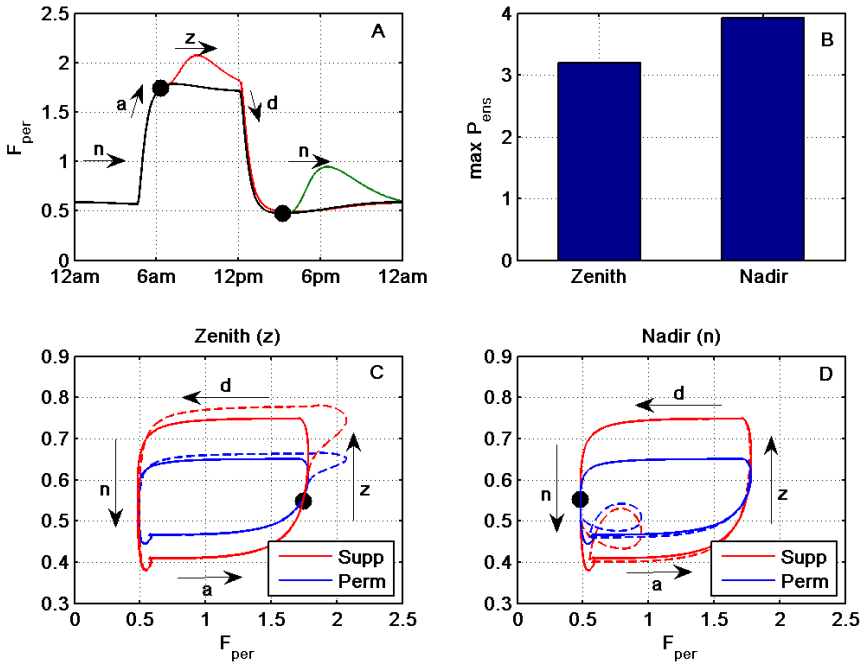

Figure B 3: Administration of LPS stimulus at cortisol's zenith (z) and nadir (n) levels. A: Cortisol profile when LPS is introduced at zenith (z) and nadir (n) levels. B: Maximum P_{ens} levels calculated for 24hr following LPS introduction at zenith or nadir levels. C: Suppressive (Supp, red line) and permissive (perm, blue line) effects in homeostasis (solid lines) and when LPS is introduced at cortisol's zenith level. Dotted point indicates the time of the stimulus. D: Suppressive (Supp, red line) and permissive (perm, blue line) effects in homeostasis (solid lines) and when LPS is introduced at cortisol's nadir levels. Permissive profile represents the cortisol mediated induction of cytokine receptors through mineralocorticoid receptor ($\frac{k_{fr,2} \cdot FMR(N)}{K_{fr,2} + FMR(N)}$) whereas suppressive the cortisol mediated inhibition of cytokines through glucocorticoid receptor ($\frac{k_{fr} \cdot FGR(N)}{K_{fr} + FGR(N)}$). Dotted point indicates the time of the stimulus.

Acknowledgements of previous publications

This dissertation contains significant portions of the following publications:

1. Scheff, J. D., P. D. Mavroudis, et al. (2011). "Modeling autonomic regulation of cardiac function and heart rate variability in human endotoxemia." Physiol Genomics **43**(16): 951-64.

2. Mavroudis, P. D., J. D. Scheff, et al. (2012). "Entrainment of peripheral clock genes by cortisol." Physiol Genomics **44**(11): 607-21.

3. Scheff, J. D., P. D. Mavroudis, et al. (2012). "Modeling physiologic variability in human endotoxemia." Crit Rev Biomed Eng **40**(4): 313-22.

4. Mavroudis, P. D., J. D. Scheff, et al. (2013). "Systems biology of circadian-immune interactions." J Innate Immun **5**(2): 153-62.

5. Scheff, J. D., P. D. Mavroudis, et al. (2013). "A multiscale modeling approach to inflammation: A case study in human endotoxemia." Journal of Computational Physics **244**(0): 279-289.

6. Scheff, J. D., P. D. Mavroudis, et al. (2013). "Translational applications of evaluating physiologic variability in human endotoxemia." J Clin Monit Comput **27**(4): 405-15.

7. Mavroudis, P. D., S. A. Corbett, et al. (2014). "Mathematical modeling of light mediated HPA axis activity and downstream implications on the entrainment of peripheral clock genes." Physiol Genomics **in press**.

8. Mavroudis, P. D., S. A. Corbett, et al. (2014). " Circadian characteristics of permissive and suppressive effects of cortisol and their role in homeostasis and the acute inflammatory response." Math Biosci **submitted**.

References

Abraham, U., A. E. Granada, et al. (2010). "Coupling governs entrainment range of circadian clocks." Mol Syst Biol **6**: 438.

Abraham, U., A. E. Granada, et al. (2010). "Coupling governs entrainment range of circadian clocks." Mol Syst Biol **6**.

Adams, K. L., O. Castanon-Cervantes, et al. (2013). "Environmental circadian disruption elevates the IL-6 response to lipopolysaccharide in blood." J Biol Rhythms **28**(4): 272-7.

Akahoshi, T., J. J. Oppenheim, et al. (1988). "Induction of high-affinity interleukin 1 receptor on human peripheral blood lymphocytes by glucocorticoid hormones." J Exp Med **167**(3): 924-36.

Akira, S., T. Hirano, et al. (1990). "Biology of multifunctional cytokines: IL 6 and related molecules (IL 1 and TNF)." Faseb J **4**(11): 2860-7.

Alamili, M., K. Bendtzen, et al. (2014). "Pronounced inflammatory response to endotoxaemia during nighttime: a randomised cross-over trial." PLoS One **9**(1): e87413.

Alesci, S., P. E. Martinez, et al. (2005). "Major depression is associated with significant diurnal elevations in plasma interleukin-6 levels, a shift of its circadian rhythm, and loss of physiological complexity in its secretion: clinical implications." J Clin Endocrinol Metab **90**(5): 2522-30.

Almon, R. R., D. C. DuBois, et al. (2002). "Pharmacodynamics and pharmacogenomics of diverse receptor-mediated effects of methylprednisolone in rats using microarray analysis." J Pharmacokinet Pharmacodyn **29**(2): 103-29.

Almon, R. R., D. C. Dubois, et al. (2005). "Pharmacogenomic responses of rat liver to methylprednisolone: an approach to mining a rich microarray time series." Aaps J **7**(1): E156-94.

Almon, R. R., D. C. DuBois, et al. (2007). "A microarray analysis of the temporal response of liver to methylprednisolone: a comparative analysis of two dosing regimens." Endocrinology **148**(5): 2209-25.

Almon, R. R., W. Lai, et al. (2005). "Corticosteroid-regulated genes in rat kidney: mining time series array data." Am J Physiol Endocrinol Metab **289**(5): E870-82.

Alvarez, S. M., M. Katsamanis Karavidas, et al. (2007). "Low-dose steroid alters in vivo endotoxin-induced systemic inflammation but does not influence autonomic dysfunction." J Endotoxin Res **13**(6): 358-68.

Amano, Y., S. W. Lee, et al. (1993). "Inhibition by glucocorticoids of the formation of interleukin-1 alpha, interleukin-1 beta, and interleukin-6: mediation by decreased mRNA stability." Mol Pharmacol **43**(2): 176-82.

An, G. (2004). "In silico experiments of existing and hypothetical cytokine-directed clinical trials using agent-based modeling." Crit Care Med **32**(10): 2050-60.

An, G. (2008). "Introduction of an agent-based multi-scale modular architecture for dynamic knowledge representation of acute inflammation." Theor Biol Med Model **5**: 11.

Andreasen, A. S., K. S. Krabbe, et al. (2008). "Human endotoxemia as a model of systemic inflammation." Curr Med Chem **15**(17): 1697-705.

Angus, D. C. (2011). "The search for effective therapy for sepsis: back to the drawing board?" Jama **306**(23): 2614-5.

Antle, M. C., D. K. Foley, et al. (2003). "Gates and oscillators: a network model of the brain clock." J Biol Rhythms **18**(4): 339-50.

Antle, M. C., N. C. Foley, et al. (2007). "Gates and oscillators II: zeitgebers and the network model of the brain clock." J Biol Rhythms **22**(1): 14-25.

Antoni, F. A. (1986). "Hypothalamic control of adrenocorticotropin secretion: advances since the discovery of 41-residue corticotropin-releasing factor." Endocr Rev **7**(4): 351-78.

Arjona, A. and D. K. Sarkar (2008). "Are circadian rhythms the code of hypothalamic-immune communication? Insights from natural killer cells." Neurochem Res **33**(4): 708-18.

Arriza, J. L., C. Weinberger, et al. (1987). "Cloning of human mineralocorticoid receptor complementary DNA: structural and functional kinship with the glucocorticoid receptor." Science **237**(4812): 268-75.

Aschoff, J. (1960). "Exogenous and endogenous components in circadian rhythms." Cold Spring Harb Symp Quant Biol **25**: 11-28.

Azama, T., M. Yano, et al. (2007). "Altered expression profiles of clock genes hPer1 and hPer2 in peripheral blood mononuclear cells of cancer patients undergoing surgery." Life Sci **80**(12): 1100-8.

Baker, J. B., G. S. Barsh, et al. (1978). "Dexamethasone modulates binding and action of epidermal growth factor in serum-free cell culture." Proc Natl Acad Sci U S A **75**(4): 1882-6.

Balsalobre, A. (2002). "Clock genes in mammalian peripheral tissues." Cell Tissue Res **309**(1): 193-9.

Balsalobre, A., S. A. Brown, et al. (2000). "Resetting of circadian time in peripheral tissues by glucocorticoid signaling." Science **289**(5488): 2344-7.

Balsalobre, A., F. Damiola, et al. (1998). "A serum shock induces circadian gene expression in mammalian tissue culture cells." Cell **93**(6): 929-37.

Barber, A. E., S. M. Coyle, et al. (1993). "Glucocorticoid therapy alters hormonal and cytokine responses to endotoxin in man." The Journal of Immunology **150**(5): 1999-2006.

Barnes, P. J. (1998). "Anti-inflammatory actions of glucocorticoids: molecular mechanisms." Clin Sci (Lond) **94**(6): 557-72.

Batada, N. N., L. A. Shepp, et al. (2004). "Stochastic model of protein-protein interaction: Why signaling proteins need to be colocalized." Proceedings of the National Academy of Sciences of the United States of America **101**(17): 6445-6449.

Bayly, E. J. (1968). "Spectral analysis of pulse frequency modulation in the nervous systems." IEEE Trans Biomed Eng **15**(4): 257-65.

Bayston, K. F. and J. Cohen (1990). "Bacterial endotoxin and current concepts in the diagnosis and treatment of endotoxaemia." J Med Microbiol **31**(2): 73-83.

Becker-Weimann, S., J. Wolf, et al. (2004). "Modeling feedback loops of the Mammalian circadian oscillator." Biophys J **87**(5): 3023-34.

Beishuizen, A. and L. G. Thijs (2003). "Endotoxin and the hypothalamo-pituitary-adrenal (HPA) axis." J Endotoxin Res **9**(1): 3-24.

Bernard, S., D. Gonze, et al. (2007). "Synchronization-induced rhythmicity of circadian oscillators in the suprachiasmatic nucleus." PLoS Comput Biol **3**(4): e68.

Beynon, A. L. and A. N. Coogan (2010). "Diurnal, age, and immune regulation of interleukin-1beta and interleukin-1 type 1 receptor in the mouse suprachiasmatic nucleus." Chronobiol Int **27**(8): 1546-63.

Bilbo, S. D., D. L. Drazen, et al. (2002). "Short day lengths attenuate the symptoms of infection in Siberian hamsters." Proc Biol Sci **269**(1490): 447-54.

Boivin, D. B. and C. A. Czeisler (1998). "Resetting of circadian melatonin and cortisol rhythms in humans by ordinary room light." Neuroreport **9**(5): 779-82.

Boivin, D. B., F. O. James, et al. (2003). "Circadian clock genes oscillate in human peripheral blood mononuclear cells." Blood **102**(12): 4143-5.

Bornstein, S. R., J. Licinio, et al. (1998). "Plasma leptin levels are increased in survivors of acute sepsis: associated loss of diurnal rhythm, in cortisol and leptin secretion." J Clin Endocrinol Metab **83**(1): 280-3.

Boyle, M. P., J. A. Brewer, et al. (2005). "Acquired deficit of forebrain glucocorticoid receptor produces depression-like changes in

adrenal axis regulation and behavior." Proc Natl Acad Sci U S A **102**(2): 473-8.

Brennan, M., M. Palaniswami, et al. (2001). "Do existing measures of Poincare plot geometry reflect nonlinear features of heart rate variability?" IEEE Trans Biomed Eng **48**(11): 1342-7.

Brennan, M., M. Palaniswami, et al. (2002). "Poincare plot interpretation using a physiological model of HRV based on a network of oscillators." Am J Physiol Heart Circ Physiol **283**(5): H1873-86.

Brown, E. N., P. M. Meehan, et al. (2001). "A stochastic differential equation model of diurnal cortisol patterns." Am J Physiol Endocrinol Metab **280**(3): E450-61.

Brown, S. A., F. Fleury-Olela, et al. (2005). "The period length of fibroblast circadian gene expression varies widely among human individuals." PLoS Biol **3**(10): e338.

Buchman, T. G. (1996). "Physiologic stability and physiologic state." J Trauma **41**(4): 599-605.

Buchman, T. G. (2009). "The digital patient: predicting physiologic dynamics with mathematical models." Crit Care Med **37**(3): 1167-8.

Buckley, T. M. and A. F. Schatzberg (2005). "On the interactions of the hypothalamic-pituitary-adrenal (HPA) axis and sleep: normal HPA axis activity and circadian rhythm, exemplary sleep disorders." J Clin Endocrinol Metab **90**(5): 3106-14.

Burger, A. J., M. Charlamb, et al. (1999). "Circadian patterns of heart rate variability in normals, chronic stable angina and diabetes mellitus." International Journal of Cardiology **71**(1): 41-48.

Burgess, H. J., J. Trinder, et al. (1997). "Sleep and circadian influences on cardiac autonomic nervous system activity." Am J Physiol Heart Circ Physiol **273**(4): H1761-1768.

Burioka, N., M. Takata, et al. (2005). "Dexamethasone influences human clock gene expression in bronchial epithelium and peripheral blood mononuclear cells in vitro." Chronobiol Int **22**(3): 585-90.

Buttenschoen, K., M. Kornmann, et al. (2008). "Endotoxemia and endotoxin tolerance in patients with ARDS." Langenbecks Arch Surg **393**(4): 473-8.

Campbell, S. S., D. Dawson, et al. (1993). "When the human circadian system is caught napping: evidence for endogenous rhythms close to 24 hours." Sleep **16**(7): 638-40.

Carlson, D. E. and W. C. Chiu (2008). "The absence of circadian cues during recovery from sepsis modifies pituitary-adrenocortical function and impairs survival." Shock **29**(1): 127-32.

Castanon-Cervantes, O., M. Wu, et al. (2010). "Dysregulation of inflammatory responses by chronic circadian disruption." J Immunol **185**(10): 5796-805.

Cavadini, G., S. Petrzilka, et al. (2007). "From the Cover: TNF-{alpha} suppresses the expression of clock genes by interfering with E-box-mediated transcription." PNAS **104**(31): 12843-12848.

Chakraborty, A., W. Krzyzanski, et al. (1999). "Mathematical Modeling of Circadian Cortisol Concentrations Using Indirect Response Models: Comparison of Several Methods." Journal of Pharmacokinetics and Pharmacodynamics **27**(1): 23-43.

Chakraborty, A., W. Krzyzanski, et al. (1999). "Mathematical modeling of circadian cortisol concentrations using indirect response models: comparison of several methods." J Pharmacokinet Biopharm **27**(1): 23-43.

Chang, L. and M. Karin (2001). "Mammalian MAP kinase signalling cascades." Nature **410**(6824): 37-40.

Charloux, A., C. Gronfier, et al. (1999). "Aldosterone release during the sleep-wake cycle in humans." Am J Physiol **276**(1 Pt 1): E43-9.

Charmandari, E., G. P. Chrousos, et al. (2011). "Peripheral CLOCK Regulates Target-Tissue Glucocorticoid Receptor Transcriptional Activity in a Circadian Fashion in Man." PLoS ONE **6**(9): e25612.

Chiu, H. W. and T. Kao (2001). "A mathematical model for autonomic control of heart rate variation." IEEE Eng Med Biol Mag **20**(2): 69-76.

Chrousos, G. P. (1995). "The Hypothalamic-Pituitary-Adrenal Axis and Immune-Mediated Inflammation." N Engl J Med **332**(20): 1351-1363.

Chrousos, G. P. (2009). "Stress and disorders of the stress system." Nat Rev Endocrinol **5**(7): 374-81.

Chrousos, G. P. and P. W. Gold (1998). "A healthy body in a healthy mind--and vice versa--the damaging power of "uncontrollable" stress." J Clin Endocrinol Metab **83**(6): 1842-5.

Chrousos, G. P. and T. Kino (2005). "Intracellular glucocorticoid signaling: a formerly simple system turns stochastic." Sci STKE **2005**(304): pe48.

Cohen, M. C., K. M. Rohtla, et al. (1997). "Meta-analysis of the morning excess of acute myocardial infarction and sudden cardiac death." The American journal of cardiology **79**(11): 1512-6.

Cooley, J. W. and J. W. Tukey (1965). "An Algorithm for the Machine Calculation of Complex Fourier Series." Mathematics of Computation **19**(90): 297-301.

Cuninkova, L. and S. A. Brown (2008). "Peripheral circadian oscillators: interesting mechanisms and powerful tools." Ann N Y Acad Sci **1129**: 358-70.

Czeisler, C. A., J. F. Duffy, et al. (1999). "Stability, precision, and near-24-hour period of the human circadian pacemaker." Science **284**(5423): 2177-81.

Czeisler, C. A., R. E. Kronauer, et al. (1989). "Bright light induction of strong (type 0) resetting of the human circadian pacemaker." Science **244**(4910): 1328-33.

De Kloet, E. R., E. Vreugdenhil, et al. (1998). "Brain corticosteroid receptor balance in health and disease." Endocr Rev **19**(3): 269-301.

Dibner, C., U. Schibler, et al. (2010). "The mammalian circadian timing system: organization and coordination of central and peripheral clocks." Annu Rev Physiol **72**: 517-49.

Dickmeis, T. (2009). "Glucocorticoids and the circadian clock." J Endocrinol **200**(1): 3-22.

Dimitrov, S., C. Benedict, et al. (2009). "Cortisol and epinephrine control opposing circadian rhythms in T cell subsets." Blood **113**(21): 5134-43.

Dinges, D. F., S. D. Douglas, et al. (1995). "Sleep deprivation and human immune function." Adv Neuroimmunol **5**(2): 97-110.

Dobson, C. M., A. Šali, et al. (1998). "Protein Folding: A Perspective from Theory and Experiment." Angewandte Chemie International Edition **37**(7): 868-893.

Donadio, V., P. Cortelli, et al. (2008). "Isolated generalised anhidrosis induced by postganglionic sympathetic skin nerve fibre degeneration: an incomplete Ross syndrome?" J Neurol Neurosurg Psychiatry **79**(8): 959-61.

DuBois, D. C., Z. X. Xu, et al. (1995). "Differential dynamics of receptor down-regulation and tyrosine aminotransferase induction following glucocorticoid treatment." J Steroid Biochem Mol Biol **54**(5-6): 237-43.

Duffy, J. F., S. W. Cain, et al. (2011). "Sex difference in the near-24-hour intrinsic period of the human circadian timing system." Proc Natl Acad Sci U S A **108 Suppl 3**: 15602-8.

Duffy, J. F. and D. J. Dijk (2002). "Getting through to circadian oscillators: why use constant routines?" J Biol Rhythms **17**(1): 4-13.

Edery, I. (2000). "Circadian rhythms in a nutshell." Physiol Genomics **3**(2): 59-74.

Elenkov, I. J., R. L. Wilder, et al. (2000). "The sympathetic nerve--an integrative interface between two supersystems: the brain and the immune system." Pharmacol Rev **52**(4): 595-638.

Faghih, R. T., K. Savla, et al. (2011). "A feedback control model for cortisol secretion." Conf Proc IEEE Eng Med Biol Soc **2011**: 716-9.

Faraut, B., K. Z. Boudjeltia, et al. (2012). "Immune, inflammatory and cardiovascular consequences of sleep restriction and recovery." Sleep Med Rev **16**(2): 137-49.

Feillet, C. A., U. Albrecht, et al. (2006). ""Feeding time" for the brain: a matter of clocks." J Physiol Paris **100**(5-6): 252-60.

Filipski, E., F. Delaunay, et al. (2004). "Effects of chronic jet lag on tumor progression in mice." Cancer Res **64**(21): 7879-85.

Filipski, E., V. M. King, et al. (2002). "Host circadian clock as a control point in tumor progression." J Natl Cancer Inst **94**(9): 690-7.

Filipski, E. and F. Levi (2009). "Circadian disruption in experimental cancer processes." Integr Cancer Ther **8**(4): 298-302.

Forger, D. B. and C. S. Peskin (2005). "Stochastic simulation of the mammalian circadian clock." Proceedings of the National Academy of Sciences of the United States of America **102**(2): 321-324.

Foteinou, P. T., S. E. Calvano, et al. (2009). "In silico simulation of corticosteroids effect on an NFkB- dependent physicochemical model of systemic inflammation." PLoS One **4**(3): e4706.

Foteinou, P. T., S. E. Calvano, et al. (2009). "Modeling endotoxin-induced systemic inflammation using an indirect response approach." Mathematical Biosciences **217**(1): 27-42.

Foteinou, P. T., S. E. Calvano, et al. (2009). "Modeling endotoxin-induced systemic inflammation using an indirect response approach." Math Biosci **217**(1): 27-42.

Foteinou, P. T., S. E. Calvano, et al. (2009). "Translational potential of systems-based models of inflammation." Clin Transl Sci **2**(1): 85-9.

Foteinou, P. T., S. E. Calvano, et al. (2010). "Multiscale model for the assessment of autonomic dysfunction in human endotoxemia." Physiol Genomics **42**(1): 5-19.

Foteinou, P. T., S. E. Calvano, et al. (2011). "A physiological model for autonomic heart rate regulation in human endotoxemia." Shock **35**(3): 229-39.

Frey, F. J., A. Odermatt, et al. (2004). "Glucocorticoid-mediated mineralocorticoid receptor activation and hypertension." Curr Opin Nephrol Hypertens **13**(4): 451-8.

Fu, L. and C. C. Lee (2003). "The circadian clock: pacemaker and tumour suppressor." Nat Rev Cancer **3**(5): 350-61.

Funder, J. W. (1993). "Mineralocorticoids, glucocorticoids, receptors and response elements." Science **259**(5098): 1132-3.

Gachon, F., E. Nagoshi, et al. (2004). "The mammalian circadian timing system: from gene expression to physiology." Chromosoma **113**(3): 103-12.

Gallego, M., E. J. Eide, et al. (2006). "An opposite role for tau in circadian rhythms revealed by mathematical modeling." Proc Natl Acad Sci U S A **103**(28): 10618-23.

Garcia-Ojalvo, J., M. B. Elowitz, et al. (2004). "Modeling a synthetic multicellular clock: repressilators coupled by quorum sensing." Proc Natl Acad Sci U S A **101**(30): 10955-60.

Geier, F., S. Becker-Weimann, et al. (2005). "Entrainment in a model of the mammalian circadian oscillator." J Biol Rhythms **20**(1): 83-93.

Gherghel, D., S. L. Hosking, et al. (2004). "Autonomic nervous system, circadian rhythms, and primary open-angle glaucoma." Surv Ophthalmol **49**(5): 491-508.

Gillespie, D. T. (2000). "The chemical Langevin equation." The Journal of Chemical Physics **113**(1): 297-306.

Godin, P. J. and T. G. Buchman (1996). "Uncoupling of biological oscillators: A complementary hypothesis concerning the pathogenesis of multiple organ dysfunction syndrome." Critical Care Medicine **24**(7): 1107-1116.

Godin, P. J. and T. G. Buchman (1996). "Uncoupling of biological oscillators: a complementary hypothesis concerning the pathogenesis of multiple organ dysfunction syndrome." Crit Care Med **24**(7): 1107-16.

Godin, P. J., L. A. Fleisher, et al. (1996). "Experimental human endotoxemia increases cardiac regularity: Results from a prospective, randomized, crossover trial." Critical Care Medicine **24**(7): 1117-1124.

Godin, P. J., L. A. Fleisher, et al. (1996). "Experimental human endotoxemia increases cardiac regularity: results from a prospective, randomized, crossover trial." Crit Care Med **24**(7): 1117-24.

Gonze, D., S. Bernard, et al. (2005). "Spontaneous synchronization of coupled circadian oscillators." Biophys J **89**(1): 120-9.

Gottschall, P. E., K. Koves, et al. (1991). "Glucocorticoid upregulation of interleukin 1 receptor expression in a glioblastoma cell line." Am J Physiol **261**(3 Pt 1): E362-8.

Griffin, M. P., T. M. O'Shea, et al. (2003). "Abnormal heart rate characteristics preceding neonatal sepsis and sepsis-like illness." Pediatr Res **53**(6): 920-6.

Haimovich, B., J. Calvano, et al. (2010). "In vivo endotoxin synchronizes and suppresses clock gene expression in human peripheral blood leukocytes." Crit Care Med **38**(3): 751-8.

Haimovich, B., M. T. Reddell, et al. (2010). "A novel model of common Toll-like receptor 4- and injury-induced transcriptional themes in human leukocytes." Crit Care **14**(5): R177.

Hampton, S. M., L. M. Morgan, et al. (1996). "Postprandial hormone and metabolic responses in simulated shift work." J Endocrinol **151**(2): 259-67.

Hastings, M., J. S. O'Neill, et al. (2007). "Circadian clocks: regulators of endocrine and metabolic rhythms." J Endocrinol **195**(2): 187-98.

Hastings, M. H., A. B. Reddy, et al. (2003). "A clockwork web: circadian timing in brain and periphery, in health and disease." Nat Rev Neurosci **4**(8): 649-61.

Haus, E. and M. H. Smolensky (1999). "Biologic rhythms in the immune system." Chronobiol Int **16**(5): 581-622.

Hermann, C., S. von Aulock, et al. (2006). "Endogenous cortisol determines the circadian rhythm of lipopolysaccharide-- but not lipoteichoic acid--inducible cytokine release." Eur J Immunol **36**(2): 371-9.

Hobson, K. G., P. J. Havel, et al. (2004). "Circulating leptin and cortisol after burn injury: loss of diurnal pattern." J Burn Care Rehabil **25**(6): 491-9.

Hobson, K. G., P. J. Havel, et al. (2004). "Circulating Leptin and Cortisol After Burn Injury: Loss of Diurnal Pattern." Journal of Burn Care & Research **25**(6): 491-499.

Hotchkiss, R. S. and I. E. Karl (2003). "The pathophysiology and treatment of sepsis." N Engl J Med **348**(2): 138-50.

Hrushesky, W. J. and P. A. Wood (1997). "Circadian time structure of septic shock: timing is everything." J Infect Dis **175**(5): 1283-4.

Hrushesky, W. J. M., T. Langevin, et al. (1994). "Circadian Dynamics of Tumor-Necrosis-Factor-Alpha (Cachectin) Lethality." Journal of Experimental Medicine **180**(3): 1059-1065.

Hrushesky, W. J. M. and P. A. Wood (1997). "Circadian time structure of septic shock: Timing is everything." Journal of Infectious Diseases **175**(5): 1283-1284.

Huikuri, H. V., M. J. Niemela, et al. (1994). "Circadian rhythms of frequency domain measures of heart rate variability in healthy subjects and patients with coronary artery disease. Effects of arousal and upright posture." Circulation **90**(1): 121-6.

Ihekwaba, A. E., D. S. Broomhead, et al. (2004). "Sensitivity analysis of parameters controlling oscillatory signalling in the NF-kappaB pathway: the roles of IKK and IkappaBalpha." Syst Biol (Stevenage) **1**(1): 93-103.

Ingle, D. J. (1954). "Permissibility of hormone action; a review." Acta Endocrinol (Copenh) **17**(1-4): 172-86.

James, F. O., C. D. Walker, et al. (2004). "Controlled exposure to light and darkness realigns the salivary cortisol rhythm in night shift workers." Chronobiol Int **21**(6): 961-72.

Jan, B. U., S. M. Coyle, et al. (2010). "Relationship of basal heart rate variability to in vivo cytokine responses after endotoxin exposure." Shock **33**(4): 363-8.

Jan, B. U., S. M. Coyle, et al. (2009). "Influence of acute epinephrine infusion on endotoxin-induced parameters of heart rate variability: a randomized controlled trial." Ann Surg **249**(5): 750-6.

Javorka, M., I. Zila, et al. (2002). "Heart rate recovery after exercise: relations to heart rate variability and complexity." Braz J Med Biol Res **35**(8): 991-1000.

Jefferies, W. M. (1991). "Cortisol and immunity." Med Hypotheses **34**(3): 198-208.

Jefferies, W. M. (1994). "Mild adrenocortical deficiency, chronic allergies, autoimmune disorders and the chronic fatigue syndrome: a continuation of the cortisone story." Med Hypotheses **42**(3): 183-9.

Jelic, S., Z. Cupic, et al. (2005). "Mathematical modeling of the hypothalamic-pituitary-adrenal system activity." Math Biosci **197**(2): 173-87.

Jeyaraj, D., S. M. Haldar, et al. (2012). "Circadian rhythms govern cardiac repolarization and arrhythmogenesis." Nature **483**(7387): 96-9.

Jin, J. Y., R. R. Almon, et al. (2003). "Modeling of corticosteroid pharmacogenomics in rat liver using gene microarrays." J Pharmacol Exp Ther **307**(1): 93-109.

Jin, J. Y., R. R. Almon, et al. (2003). "Modeling of Corticosteroid Pharmacogenomics in Rat Liver Using Gene Microarrays." Journal of Pharmacology and Experimental Therapeutics **307**(1): 93-109.

Joels, M. and E. R. de Kloet (1994). "Mineralocorticoid and glucocorticoid receptors in the brain. Implications for ion permeability and transmitter systems." Prog Neurobiol **43**(1): 1-36.

Jung, C. M., S. B. Khalsa, et al. (2010). "Acute effects of bright light exposure on cortisol levels." J Biol Rhythms **25**(3): 208-16.

Jusko, W. J. (1994). "Receptor-mediated pharmacodynamics of corticosteroids." Prog Clin Biol Res **387**: 261-70.

Jusko, W. J., D. DuBois, et al. (2005). "Sixth-Generation Model for Corticosteroid Pharmacodynamics: Multi-Hormonal Regulation of Tyrosine Aminotransferase in Rat Liver." J Pharmacokin Pharmacodyn.

Kaern, M., T. C. Elston, et al. (2005). "Stochasticity in gene expression: from theories to phenotypes." Nat Rev Genet **6**(6): 451-64.

Kalsbeek, A., R. M. Buijs, et al. (1992). "Vasopressin-containing neurons of the suprachiasmatic nuclei inhibit corticosterone release." Brain Res **580**(1-2): 62-7.

Kalsbeek, A., E. Fliers, et al. (2010). "Vasopressin and the output of the hypothalamic biological clock." J Neuroendocrinol **22**(5): 362-72.

Kamisoglu, K., K. Sleight, et al. (2013). "Effects of coupled dose and rhythm manipulation of plasma cortisol levels on leukocyte transcriptional response to endotoxin challenge in humans." Innate Immun.

Karemaker, J. M. (1999). "Autonomic integration: the physiological basis of cardiovascular variability." J Physiol **517 (Pt 2)**: 316.

Keller, M., J. Mazuch, et al. (2009). "A circadian clock in macrophages controls inflammatory immune responses." Proceedings of the National Academy of Sciences.

Khalsa, S. B., M. E. Jewett, et al. (2003). "A phase response curve to single bright light pulses in human subjects." J Physiol **549**(Pt 3): 945-52.

Kino, T., M. U. De Martino, et al. (2003). "Tissue glucocorticoid resistance/hypersensitivity syndromes." J Steroid Biochem Mol Biol **85**(2-5): 457-67.

Kleiger, R. E., J. P. Miller, et al. (1987). "Decreased heart rate variability and its association with increased mortality after acute myocardial infarction." Am J Cardiol **59**(4): 256-62.

Knudsen, P. J., C. A. Dinarello, et al. (1987). "Glucocorticoids inhibit transcriptional and post-transcriptional expression of interleukin 1 in U937 cells." J Immunol **139**(12): 4129-34.

Knutsson, A., J. Hallquist, et al. (1999). "Shiftwork and myocardial infarction: a case-control study." Occup Environ Med **56**(1): 46-50.

Korpelainen, J. T., K. A. Sotaniemi, et al. (1997). "Circadian rhythm of heart rate variability is reversibly abolished in ischemic stroke." Stroke **28**(11): 2150-4.

Kostoglou-Athanassiou, I., D. F. Treacher, et al. (1998). "Bright light exposure and pituitary hormone secretion." Clin Endocrinol (Oxf) **48**(1): 73-9.

Koyanagi, S. and S. Ohdo (2002). "Alteration of intrinsic biological rhythms during interferon treatment and its possible mechanism." Mol Pharmacol **62**(6): 1393-9.

Kronfol, Z., M. Nair, et al. (1997). "Circadian immune measures in healthy volunteers: relationship to hypothalamic-pituitary-adrenal axis hormones and sympathetic neurotransmitters." Psychosom Med **59**(1): 42-50.

Kutteh, W. H., W. E. Rainey, et al. (1991). "Glucocorticoids inhibit lipopolysaccharide-induced production of tumor necrosis factor-alpha by human fetal Kupffer cells." J Clin Endocrinol Metab **73**(2): 296-301.

Kwak, Y., G. B. Lundkvist, et al. (2008). "Interferon-gamma alters electrical activity and clock gene expression in suprachiasmatic nucleus neurons." J Biol Rhythms **23**(2): 150-9.

Kyrylov, V., L. A. Severyanova, et al. (2005). "Modeling robust oscillatory behavior of the hypothalamic-pituitary-adrenal axis." IEEE Trans Biomed Eng **52**(12): 1977-83.

Laakso, M. L., T. Porkka-Heiskanen, et al. (1994). "Twenty-four-hour rhythms in relation to the natural photoperiod: a field study in humans." J Biol Rhythms **9**(3-4): 283-93.

Lahiri, M. K., P. J. Kannankeril, et al. (2008). "Assessment of autonomic function in cardiovascular disease: physiological basis and prognostic implications." J Am Coll Cardiol **51**(18): 1725-33.

Lake, D. E., J. S. Richman, et al. (2002). "Sample entropy analysis of neonatal heart rate variability." Am J Physiol Regul Integr Comp Physiol **283**(3): R789-97.

Lange, T., S. Dimitrov, et al. (2010). "Effects of sleep and circadian rhythm on the human immune system." Ann N Y Acad Sci **1193**: 48-59.

Lavoie, S., J. Paquet, et al. (2003). "Vigilance levels during and after bright light exposure in the first half of the night." Chronobiol Int **20**(6): 1019-38.

Lee, J. E. and I. Edery (2008). "Circadian regulation in the ability of Drosophila to combat pathogenic infections." Curr Biol **18**(3): 195-9.

Leloup, J. C. and A. Goldbeter (2003). "Toward a detailed computational model for the mammalian circadian clock." Proc Natl Acad Sci U S A **100**(12): 7051-6.

Leproult, R., E. F. Colecchia, et al. (2001). "Transition from dim to bright light in the morning induces an immediate elevation of cortisol levels." J Clin Endocrinol Metab **86**(1): 151-7.

Leproult, R., O. Van Reeth, et al. (1997). "Sleepiness, performance, and neuroendocrine function during sleep deprivation: effects of exposure to bright light or exercise." J Biol Rhythms **12**(3): 245-58.

Lewy, A. J., J. Emens, et al. (2006). "Circadian uses of melatonin in humans." Chronobiol Int **23**(1-2): 403-12.

Li, X. M., F. Delaunay, et al. (2010). "Cancer inhibition through circadian reprogramming of tumor transcriptome with meal timing." Cancer Res **70**(8): 3351-60.

Lipiner-Friedman, D., C. L. Sprung, et al. (2007). "Adrenal function in sepsis: The retrospective Corticus cohort study." Critical Care Medicine **35**(4): 1012-1018 10.1097/01.CCM.0000259465.92018.6E.

Liu, A. C., D. K. Welsh, et al. (2007). "Intercellular coupling confers robustness against mutations in the SCN circadian clock network." Cell **129**(3): 605-16.

Logan, R. W. and D. K. Sarkar (2012). "Circadian nature of immune function." Mol Cell Endocrinol **349**(1): 82-90.

Lombardi, F., A. Malliani, et al. (1996). "Heart rate variability and its sympatho-vagal modulation." Cardiovasc Res **32**(2): 208-16.

Lowry, S. F. (2005). "Human Endotoxemia: A Model for Mechanistic Insight and Therapeutic Targeting." Shock **24**: 94-100.

Lowry, S. F. (2005). "Human endotoxemia: a model for mechanistic insight and therapeutic targeting." Shock **24 Suppl 1**: 94-100.

Lowry, S. F. (2009). "The stressed host response to infection: the disruptive signals and rhythms of systemic inflammation." Surg Clin North Am **89**(2): 311-26, vii.

Lowry, S. F. (2009). "The Stressed Host Response to Infection: The Disruptive Signals and Rhythms of Systemic Inflammation." Surgical Clinics of North America **89**(2): 311-326.

Lowry, S. F. and S. E. Calvano (2008). "Challenges for modeling and interpreting the complex biology of severe injury and inflammation." J Leukoc Biol **83**(3): 553-7.

Marpegan, L., M. J. Leone, et al. (2009). "Diurnal variation in endotoxin-induced mortality in mice: correlation with proinflammatory factors." Chronobiol Int **26**(7): 1430-42.

Marshall, J. C. (2003). "Such stuff as dreams are made on: mediator-directed therapy in sepsis." Nat Rev Drug Discov **2**(5): 391-405.

Martin, G. S., D. M. Mannino, et al. (2003). "The epidemiology of sepsis in the United States from 1979 through 2000." N Engl J Med **348**(16): 1546-54.

Mavroudis, P. D., S. A. Corbett, et al. (2014). "Mathematical modeling of light mediated HPA axis activity and downstream implications on the entrainment of peripheral clock genes." Physiol Genomics **in press**.

Mavroudis, P. D., J. D. Scheff, et al. (2013). "Systems biology of circadian-immune interactions." J Innate Immun **5**(2): 153-62.

Mavroudis, P. D., J. D. Scheff, et al. (2012). "Entrainment of peripheral clock genes by cortisol." Physiol Genomics.

Mavroudis, P. D., J. D. Scheff, et al. (2012). "Entrainment of peripheral clock genes by cortisol." Physiol Genomics **44**(11): 607-21.

Meyer-Hermann, M., M. T. Figge, et al. (2009). "Mathematical modeling of the circadian rhythm of key neuroendocrine-immune system players in rheumatoid arthritis: a systems biology approach." Arthritis Rheum **60**(9): 2585-94.

Meyer-Hermann, M., M. T. Figge, et al. (2009). "Mathematical modeling of the circadian rhythm of key neuroendocrine–immune

system players in rheumatoid arthritis: A systems biology approach." Arthritis & Rheumatism **60**(9): 2585-2594.

Mi, Q., B. Riviere, et al. (2007). "Agent-based model of inflammation and wound healing: insights into diabetic foot ulcer pathology and the role of transforming growth factor-beta1." Wound Repair Regen **15**(5): 671-82.

Miles, L. E., D. M. Raynal, et al. (1977). "Blind man living in normal society has circadian rhythms of 24.9 hours." Science **198**(4315): 421-3.

Miller, G. E., E. Chen, et al. (2007). "If it goes up, must it come down? Chronic stress and the hypothalamic-pituitary-adrenocortical axis in humans." Psychol Bull **133**(1): 25-45.

Mirsky, H. P., A. C. Liu, et al. (2009). "A model of the cell-autonomous mammalian circadian clock." Proc Natl Acad Sci U S A **106**(27): 11107-12.

Miyata, T. and M. Torisu (1986). "Plasma endotoxin levels and functions of peripheral granulocytes in surgical patients with respiratory distress syndrome." Jpn J Surg **16**(6): 412-7.

Mondragon-Palomino, O., T. Danino, et al. (2011). "Entrainment of a population of synthetic genetic oscillators." Science **333**(6047): 1315-9.

Mormont, M. C. and F. Levi (1997). "Circadian-system alterations during cancer processes: a review." Int J Cancer **70**(2): 241-7.

Mormont, M. C., J. Waterhouse, et al. (2000). "Marked 24-h rest/activity rhythms are associated with better quality of life, better response, and longer survival in patients with metastatic colorectal cancer and good performance status." Clin Cancer Res **6**(8): 3038-45.

Morris, J. A., Jr., P. R. Norris, et al. (2007). "Adrenal insufficiency, heart rate variability, and complex biologic systems: a study of 1,871 critically ill trauma patients." J Am Coll Surg **204**(5): 885-92; discussion 892-3.

Munck, A. and A. Naray-Fejes-Toth (1992). "The ups and downs of glucocorticoid physiology. Permissive and suppressive effects revisited." Mol Cell Endocrinol **90**(1): C1-4.

Mundigler, G., G. Delle-Karth, et al. (2002). "Impaired circadian rhythm of melatonin secretion in sedated critically ill patients with severe sepsis." Crit Care Med **30**(3): 536-40.

Nader, N., G. P. Chrousos, et al. (2009). "Circadian rhythm transcription factor CLOCK regulates the transcriptional activity of the glucocorticoid receptor by acetylating its hinge region lysine cluster: potential physiological implications." Faseb J **23**(5): 1572-83.

Nader, N., G. P. Chrousos, et al. (2010). "Interactions of the circadian CLOCK system and the HPA axis." Trends Endocrinol Metab **21**(5): 277-86.

Nagoshi, E., C. Saini, et al. (2004). "Circadian gene expression in individual fibroblasts: cell-autonomous and self-sustained oscillators pass time to daughter cells." Cell **119**(5): 693-705.

Nakagawa, H., R. L. Sack, et al. (1992). "Sleep propensity free-runs with the temperature, melatonin and cortisol rhythms in a totally blind person." Sleep **15**(4): 330-6.

Nakagawa, M., T. Iwao, et al. (1998). "Circadian rhythm of the signal averaged electrocardiogram and its relation to heart rate variability in healthy subjects." Heart **79**(5): 493-6.

Nakao, M., M. Norimatsu, et al. (1997). "Spectral distortion properties of the integral pulse frequency modulation model." IEEE Trans Biomed Eng **44**(5): 419-26.

Nava, F., G. Carta, et al. (2000). "Lipopolysaccharide increases arginine-vasopressin release from rat suprachiasmatic nucleus slice cultures." Neuroscience Letters **288**(3): 228-230.

Niklasson, U., U. Wiklund, et al. (1993). "Heart-rate variation: what are we measuring?" Clin Physiol **13**(1): 71-9.

Novak, B. and J. J. Tyson (2008). "Design principles of biochemical oscillators." Nat Rev Mol Cell Biol **9**(12): 981-91.

Oakley, R. H. and J. A. Cidlowski (1993). "Homologous down regulation of the glucocorticoid receptor: the molecular machinery." Critical reviews in eukaryotic gene expression **3**(2): 63-88.

Octavio, J. A., A. E. Rodriguez, et al. (2004). "[Circadian profiles of heart rate and its instantaneous variability in patients with chronic Chagas' disease]." Rev Esp Cardiol **57**(2): 130-7.

Okada, K., M. Yano, et al. (2008). "Injection of LPS causes transient suppression of biological clock genes in rats." J Surg Res **145**(1): 5-12.

Opal, S. M. and V. A. DePalo (2000). "Anti-inflammatory cytokines." Chest **117**(4): 1162-72.

Opal, S. M., P. J. Scannon, et al. (1999). "Relationship between plasma levels of lipopolysaccharide (LPS) and LPS-binding protein in patients with severe sepsis and septic shock." J Infect Dis **180**(5): 1584-9.

Orth, D. N., G. M. Besser, et al. (1979). "Free-running circadian plasma cortisol rhythm in a blind human subject." Clin Endocrinol (Oxf) **10**(6): 603-17.

Otsuka, T., M. Goto, et al. (2012). "Photoperiod regulates corticosterone rhythms by altered adrenal sensitivity via melatonin-independent mechanisms in Fischer 344 rats and C57BL/6J mice." PLoS One **7**(6): e39090.

Pagani, M. (2000). "Heart rate variability and autonomic diabetic neuropathy." Diabetes Nutr Metab **13**(6): 341-6.

Paladino, N., M. J. Leone, et al. (2010). "Paying the circadian toll: the circadian response to LPS injection is dependent on the Toll-like receptor 4." J Neuroimmunol **225**(1-2): 62-7.

Paliogianni, F. and D. T. Boumpas (1995). "Glucocorticoids regulate calcineurin-dependent trans-activating pathways for interleukin-2 gene transcription in human T lymphocytes." Transplantation **59**(9): 1333-9.

Papaikonomou, E. (1977). "Rat adrenocortical dynamics." J Physiol **265**(1): 119-31.

Parrillo, J. E. (1993). "Pathogenetic mechanisms of septic shock." N Engl J Med **328**(20): 1471-7.

Peng, C. K., S. Havlin, et al. (1995). "Quantification of scaling exponents and crossover phenomena in nonstationary heartbeat time series." Chaos **5**(1): 82-7.

Petrovsky, N. and L. C. Harrison (1997). "Diurnal rhythmicity of human cytokine production: a dynamic disequilibrium in T helper cell type 1/T helper cell type 2 balance?" J Immunol **158**(11): 5163-8.

Petrovsky, N. and L. C. Harrison (1998). "The chronobiology of human cytokine production." Int Rev Immunol **16**(5-6): 635-49.

Petrovsky, N., P. McNair, et al. (1998). "Diurnal rhythms of pro-inflammatory cytokines: regulation by plasma cortisol and therapeutic implications." Cytokine **10**(4): 307-12.

Pigolotti, S., S. Krishna, et al. (2007). "Oscillation patterns in negative feedback loops." Proc Natl Acad Sci U S A **104**(16): 6533-7.

Pincus, S. M. (1994). "Greater signal regularity may indicate increased system isolation." Math Biosci **122**(2): 161-81.

Polk, D. E., S. Cohen, et al. (2005). "State and trait affect as predictors of salivary cortisol in healthy adults." Psychoneuroendocrinology **30**(3): 261-72.

Pollmacher, T., J. Mullington, et al. (1996). "Diurnal variations in the human host response to endotoxin." J Infect Dis **174**(5): 1040-5.

Ponikowski, P., S. D. Anker, et al. (1997). "Depressed heart rate variability as an independent predictor of death in chronic congestive heart failure secondary to ischemic or idiopathic dilated cardiomyopathy." Am J Cardiol **79**(12): 1645-50.

Pratt, W. B. (1990). "Glucocorticoid receptor structure and the initial events in signal transduction." Prog Clin Biol Res **322**: 119-32.

Prendergast, B. J., A. K. Hotchkiss, et al. (2003). "Photoperiodic adjustments in immune function protect Siberian hamsters from lethal endotoxemia." J Biol Rhythms **18**(1): 51-62.

Ramakrishnan, R., D. C. DuBois, et al. (2002). "Fifth-generation model for corticosteroid pharmacodynamics: application to steady-state receptor down-regulation and enzyme induction patterns during

seven-day continuous infusion of methylprednisolone in rats." J Pharmacokinet Pharmacodyn **29**(1): 1-24.

Rassias, A. J., P. T. Holzberger, et al. (2005). "Decreased physiologic variability as a generalized response to human endotoxemia." Crit Care Med **33**(3): 512-9.

Rassias, A. J., P. T. Holzberger, et al. (2005). "Decreased physiologic variability as a generalized response to human endotoxemia *." Critical Care Medicine **33**(3): 512-519 10.1097/01.CCM.0000155908.46346.ED.

Re, F., M. Muzio, et al. (1994). "The type II "receptor" as a decoy target for interleukin 1 in polymorphonuclear leukocytes: characterization of induction by dexamethasone and ligand binding properties of the released decoy receptor." J Exp Med **179**(2): 739-43.

Reilly, D. F., E. J. Westgate, et al. (2007). "Peripheral circadian clocks in the vasculature." Arterioscler Thromb Vasc Biol **27**(8): 1694-705.

Reiter, R. J. (1993). "The melatonin rhythm: both a clock and a calendar." Cellular and Molecular Life Sciences **49**(8): 654-664.

Relogio, A., P. O. Westermark, et al. (2011). "Tuning the Mammalian circadian clock: robust synergy of two loops." PLoS Comput Biol **7**(12): e1002309.

Reppert, S. M., M. J. Perlow, et al. (1981). "Effects of damage to the suprachiasmatic area of the anterior hypothalamus on the daily melatonin and cortisol rhythms in the rhesus monkey." J Neurosci **1**(12): 1414-25.

Reppert, S. M. and D. R. Weaver (2002). "Coordination of circadian timing in mammals." Nature **418**(6901): 935-41.

Richman, J. S. and J. R. Moorman (2000). "Physiological time-series analysis using approximate entropy and sample entropy." Am J Physiol Heart Circ Physiol **278**(6): H2039-49.

Rosmond, R., M. F. Dallman, et al. (1998). "Stress-Related Cortisol Secretion in Men: Relationships with Abdominal Obesity and Endocrine, Metabolic and Hemodynamic Abnormalities." J Clin Endocrinol Metab **83**(6): 1853-1859.

Ruiz, F. S., M. L. Andersen, et al. (2012). "Immune alterations after selective rapid eye movement or total sleep deprivation in healthy male volunteers." Innate Immun **18**(1): 44-54.

Sack, R. L., D. Auckley, et al. (2007). "Circadian rhythm sleep disorders: part I, basic principles, shift work and jet lag disorders. An American Academy of Sleep Medicine review." Sleep **30**(11): 1460-83.

Sack, R. L., A. J. Lewy, et al. (1992). "Circadian rhythm abnormalities in totally blind people: incidence and clinical significance." J Clin Endocrinol Metab **75**(1): 127-34.

Saito, Y., T. Shimizu, et al. (1996). "Effect of bright light exposure on muscle sympathetic nerve activity in human." Neuroscience Letters **219**(2): 135-137.

Sapolsky, R. M., L. M. Romero, et al. (2000). "How Do Glucocorticoids Influence Stress Responses? Integrating Permissive, Suppressive, Stimulatory, and Preparative Actions." Endocr Rev **21**(1): 55-89.

Sathiyaa, R. and M. M. Vijayan (2003). "Autoregulation of glucocorticoid receptor by cortisol in rainbow trout hepatocytes." Am J Physiol Cell Physiol **284**(6): C1508-15.

Sayk, F., A. Vietheer, et al. (2008). "Endotoxemia causes central downregulation of sympathetic vasomotor tone in healthy humans." Am J Physiol Regul Integr Comp Physiol **295**(3): R891-8.

Schaller, M. D., B. Waeber, et al. (1985). "Angiotensin II, vasopressin, and sympathetic activity in conscious rats with endotoxemia." Am J Physiol **249**(6 Pt 2): H1086-92.

Scheer, F. A. and R. M. Buijs (1999). "Light affects morning salivary cortisol in humans." J Clin Endocrinol Metab **84**(9): 3395-8.

Scheff, J. D., S. E. Calvano, et al. (2010). "Modeling the influence of circadian rhythms on the acute inflammatory response." Journal of Theoretical Biology **264**(3): 1068-1076.

Scheff, J. D., S. E. Calvano, et al. (2010). "Modeling the influence of circadian rhythms on the acute inflammatory response." J Theor Biol **264**(3): 1068-76.

Scheff, J. D., S. E. Calvano, et al. (2012). "Transcriptional implications of ultradian glucocorticoid secretion in homeostasis and in the acute stress response." Physiol Genomics **44**(2): 121-9.

Scheff, J. D., A. K. Kosmides, et al. (2011). "Pulsatile glucocorticoid secretion: origins and downstream effects." IEEE Trans Biomed Eng **58**(12): 3504-7.

Scheff, J. D., P. D. Mavroudis, et al. (2013). "Translational applications of evaluating physiologic variability in human endotoxemia." J Clin Monit Comput **27**(4): 405-15.

Scheff, J. D., P. D. Mavroudis, et al. (2011). "Modeling autonomic regulation of cardiac function and heart rate variability in human endotoxemia." Physiol Genomics **43**(16): 951-64.

Scheff, J. D., P. D. Mavroudis, et al. (2013). "A multiscale modeling approach to inflammation: A case study in human endotoxemia." Journal of Computational Physics **244**(0): 279-289.

Scheff, J. D., P. D. Mavroudis, et al. (2012). "Modeling physiologic variability in human endotoxemia." Crit Rev Biomed Eng **40**(4): 313-22.

Schmidt, H., U. Müller-Werdan, et al. (2007). Autonomic dysfunction: A relevant component in multiple organ dysfunction

syndrome. Yearbook of Intensive Care and Emergency Medicine. J. L. Vincent, Springer**:** 455-467.

Sephton, S. and D. Spiegel (2003). "Circadian disruption in cancer: a neuroendocrine-immune pathway from stress to disease?" Brain Behav Immun **17**(5): 321-8.

Sephton, S. E., E. Lush, et al. (2013). "Diurnal cortisol rhythm as a predictor of lung cancer survival." Brain Behav Immun **30 Suppl**: S163-70.

Sephton, S. E., R. M. Sapolsky, et al. (2000). "Diurnal Cortisol Rhythm as a Predictor of Breast Cancer Survival." Journal of the National Cancer Institute **92**(12): 994-1000.

Sephton, S. E., R. M. Sapolsky, et al. (2000). "Diurnal cortisol rhythm as a predictor of breast cancer survival." J Natl Cancer Inst **92**(12): 994-1000.

Seydnejad, S. R. and R. I. Kitney (2001). "Modeling of Mayer waves generation mechanisms." IEEE Eng Med Biol Mag **20**(2): 92-100.

Shanahan, T. L. and C. A. Czeisler (1991). "Light exposure induces equivalent phase shifts of the endogenous circadian rhythms of circulating plasma melatonin and core body temperature in men." J Clin Endocrinol Metab **73**(2): 227-35.

Shanahan, T. L., R. E. Kronauer, et al. (1999). "Melatonin rhythm observed throughout a three-cycle bright-light stimulus designed to reset the human circadian pacemaker." J Biol Rhythms **14**(3): 237-53.

Shanker, B.-A., S. M. Coyle, et al. "Modeling the human injury response." Journal of the American College of Surgeons **211**(3, Supplement 1): S53-S54.

Shanker, B.-A., S. M. Coyle, et al. "Modeling the human injury response." Journal of the American College of Surgeons **211**(3): S53-S54.

Silver, A. C., A. Arjona, et al. (2012). "The circadian clock controls toll-like receptor 9-mediated innate and adaptive immunity." Immunity **36**(2): 251-61.

Snyers, L., L. De Wit, et al. (1990). "Glucocorticoid up-regulation of high-affinity interleukin 6 receptors on human epithelial cells." Proc Natl Acad Sci U S A **87**(7): 2838-42.

So, A. Y. L., T. U. Bernal, et al. (2009). "Glucocorticoid regulation of the circadian clock modulates glucose homeostasis." Proceedings of the National Academy of Sciences **106**(41): 17582-17587.

Sommer, C. and M. Kress (2004). "Recent findings on how proinflammatory cytokines cause pain: peripheral mechanisms in inflammatory and neuropathic hyperalgesia." Neurosci Lett **361**(1-3): 184-7.

Sriram, K., M. Rodriguez-Fernandez, et al. (2012). "Modeling cortisol dynamics in the neuro-endocrine axis distinguishes normal, depression, and post-traumatic stress disorder (PTSD) in humans." PLoS Comput Biol **8**(2): e1002379.

Sternberg, E. M. (2006). "Neural regulation of innate immunity: a coordinated nonspecific host response to pathogens." Nat Rev Immunol **6**(4): 318-28.

Stevens, R. G., D. E. Blask, et al. (2007). "Meeting report: the role of environmental lighting and circadian disruption in cancer and other diseases." Environ Health Perspect **115**(9): 1357-62.

Stratmann, M. and U. Schibler (2006). "Properties, entrainment, and physiological functions of mammalian peripheral oscillators." J Biol Rhythms **21**(6): 494-506.

Stricker, J., S. Cookson, et al. (2008). "A fast, robust and tunable synthetic gene oscillator." Nature **456**(7221): 516-9.

Strogatz, S. H. and I. Stewart (1993). "Coupled oscillators and biological synchronization." Sci Am **269**(6): 102-9.

Sun, Y. N., D. C. DuBois, et al. (1998). "Fourth-generation model for corticosteroid pharmacodynamics: a model for methylprednisolone effects on receptor/gene-mediated glucocorticoid receptor down-regulation and tyrosine aminotransferase induction in rat liver." J Pharmacokinet Biopharm **26**(3): 289-317.

Sun, Y. N. and W. J. Jusko (1998). "Transit compartments versus gamma distribution function to model signal transduction processes in pharmacodynamics." J Pharm Sci **87**(6): 732-7.

Task (1996). "Heart rate variability: standards of measurement, physiological interpretation and clinical use. Task Force of the European Society of Cardiology and the North American Society of Pacing and Electrophysiology." Circulation **93**(5): 1043-65.

Tass, P., M. G. Rosenblum, et al. (1998). "Detection of n:m Phase Locking from Noisy Data: Application to Magnetoencephalography." Physical Review Letters **81**(15): 3291-3294.

Touitou, Y., O. Benoit, et al. (1992). "Effects of a two-hour early awakening and of bright light exposure on plasma patterns of cortisol, melatonin, prolactin and testosterone in man." Acta Endocrinol (Copenh) **126**(3): 201-5.

Touitou, Y., A. Bogdan, et al. (1996). "Disruption of the circadian patterns of serum cortisol in breast and ovarian cancer patients: relationships with tumour marker antigens." Br J Cancer **74**(8): 1248-52.

Tousson, E. and H. Meissl (2004). "Suprachiasmatic nuclei grafts restore the circadian rhythm in the paraventricular nucleus of the hypothalamus." J Neurosci **24**(12): 2983-8.

Tracey, K. J. (2002). "The inflammatory reflex." Nature **420**(6917): 853-859.

Tracey, K. J., B. Beutler, et al. (1986). "Shock and tissue injury induced by recombinant human cachectin." Science **234**(4775): 470-4.

Tracey, K. J., S. F. Lowry, et al. (1987). "Cachectin/tumor necrosis factor induces lethal shock and stress hormone responses in the dog." Surg Gynecol Obstet **164**(5): 415-22.

Tsigos, C. and G. P. Chrousos (1994). "Physiology of the hypothalamic-pituitary-adrenal axis in health and dysregulation in psychiatric and autoimmune disorders." Endocrinol Metab Clin North Am **23**(3): 451-66.

Tyson, J. J., K. C. Chen, et al. (2003). "Sniffers, buzzers, toggles and blinkers: dynamics of regulatory and signaling pathways in the cell." Curr Opin Cell Biol **15**(2): 221-31.

Ullner, E., J. Buceta, et al. (2009). "Noise-induced coherence in multicellular circadian clocks." Biophys J **96**(9): 3573-81.

Van Cauter, E., J. Sturis, et al. (1994). "Demonstration of rapid light-induced advances and delays of the human circadian clock using hormonal phase markers." Am J Physiol **266**(6 Pt 1): E953-63.

van der Poll, T. (2001). "Effects of catecholamines on the inflammatory response." Sepsis **4**(2): 159-67.

van der Poll, T., S. M. Coyle, et al. (1996). "Epinephrine inhibits tumor necrosis factor-alpha and potentiates interleukin 10 production during human endotoxemia." J Clin Invest **97**(3): 713-9.

van Mark, A., S. W. Weiler, et al. (2010). "The impact of shift work induced chronic circadian disruption on IL-6 and TNF-alpha immune responses." J Occup Med Toxicol **5**: 18.

Veldhuis, J. D., D. M. Keenan, et al. (2008). "Motivations and methods for analyzing pulsatile hormone secretion." Endocr Rev **29**(7): 823-64.

Vinther, F., M. Andersen, et al. (2011). "The minimal model of the hypothalamic-pituitary-adrenal axis." J Math Biol **63**(4): 663-90.

Vodovotz, Y., G. Constantine, et al. (2009). "Mechanistic simulations of inflammation: current state and future prospects." Math Biosci **217**(1): 1-10.

Vodovotz, Y., M. Csete, et al. (2008). "Translational systems biology of inflammation." PLoS Comput Biol **4**(4): e1000014.

Vondrasova, D., I. Hajek, et al. (1997). "Exposure to long summer days affects the human melatonin and cortisol rhythms." Brain Res **759**(1): 166-70.

Walker, J. J., J. R. Terry, et al. (2010). "Origin of ultradian pulsatility in the hypothalamic-pituitary-adrenal axis." Proc Biol Sci **277**(1688): 1627-33.

Wang, X. S., M. E. Armstrong, et al. (2011). "Shift work and chronic disease: the epidemiological evidence." Occup Med (Lond) **61**(2): 78-89.

Warner, H. R. and A. Cox (1962). "A mathematical model of heart rate control by sympathetic and vagus efferent information." J Appl Physiol **17**: 349-55.

Welsh, D. K., S. H. Yoo, et al. (2004). "Bioluminescence imaging of individual fibroblasts reveals persistent, independently phased circadian rhythms of clock gene expression." Curr Biol **14**(24): 2289-95.

West, G. and H. Pohl (1973). "Effect of light-dark cycles with different LD time-ratios and different LD intensity-ratios on the activity rhythm of chaffinches." Journal of comparative physiology **83**(3): 289-302.

Westermark, P. O., D. K. Welsh, et al. (2009). "Quantification of circadian rhythms in single cells." PLoS Comput Biol **5**(11): e1000580.

Wu, M. W., X. M. Li, et al. (2004). "Effects of meal timing on tumor progression in mice." Life Sci **75**(10): 1181-93.

Wurtman, R. J., L. A. Pohorecky, et al. (1972). "Adrenocortical control of the biosynthesis of epinephrine and proteins in the adrenal medulla." Pharmacol Rev **24**(2): 411-26.

Xu, Z. X., Y. N. Sun, et al. (1995). "Third-generation model for corticosteroid pharmacodynamics: roles of glucocorticoid receptor mRNA and tyrosine aminotransferase mRNA in rat liver." J Pharmacokinet Biopharm **23**(2): 163-81.

Yamamoto, T., Y. Nakahata, et al. (2005). "Acute physical stress elevates mouse period1 mRNA expression in mouse peripheral tissues via a glucocorticoid-responsive element." J Biol Chem **280**(51): 42036-43.

Yamazaki, S., R. Numano, et al. (2000). "Resetting central and peripheral circadian oscillators in transgenic rats." Science **288**(5466): 682-5.

Yamazaki, S., M. Straume, et al. (2002). "Effects of aging on central and peripheral mammalian clocks." Proceedings of the National Academy of Sciences **99**(16): 10801-10806.

Yao, Z., D. C. DuBois, et al. (2006). "Modeling circadian rhythms of glucocorticoid receptor and glutamine synthetase expression in rat skeletal muscle." Pharm Res **23**(4): 670-9.

Yehuda, R., M. H. Teicher, et al. (1996). "Cortisol regulation in posttraumatic stress disorder and major depression: a chronobiological analysis." Biol Psychiatry **40**(2): 79-88.

Yoo, S. H., S. Yamazaki, et al. (2004). "PERIOD2::LUCIFERASE real-time reporting of circadian dynamics reveals persistent circadian

oscillations in mouse peripheral tissues." Proc Natl Acad Sci U S A **101**(15): 5339-46.

Zvonic, S., A. A. Ptitsyn, et al. (2006). "Characterization of Peripheral Circadian Clocks in Adipose Tissues." Diabetes **55**(4): 962-970.